

**THREE-DIMENSIONAL KINEMATICS OF THE UPPER LIMB
DURING FOUR FUNCTIONAL LIFTING TASKS**

by

Colin Wicks

Submitted in partial fulfillment of the requirements
for the degree of Master of Science

at

Dalhousie University
Halifax, Nova Scotia
August, 2017

© Copyright by Colin Wicks, 2017

DEDICATION PAGE

This paper is dedicated to my late grandparents, Sadie Wicks & Frank Simms.

Nature's first green is gold, Her hardest hue to hold.
 Her early leaf's a flower; But only so an hour.
Then leaf subsides to leaf. So Eden sank to grief,
 So dawn goes down today.
 Nothing gold can stay.

Table of Contents

List of Tables	iv
List of Figures	vi
Abstract	ix
List of Abbreviations Used	x
Chapter 1: Introduction	1
1.1 Significance.....	1
Chapter 2: Literature Review.....	5
2.1 Literature Review.....	5
2.2 Summary	13
Chapter 3: Methods.....	14
3.1 Study Design and Location.....	14
3.2 Participants.....	14
3.3 Experimental Protocol	15
3.4 Data Collection	26
3.5 Data Analysis	27
3.6 Conclusion	29
Chapter 4: Results	30
4.1 Qualysis & Flock of Birds Comparison.....	30
4.2 Body Segment Angular Motion Patterns	50
4.3 Lifting Load Linear Motion Patterns & Time Comparison	57
Chapter 5: Discussion	63
5.1 Qualysis - FOB System Comparison	64
5.2 Angular Motion Patterns	65
5.3 Lifting Load Trajectory.....	72
5.4 Effect of Instruction on Trial Time & Pelvic/Trunk Motion	73
5.5 Conclusion	75
References	78
Appendix A: Results Continued	83
Appendix B: Initial Screening Form.....	145
Appendix C: Pilot Study	146

List of Tables

Table 1. Visual representation of the data collection procedure.....	16
Table 2.List of bony landmarks represented by virtual marker placement.....	19
Table 3. Mean (standard deviation) maximum angular displacement (degrees) of the trunk in relation to the GCS during the normal reach lift and replace task.	33
Table 4. Average max angular displacement (Standard Deviation) of the pelvis in relation to the GCS during the normal reach lift and replace task. Standard deviation is included in brackets. Units are in degrees.	41
Table 9. Results from the paired t-tests performed to assess the effect of instruction on the time needed to perform each task. A positive result (+) indicates a significant difference between standardized and freestyle instructive conditions. All units are in seconds.....	62
Table 10. Average (Standard Deviation) max angular displacement of the trunk in relation to the GCS during the maximum reach lift and replace task. Standard deviation is included in brackets. Units are in degrees.....	84
Table 11. Average (Standard Deviation) max angular displacements of the pelvis in relation to the GCS during the maximum reach lift and replace task. Standard deviation is included in brackets. Units are in degrees.....	92
Table 12. Average (Standard Deviation) max angular displacements of the trunk in relation to the GCS during the normal reach lift and horizontal transfer task. Standard deviation is included in brackets. Units are in degrees.....	100
Table 13. Average (Standard Deviation) max angular displacements of the pelvis in relation to the GCS during the normal reach lift and horizontal transfer task. Standard deviation is included in brackets. Units are in degrees.....	107
Table 14. Average (Standard Deviation) max angular displacements of the trunk in relation to the GCS during the extended reach lift and horizontal transfer task. Standard deviation is included in brackets. Units are in degrees.....	115
Table 15. Average (Standard Deviation) max angular displacements of the pelvis in relation to the GCS during the maximum reach lift and horizontal transfer task. Standard deviation is included in brackets. Units are in degrees.....	123
Table 16. Calculated MAD of the trunk relative to the pelvis during the testing procedure.	155

Table 17. Calculated MAD for both shoulders relative to the trunk during the testing procedure..... 156

Table 18. Calculated MAD for both elbows relative to the upper arms during the testing procedure..... 159

List of Figures

Figure 1. Visual portrayal of the placement of the six triads and twenty markers being used to create the upper body model.....	17
Figure 2. Sagittal view of the two reach postures for the four lifting tasks	22
Figure 3. The experimental set-up and lifting height required for the two lifting conditions. Note that the subject is in the maximum reach position and would have their elbows at 90 degrees during the normal reach condition, even though the lifting height did not change for either condition.	24
Figure 4. Shown above are the one, three and five second positions, in appropriate order, for the horizontal transfer task. Note the 60 degree starting and end lines located on the table, which will be used for both reach conditions of the transfer task to control the start and end positions of the load for each participant.	26
Figure 5. Proposed biomechanical model detailing the degrees of freedom being examined at both the shoulder and elbow joints. (Abdullah et al., 2007).....	29
Figure 6. Angular displacement-time graphs showing the angular position of the trunk with reference to the GCS for both the standardized and freestyle conditions as recorded by the Qualysis system. Forward flexion and movements to the left are negative; Trunk extension and lateral bending to the right are positive values.	33
Figure 7. Graphical representation of the output from the univariate ANOVA results....	34
Figure 8. Bland-Altman Plot demonstrating the agreement between the FOB and Qualysis systems while recording trunk flexion/extension during the lifting task normal reach task.	35
Figure 9. Graphical representation of the output from the univariate ANOVA results....	36
Figure 10. Bland-Altman Plot demonstrating the agreement between the FOB and Qualysis systems while recording trunk lateral flexion during the lifting task normal reach task. The dotted red lines represent the upper and lower limits of the 95% confidence interval. The solid black line represents the mean of the differences calculated between the two systems.....	37
Figure 11. Graphical representation of the output from the univariate ANOVA results..	38
Figure 12. Bland-Altman Plot demonstrating the agreement between the FOB and Qualysis systems while recording trunk axial rotation during the lift and replace normal reach task.	39

Figure 13. Angle-time graphs showing the angular position of the pelvis with reference to the GCS for both the standardized and freestyle conditions for the Qualysis system. Angles are measured in degrees. Forward flexion and movements in the left are negative values; extension and movements to the right are positive values.....	40
Figure 14. Graphical representation of the output from the univariate ANOVA results..	42
Figure 15. Bland-Altman Plot demonstrating the agreement between the FOB and Qualysis systems while recording pelvic flexion/extension during the lift and replace normal reach task.....	43
Figure 16. Graphical representation of the output from the univariate ANOVA results..	44
Figure 17. Bland-Altman Plot demonstrating the agreement between the FOB and Qualysis systems while recording pelvic lateral tilt during the lift and replace normal reach task.	45
Figure 18. Graphical representation of the output from the univariate ANOVA results..	46
Figure 19. Bland-Altman Plot demonstrating the agreement between the FOB and Qualysis systems while recording axial rotation during the lift and replace normal reach task.	47
Figure 20. Angle-time graphs showing the angular position of the trunk with reference to the pelvis during the Lift & Replace Normal Reach task.	52
Figure 21. Angle-time graphs showing the angular position of the right upper arm with reference to the torso during the Lift & Replace Normal Reach task.	53
Figure 22. Angle-time graphs showing the angular position of the left upper arm with reference to the torso during the Lift & Replace Normal Reach task.	54
Figure 23. Angle-time graphs showing the angular position of the right lower arm with reference to the right upper arm during the Lift & Replace Normal Reach task.	55
Figure 24. Angle-time graphs showing the angular position of the left lower arm with reference to the left upper arm during the Lift & Replace Normal Reach task.	56
Figure 25. Linear movement patterns for the lifting load during the lift and replace normal reach condition. Distance units are in meters (m). X = Subject Frontal Plane, Y= Subject Transverse Plane, Z = Subject Sagittal Plane.	58
Figure 26. Linear movement patterns for the lifting load during the lift and replace extended reach condition. Distance units are in meters (m). X = Subject Frontal Plane, Y= Subject Transverse Plane, Z = Subject Sagittal Plane.	59

Figure 27. Linear movement patterns for the lifting load during the normal reach variant of the horizontal transfer task condition. The red line signifies the moment the load was transferred between hands. Distance units are in meters (m). X = Subject Frontal Plane, Y= Subject Transverse Plane, Z = Subject Sagittal Plane. 60

Figure 28. Linear movement patterns for the lifting load during the extended reach variant of the horizontal transfer task condition. The red line signifies the moment the load was transferred between hands. Distance units are in meters (m). X = Subject Frontal Plane, Y= Subject Transverse Plane, Z = Subject Sagittal Plane. 61

Abstract

Kinematics is a branch of classical mechanics responsible for the description of the motion of an object, or series of objects, in space. This study uses 3-D motion capture to record the motion of the torso and upper extremities during four functional lifting tasks. The tasks are part of a series of standardized tests developed to assess difference in healthy and sub-acute low back-injured populations. The purpose of the study is to develop a method to quantify the 3-D kinematics of the upper extremity and trunk during while comparing the FOB and Qualysis motion capture systems during two separate instructional conditions. Healthy participants between the ages of 18-35 were recruited to perform a one-day repeated measures protocol. The data collected allowed for the angular movement patterns of the general healthy population. In the future, these motion patterns will be used for to the development of kinetic models of the motion.

List of Abbreviations Used

LTN	Lift & Replace Normal Reach
LTM	Lift & Replace Maximum Reach
HTTN	Horizontal Transfer Task Normal Reach
HTTM	Horizontal Transfer Task Maximum Reach
GCS	Global Coordinate System
ACS	Anatomical Coordinate System
UX	Upper Extremity
LX	Lower Extremity
FOB	Flock of Birds Motion Capture System
QTM	Qualysis Track Manager Software Program
MAD	Max Angular Displacement
SPSS	Statistical Package for the Social Sciences
GLM	General Linear Model
df	Degrees of Freedom
SE	Standard Error
SD	Standard Deviation

Chapter 1: Introduction

Kinematics is a branch of classical mechanics responsible for the description of the linear and angular motion of an object, or series of objects, in space (Zatsiorsky, 1998). Researchers using a kinematic method focus on examining the motion of an object and not the causes of the motion. These motions hold particular interest to health researchers because they allow for the measurement and modeling of the active human body in space. For example, the movement patterns observed from these models can give valuable insight into outcomes of mechanical differences between healthy and injured populations (Gage et al., 2001; Mercer et al., 2006; van Andel et al., 2008). These models allow for irregularities within the motion to be easily quantified, which can provide researchers and clinicians with insights into treatment methods for individuals with biomechanical pathologies. They also give researchers the ability to develop injury prevention strategies in order to prevent future injury from occurring, especially in the occupational and ergonomic disciplines.

1.1 Significance

Extensive research has been performed in the fields of biomechanics and ergonomics, sometimes called occupational biomechanics, to try and establish a relationship between material handling technique and lower back injury (Wrigley et al., 2005). Both qualitative and quantitative approaches have been used to examine the lower back and pelvis in hopes of finding the cause or predictive risk factors for the high prevalence of back injury in the workforce (Garg et al., 1985; Park et al., 1974).

Kinematic analyses are a form of descriptive analysis that have been performed using both 2-D and 3-D motion capture techniques to record the motion of healthy and injured populations. The models created from these analyses are then used for direct comparison within and between sub-populations of individuals. The models can also provide insight into the effectiveness of treatment programs meant to aid in the restoration of normal movement patterns in injured populations (Wu et al., 2007). The next step once the kinematic analysis is performed would be to examine the kinetics of the motion, meaning the forces and moments acting within the body while the motion is occurring. These forces give even greater insight into the nature of the activities performed (Mercer et al., 2006).

One example of the use of biomechanical measures in combination with other measures is the work of Hubley-Kozey and her colleagues who have used complex measures of electromyography of the trunk musculature to establish representative patterns of muscle activation in healthy and low-back injured groups (Butler et al., 2007, 2009, 2013). This work has also been extended (Hubley-Kozey et al., 2014) to examine the effects of aging and sex on trunk and spinal stability. While they have collected trunk and pelvic motion in the past, one of the shortcomings of their work was the absence of a direct measure of the upper extremity motion. This motion and the motion of the external load creates the moment of force being compensated for by trunk muscle activation. A direct measure of this motion would provide more detailed information of the interactions between upper extremity motion and the EMG patterns throughout the task. As well, they have assumed the position of the load did not vary substantially from trial to trial. Up

until this point, the moment acting about the spinal-pelvic juncture has been assumed and controlled through instruction and control but no direct measure has been taken.

This study used 3-D motion capture to record the motion of the torso and upper extremities during the four different load transfer tasks used in the studies performed by Hubley-Kozey at al. The motion tasks are part of a series of tests developed to assess differences in healthy and sub-acute low back injured populations (Butler et al., 2007, 2009). These tasks were performed in an erect posture during which the participants lifted and moved a standardized load during 2 conditions of reach (normal and maximum) and two conditions of motion, first in the sagittal plane and second on the horizontal plane. During these movements the participants are asked to minimize the motion of the trunk and pelvis. This was done to minimize the change in moments created by the motion of the individual's trunk. Until now, the Flock of Birds (FOB) system has been the only means used to assess trunk and pelvic motion. The purpose of this study was to develop a model to quantify the 3-D kinematics of the upper limb, trunk and pelvis during these four standardized load transfer tasks. This will provide the basis for a more complete analysis of the similarities and the differences between the study groups with respect to trunk and pelvis stability. Healthy participants between the ages of 18-35 were recruited to perform a one-day repeated measures protocol. The age range was selected to reduce any age-related changes to the motion patterns. Participants were asked to perform the lifting tasks under 2 instructional conditions, freestyle and standardized, to assess the effect motion control and instruction had on the motion of the trunk. The information collected allowed for the creation of the average linear and angular movements patterns

of the general healthy population when performing the four tasks. The proposed study had four primary objectives:

1. Determine the differences between the FOB and Qualysis motion tracking systems as they record the motion of the trunk and pelvis.
2. Measure and document the angular displacement time graphs about the lower back & upper extremity for the healthy population throughout the four lifting conditions.
3. Document the linear movement patterns of the lifting load during the four conditions.
4. Examine the effect that instruction and control has on the four conditions.

(Freestyle vs. Standardized)

Chapter 2: Literature Review

2.1 Literature Review

Kinematics is the field of biomechanics that describes human motion, without regard for the causes of the motion. Often referred to as the “geometry of motion”, kinematic principles have been used in many scientific disciplines as a means of observing and recording the angular or linear motion of an object of interest (Pozrikidis, 2009; Zatsiorsky, 1998). In order to easily collect and observe the motion, the trajectory of the object of interest in either two or three-dimensional space is recorded. When the measurement duration or the temporal measurement increment is recorded, other differential properties such as the velocity and acceleration of the object can be calculated as well. These common principles allow biomechanists to describe the motion of the human body.

Many systems have been used to collect motion over the years: stroboscopic photography, movie cameras, TV picture analysis, TV signal analysis, chronocyclographical measurement, polarised light goniometer, the "Selspot" system, parallelogram goniometers, exoskeleton goniometers (Kozey et al., 1997; Rowe et al., 2001; Stanic et al., 1976). Early motion capture methods used to collect motion tended to be restrictive and generally inaccurate, limiting the number of degrees of freedom which could be described accurately (DiFranco et al., 2001). The earliest method of collecting kinematics involved taking a series of pictorial images of the activity of interest, a process known as chronophotography. This process first arose in the late 1800's with its main restriction being that it was incredibly time consuming (Al-Zahrani et al., 2008). It

also only allowed researchers to examine joint angles in two dimensions. Many of the early studies performed used this method to analyze gait patterns of pathologic populations, while advancements in the methods used to collect the kinematic data continued.

Two types of motion capture systems are currently commercially available, the optical and magnetic (Bodenheimer et al., 1997; Maletsky et al., 2007; Meskers et al., 1999). It is generally accepted that the optic systems are more accurate than their magnetic counterparts (Maletsky et al., 2007) but this accuracy comes at a cost as they tend to be more expensive systems to purchase. Camera system setups can use a single or multiple cameras depending on the size number of dimensions and the field of view needed to collect the activity of interest and the desired accuracy. These motion capture systems simplified the amount of data processing required while multiple camera set-ups allowed researchers to examine activities in the third dimension. Early optical systems used passive reflective markers to reflect infrared light back at the camera recording, similar to the Qualysis “Proflex” camera system (Model number: MCU 240, Gothenburg, Sweden). These systems were limited by the fact that they had to be in proper lighting (i.e. laboratory, staged setting) to reliably detect the markers. The markers also needed to be labeled manually once the data collection was complete, a task that could become quite tedious depending on the number of markers involved in the experimental set up. For these reasons, systems like the Vicon and Qualysis are known as passive camera systems.

More recent models of optical motion capture systems, like the Certus (Northern Digital Inc., Waterloo, Canada), utilize multiple cameras to track active light-emitting markers with much higher accuracy than the magnetic or passive systems (Maletsky et al., 2007). Both the passive and active optical systems, use the method of triangulation to calculate the three dimensional location of any number of markers with reference to a fixed global coordinate system (Bodenheimer et al., 1997). The active systems are, however, still limited by their requirement of being in a clinical setting. They also require a number of cables to link the markers for experimental set up.

Both active and passive systems allow for the calculation of “imaginary or virtual” markers with reference to “smart triads” of three non-collinear markers (Wang et al., 2009). Assuming the object being tracked is a rigid body allows for anatomical landmarks occluded from the view of the cameras to be estimated in space, as long as the three non-collinear markers are visible to the camera. This is because the smart triad forms a local coordinate system, a set of 3 orthogonal axis found within the pre-established global coordinate system. By knowing the location of the anatomical landmark with respect to the local coordinate, the system is able to calculate the location with reference to the global coordinate axis as long as the three triad markers forming the local coordinate system are in the field of view of the cameras and visible. By placing enough markers on a subject, the researcher is able to generate a human animation (Bodenheimer et al, 1997). This holds major implications for those interested in creating models of multi-linked systems in space, as it allows for fewer markers to be used when developing more complex models, such as the human body.

Biomechanists use motion capture systems to create functional activity models about the nature of human movement. These movement analyses show potential to become important tools when assessing orthopedic and neurological disorders in the clinical setting (Gage & Novacledi, 2001; Mercer et al., 2006; Park & Chaffin, 1974; van Andel et al., 2008; Whiting et al., 1988). Much has been done in the past to establish the use of gait analysis in treatment of conditions of the lower extremity (LX) (Gage et al., 2001), perhaps because of the general interest in the area of mobility, which leads to independence. The opposite is true for the upper extremity (UX), which has largely been neglected due to its multi-joint anatomy and high degrees of freedom when compared to the LX. The limited studies that have been done have focused on the kinematics of activities of daily living (AODL) (van Andel et al., 2008) in hopes of establishing UX analysis reports similar to those created for the LX (Veeger & Yu, 1996). Earlier work was performed before the introduction of active motion capture systems and their “imaginary” markers, therefore limiting the ways of describing the many degrees of freedom of the UX, resulting in the over simplification of many of the models created (Whiting et al., 1988). Imaginary or virtual markers have allowed for more complex rigid body models of the human body to be created that allow for anatomically relevant kinematics to be calculated. A methodology for standardizing the calculation of the anatomical co-ordinate systems and resulting angles was needed in order to allow for easy communication between researchers. Thus, the Standardization and Terminology Committee (STC) of the International Society of Biomechanics presented their recommendations for this process (Wu et al., 2005). These recommendations have provided a basis from which researchers can continue to create standardized models of

human motion, which can then be used to help researchers gain more insight into the pathologies that effect human movement, such as lower back injury. More importantly, the efforts for standardization have been focused on making inter-lab comparisons easier and more reliable.

Research has been performed in the field of biomechanics and ergonomics to establish a relationship between lifting technique and lower back injury (Marras et al., 2009; McClure et al., 1997). Much of this research has tried to quantify the moments about the lower back and hip in hopes of finding the cause of the high precedence of back injury in the workforce (Park et al., 1974), something that is not an easy task when one considers the number of joints involved in that area of the body. Interest in the problem continues to grow as worker's compensation claims and lost worker hours increase. With a staggering 31.6% of work place injuries involving the back in Nova Scotia alone (Workers' Comp. Board of Nova Scotia, 2011), it is understandable why there is still a great amount of interest and time put into finding the causes of these injuries to help prevent them in the future.

Much of the early work performed before the 1970's focused on difference in techniques and the different effects they have on the load being placed on the lower spine. Since the 1930's, studies have attempted to quantify a range of values from joint pressures (Hodges et al., 1999) to abdominal muscle force outputs (Park et al., 1974) in hopes of understanding the high incidence of injury in the work force. This research recommended that all lifting should be performed with the back in a straight, near vertical, position with the knees bent. The basis of this recommendation is that it shifts

the stresses from the lower back. This assertion has since been proven true for certain conditions but not all (Wrigley et al., 2005). When the load being lifted is placed close to the feet, the recommended technique is in fact more effective at reducing the moment in the lower back, but was shown to create a 50% greater moment when the load was held away from the body (Park et al., 1974). Further research examining the physiological cost of bent knee technique showed it to be far more physiologically taxing than the “free-style” lifting teaching and therefore less efficient for those in an industrial setting to perform (Garg et al., 1985). The National Institute of Occupational Safety and Health (NIOSH) developed a lifting guide in 1990’s with hopes that it would be applied to the gross population of manual workers (Waters et al., 1994). The guide featured an equation for lifting that took into account many of the risk factors identified in previous work, such as load, load distance and number of lifts performed. This guide and its derivatives remain one of the most applicable aids in helping deter workplace lower back injury.

Recent research has looked at the activity response patterns of the trunk muscles when forces are applied to the back (Butler et al., 2007, 2009, 2013). They examined the physiological alterations in the trunk musculature as an objective marker of recovery that could provide insight into re-injury mechanisms (Hubley-Kozey et al., 2014). Their rationale for doing so stems from previous theoretical (Panjabi et al., 2006) and modeling research (Cholewiak and McGill, 1996), which has linked trunk neuromuscular alterations to mechanical spinal instability and lower back injury. When the spine and body are in a neutral posture, the passive components of the musculoskeletal system, the ligaments and bone, are vulnerable to forces that exceed their injury thresholds. The active components

of the musculoskeletal system are the muscles, which provide active joint stiffness that increases joint stability while an individual is in a non-neutral position. The act of lifting an object at a horizontal distance from the spinal pelvic juncture creates a moment that in turn increases the internal forces acting on the body. A longer horizontal moment arm theoretically will result in a greater internal force acting on the lower back, increasing the risk of injury. While the structural anatomy of the spinal ligaments and bone provide a great amount of resistance to force, the muscles are the only active tissue to stop tissue failure and injury from occurring.

The active components in the torso are the abdominal and back extensor muscles. These muscles respond to any added forces through agonist and antagonist co-activation, therefore increasing active stiffness and enhancing spinal stability (Cholewicki and McGill, 1996). The research by Hubley-Kozey et al. (Butler et al., 2009, 2013) has examined the activation patterns of these different muscles to better understand any differences between the healthy and the lower back injured populations. To do so, they used an electromyogram (EMG) to record the temporal activity patterns of a comprehensive set of twenty-four trunk muscle sites while participants performed a series of tasks that would require the activation of the trunk muscles. Forces were created by having the participants perform symmetrical and asymmetrical lift and replace tasks, which alternated sagittal and frontal plane moments (Butler et al., 2009, 2013). These muscles were required to counter balance the dynamic moments produced by the lifting tasks. By comparing the relative amplitudes of the two population groups, they found that an altered muscle activation pattern is present in individuals who have endured a lower back injury, even when the individual was deemed recovered (Butler et al., 2013). This

suggests that residual muscle activation alterations may remain even after symptoms dissipate.

During these studies the motion of the trunk and pelvis were monitored using a Flock of Birds (FOB) electromagnetic system, which provided 3-D angular measurements of the two segments. While the motion of the upper extremities was not monitored, the actions were performed in a standardized, timed fashion. Standardizing the time was done to control the acceleration of the load and upper extremities and resulting moment of force on the spine between participants. Participants were also required to keep their trunk and pelvis stationary to further restrict any additional moments being introduced to the subject's spine. In the past, the FOB has been important in its role to ensure there was not more than 10 degrees of motion in these segments and if so, the trials were repeated (Butler et al., 2009, 2013). This standardization would reduce some the inter-subject variability but does not provide the detailed upper extremity kinematic patterns of each participant. Nor does it allow for the calculation of the motion kinetics moments about each joint center. In the future, having this information, along with other time derivatives such as velocity and acceleration, will help to explain some of the differences between the healthy and low back injury groups.

2.2 Summary

Based on the review of the related literature, the proposed study looked to extend the current research conducted in the Neuromuscular Function Laboratory at Dalhousie University lab by quantifying the complete upper extremity kinematics of the lifting tasks used in the lower back injury studies (Butler et al., 2002, 2009, 2013). Until now, electromagnetic sensors (Butler et al., 2013) have been used to record the movement of the relative motion of the pelvis and torso during the lifting tasks. The subjects were asked to maintain as erect a standing posture as possible throughout the trials. The electromagnetic sensor was used to ensure this, with any trials with an overt violation of over 10 degrees of trunk motion being redone. The position of the arms during the trials was not recorded, but was controlled using the placement of the lifting load and resulting reach required for each participant to lift it.

The proposed study looked to compliment the electromagnetic sensors with passive optic tracking to produce a more robust representation of the movement patterns present during the lifting tasks. Video camera technology was used to track the upper extremity as an open chain rigid body model from which the joint angles at each juncture was calculated and normalized for the activity. The system also tracked the linear movement of the load in three-dimensional space in order to establish a linear movement pattern for each of the four conditions. Based upon the review of relevant literature this project set out to determine the extent to which the angular measures of the pelvis and trunk would be in agreement or not. As well the project attempted to document the effect the movement controls had on the temporal and kinematic patterns of the four tasks.

Chapter 3: Methods

3.1 Study Design and Location

The research project used a repeated measures design involving the collection of the motion from the upper extremity, trunk and pelvis during four functional lifting tasks. The design of the study allowed for the measurement of the linear and angular movements patterns of a sample of individuals who had not experienced a low back injury within the 12 months prior to testing. The load transfer tasks are part of a series of tests developed to assess differences in healthy and low back injury populations (Butler et al., 2002). The lift and transfer tasks were performed in both a normal and maximum reach to create varying joint moments about the subject's spine in both the transverse and sagittal planes. These moments must be counterbalanced through internal forces achieved through activation of specific trunk muscles which relates to the level of activation required from the musculature. All testing was performed at the JAR Musculoskeletal Research Suite, School of Physiotherapy of Dalhousie University, Halifax, Nova Scotia.

3.2 Participants

The study sample consisted of 20 individuals of both sexes (M 17, F 3) between the ages of 18-35 years. Ethics approval was obtained prior to participation which including screening each participant to ensure they had no acute or chronic health conditions which would affect their ability to perform the functional lifting tasks. In general, individuals who fit the age range and were asymptomatic of injuries or pain in the upper extremities, back and pelvis were deemed eligible to participate. Participants

were deemed ineligible if they (a) were not between the ages of 18-35; (b) had answered, “yes” to any of the questions on the Initial Screening Questionnaire (Appendix A); which covered general health issues as well as impairments of the back and upper extremity. Recruiting for the study was performed through flyers and word of mouth at Dalhousie University and the surrounding Halifax community.

3.3 Experimental Protocol

The testing consisted of one session of data collection, taking approximately 60-75 minutes per participant (Table 1). Potential participants, upon providing notice of interest, received a copy of the study’s Informed Consent Form and Initial Screening Questionnaire via email prior to attending the testing session. They were told to review each of the forms completely to ensure they were willing and eligible to complete the study. If they found themselves unwilling or ineligible, they were thanked for their time and all information collected from the individual was destroyed. Potential participants who passed the initial screening were scheduled to perform the one-day testing, while still being informed that they could withdraw consent and not participate at any moment’s notice.

Table 1. Visual representation of the data collection procedure.

Day 1	TIME (minutes)									
	Preparation	Condition 1 (No Instruction)	Condition 2 (No Instruction)	Condition 3 (No Instruction)	Condition 4 (No Instruction)	Condition 1 (Instructed)	Condition 2 (Instructed)	Condition 3 (Instructed)	Condition 4 (Instructed)	Debrief & Marker Removal
	0:00- 0:20	0:20- 0:25	0:25- 0:30	0:30- 0:35	0:35- 0:40	0:40- 0:45	0:45- 0:50	0:50- 0:55	0:55- 1:00	1:00- 1:15
Informed Consent, Set Up										

When the participant arrived for testing, their initial forms were reviewed to ensure that all concerns and questions were handled prior to the commencement of testing. Once consent was obtained, the participant was prepared for collection by placing reflective markers on the necessary anatomical landmarks of the torso and upper extremity (Table 2). The electromagnetic Flock of Birds (FOB) sensors used in the previous experiments (Butler et al., 2002, 2009, 2013; Hubley-Kozey et al., 2014) were kept in the same trunk and pelvic locations as the previous studies (Butler et al., 2009, 2013) and were placed on the same plastic plates as the rigid body markers for the Qualisys system. The marker locations selected were based on the recommendations from the International Society for Biomechanics as presented by Wu et al (2002, 2005) for the upper extremity and trunk.

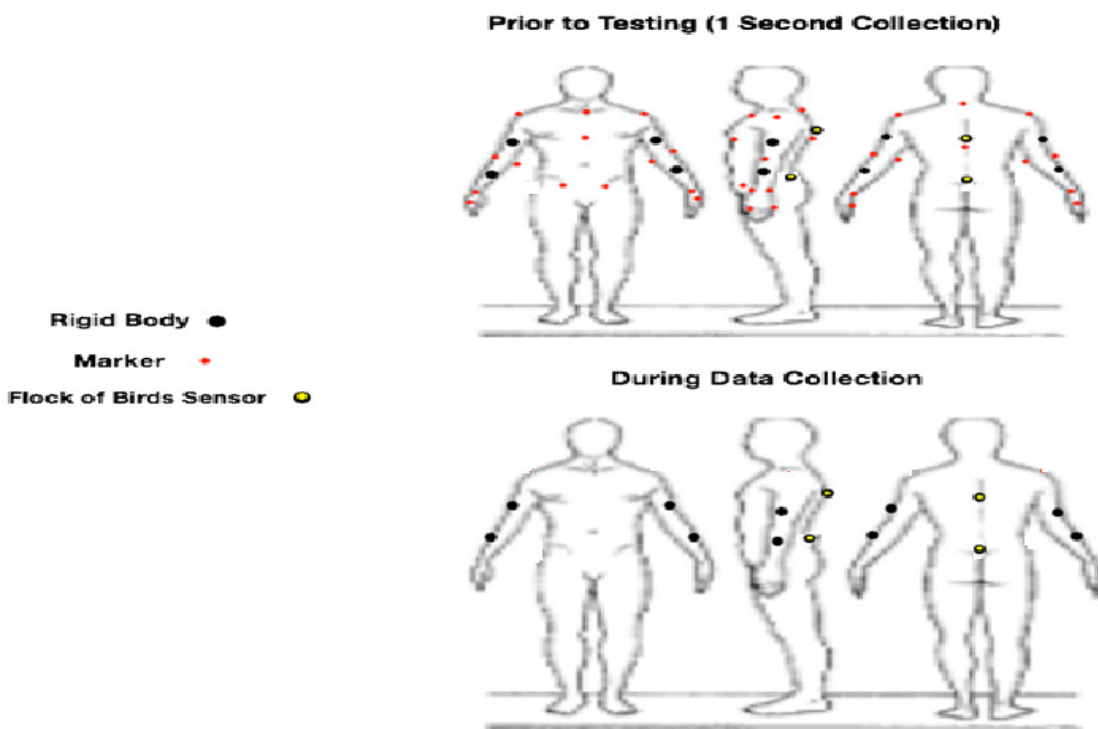


Figure 1. Visual portrayal of the placement of the six triads and twenty markers being used to create the upper body model.

The participants were prepared for measurement of the Qualysis system by placing clusters of four reflective markers, known as rigid bodies, on the posterior surface of the pelvis and thoracic spine, and bilaterally over their humerus' and forearms. The rigid bodies were attached using double-sided adhesive tape and an elastic strap. Rigid bodies were placed on the lateral aspects of the arm and forearm bilaterally. The rigid bodies gave reference to an additional 20 relative markers (Table 1, Figure 1) that were present for a short stationary calibration trial prior to collection, but were removed prior to any experimental trials. For any markers that couldn't be placed directly over the anatomical landmark, a digital prober with a pointer was placed on the location manually, thus allowing the landmark to be calculated with reference to the rigid body without the presence of a reflective marker. The markers chosen made it possible to create anatomical coordinate systems (ACS) within the body segments in order for their orientations to be calculated relative to one another in three-dimensional space. This subsequently allowed for the calculation of the joint angles about the torso, shoulder and elbow at any given frame of time. Prior to each data collection, a static calibration of the Qualysis system was performed and the RMS error was calculated. This was followed by a static recording of the participant in a static, normalization pose.

Table 2.List of bony landmarks represented by virtual marker placement

RIGID BODY (Attachment)	VIRTUAL MARKERS	DESCRIPTION
Pelvis (Sacral)	1) RASSIS: right anterior superior iliac spine 2) LASIS: left anterior superior iliac spine 3) MID-PSIS: mid-point of left and right posterior superior iliac spine (Located on Pelvic Rigid Body)	- Skin surface point at the anterior-superior iliac spine. Located by palpating proximally on the midline of the anterior thigh surface until the anterior prominence of the iliac spine is reached. - Skin surface point at the posterior-superior iliac spine. This landmark is located by palpating posteriorly along the margin of the iliac spine until the most posterior prominence is located on either side of the sacrum. The middle point between these two locations.
Thorax (T6-T10)	5) C7: processus spinous 7 th cervical vertebra 6) T10: processus spinous 8 th thoracic vertebra 7) PX: processus xiphoideus 8) IJ: incisura jugularis	- Skin surface point at the most posterior aspect of the spinous process. - Skin surface point at the inferior margin of the sternum on the midline. - Skin surface point at the superior margin of the jugular notch of the manubrium on the midline of the sternum.
Humerus (2)	9) LE: lateral epicondyle (2) 10) ME: medial epicondyle (2)	- Skin surface point at the most lateral aspect of the humeral condyle. - Skin surface point at the most medial aspect of the humeral condyle.
Forearm (2)	11) RS: radial styloid (2) 12) US: ulnar styloid (2) 13) 2M: head of the 2 nd metacarpal (2) 14) 5M: head of the 5 th metacarpal (2)	- Skin surface point at the most caudal & lateral point of the radius - Skin surface point at the most caudal & medial point of the ulna - Skin surface point at the most caudal & lateral point of the 2 nd metacarpal - Skin surface point at the most caudal & medial point of the 5 th metacarpal
Extra Markers	15) AC: Acromion Process (2)	- Skin surface point obtained by palpating the most anterior portion of the lateral margin of the acromial process of the scapula.
Flock of Birds Sensors	16) Pelvis 17) Thorax	- Will be attached to the pelvic rigid body placed over the sacrum - Will be attached to the thoracic rigid body placed on the T6-T10 region approximately

The participant, after being prepared for data collection, was positioned in front of the load-lifting table and was asked to stand erect with their arms at their sides; elbows flexed approximately 90 degrees, with their forearms parallel with the table surface, as shown in the left picture of Figure 2. The table surface was adjusted to ensure that the participant's forearms remained in this "normal reach" position while the hands gripped the handle of the load being transferred; a 2.9 kilogram paint can (Butler et al., 2013), which was resting on top of the table. The weight chosen was selected to avoid fatigue and was based on the recommended weight limit (Waters et al., 1994) for the 5th percentile female extreme reach distance. The load and handle had a combined height of approximately 30 centimeters. A motion trigger was placed directly in front of the participant, providing researchers live feedback as to whether the participants were lifting the load to the appropriate height during the trials and allowing the moment of transfer between hands to be recorded during the transfer tasks. A pressure trigger was located on the base of the load to allow for the starting and finishing times for each of the trials to be recorded. This allowed for the trials to be compared relatively as a percent completed from 0-100%.

Once the table was at the appropriate (elbow) level, the four lifts were performed twice during two different instructional conditions. First, the participants were asked to perform three trials of each of the four tasks listed below, without receiving any direction other than to lift the load high enough to break the motion sensor and to follow the cadence of the instructor while lifting. This first condition was known as

the “Freestyle” condition, and was succeeded by a further three trials of each of the four conditions, with the exception that their motion was controlled with instruction and instruments. This second condition was called standardized and always followed the freestyle trials. At this point, trials were repeated if the trial was performed out of cadence or if there was excessive trunk or pelvic motion recorded by the FOB system. The participants were also instructed to maintain an erect body posture with as little movement of the trunk and pelvis as possible. A vertical jig was placed over the participant’s mid thoracic spine to help provide proprioceptive feedback throughout the trials. A noticeable failure in performing this condition resulted in the trial being repeated. In total, there were two lift conditions – a symmetrical lift and replace in the sagittal plane and a lift and transfer in the horizontal plane from the right side to the left side of their bodies. Each of these lifts were performed in the normal reach and the maximum reach.

Two of the four lifting tasks consisted of lifting and replacing the load in the normal and maximum reach positions as shown in Figure 2. This symmetrical lift and replace used both hands simultaneously. The other two lifting tasks involved the load being lifted and moved horizontally across the front of the body in the same two reach positions (Figure 4) during both instructional conditions.

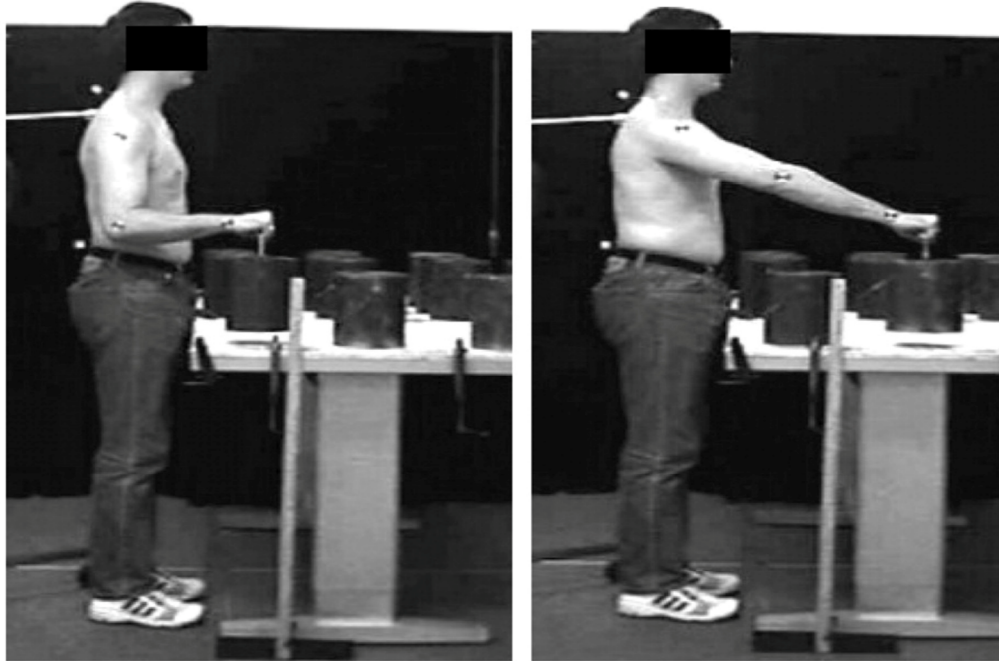


Figure 2. Sagittal view of the two reach postures for the four lifting tasks

1. Lift & Replace Normal Reach (LTN)

The subject maintained the bent arm position used in the table height calibration and bent-arm transfer, with the load placed directly underneath their hands. They had the lift demonstrated and were informed of the task's three-second cadence. The participants started standing with their hands at their sides, grabbed the load handle on the one count, lifted the load 5 centimeters above the table surface during the two count and placed the load back on the table during the third count. The motion sensor (Figure 3) facing the subject provided audio feedback to the subject when the load reached the necessary vertical height.

2. Lift & Replace Maximum Reach (LTM)

The subject was directed to extend their arms horizontally over the table as far as possible while maintaining an upright trunk position. The load was placed under their hands on the table. Once the load position was established, the tester demonstrated the lift to the subject and informed them of the three-second cadence used for the trials. The participants started with their hands at their sides, placed them on the load handle during the one count, lifted the load over 5 centimeters during the two-count and placed the load back on the table during the third count. The motion sensor (Figure 3) facing the subject provided audio feedback to the subject when the load reached the necessary vertical height.



Figure 3. The experimental set-up and lifting height required for the two lifting conditions. Note that the subject is in the maximum reach position and would have their elbows at 90 degrees during the normal reach condition, even though the lifting height did not change for either condition.

3. Horizontal Transfer Task Normal Reach (HTTN)

The participants transferred the load, using the same normal reach position used in the table height calibration for the lift and replace task, at a 60 degree angle from the patient's right hip as determined by a line on the table originating directly in front of the subject. They had the lift demonstrated and were informed of the condition's five second cadence. The participants started standing with their hands at their sides, grabbed the load handle on the one count, lifted the load between 2-5 cm off the table and about halfway from the start position to directly in front during the two-count, then transferred the load directly in front of them during the three count. Also on the third count, the participants transferred the load from their right hand to their left hand while ensuring that the can

was low enough to the table that it causes the motion sensor to provide audio feedback, then transferred the load to the three quarters complete position during the fourth count. The fifth count consisted of them placing the load on a line on the subject's left side that mirrored the 60-degree starting line. Participants were asked to keep their elbows at 90 degrees throughout the trial and the load was moved in the same right to left direction for each trial.

4. Horizontal Transfer Task Maximum Reach (HTTM)

The participants started standing with their hands at their sides with the load being placed an arm's length away, at a 60 degree angle from the patient's right hip as determined by a line on the table originating directly in front of the subject. The lift was demonstrated and they were informed of the condition's five-second cadence. The participants started with their hands at their sides; grabbed the load handle during the one count, lifted the load between 2-5 cm off the table and about halfway from the start position to directly in front during the two-count, then brought the load directly in front of them during the three count. Also on the third count, the participants transferred the load from their right hand to their left hand while ensuring that the can was low enough to the table that it causes the motion sensor to provide audio feedback, then brought the load to the three quarters complete position during the fourth count. The fifth count consisted of them placing the load on a line on the subject's left side that mirrored the 60-degree starting line. The participants tried to maintain an extended arm throughout the trials and the load was moved in the same right to left direction for each trial.

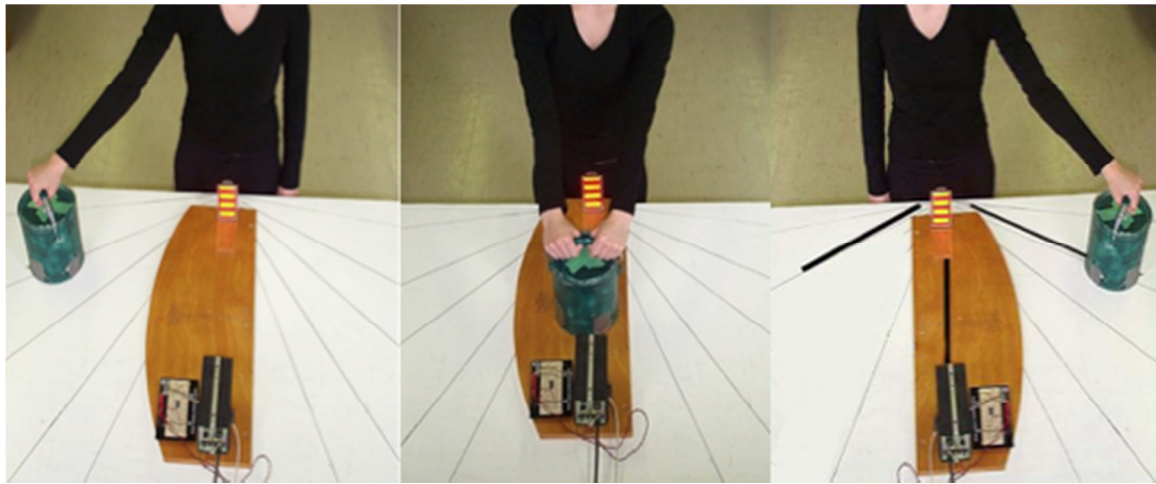


Figure 4. Shown above are the one, three and five second positions, in appropriate order, for the horizontal transfer task. Note the 60 degree starting and end lines located on the table, which will be used for both reach conditions of the transfer task to control the start and end positions of the load for each participant.

3.4 Data Collection

The motion data from the lifting tasks was collected using a Qualysis “Proflex” motion capture system (Model number: MCU 240, Goteborg, Sweden). A Flock of Birds Motion Capture™ system was used to record the absolute motion of the pelvis and trunk. The 6 Qualysis cameras were strategically placed around the laboratory to allow for a field of view that would capture motion in both the sagittal and frontal planes of the participant while they performed their trials. The system allowed for the reflective markers to be tracked in space with an accuracy of 0.1 mm and a resolution of 0.01 mm, this was confirmed prior to each collection by performing a static calibration and calculating the RMS and ensuring it was consistent. The global coordinate system axis’ (GCS) was located on top of the table in front of the subject and was established prior to the participant arriving by placing a square rigid body in its location. It was aligned in the same place relative to the FOB GCS for each participant. The multi camera system

tracked the three-dimensional position of the six marker rigid bodies highlighted in Table 1. A marker was also placed on top of the lifting load to record its three-dimensional trajectory throughout the trials. The position of these markers during each trial was sampled at 100 Hz using the Qualysis Track Manager (QTM) software.

3.5 Data Analysis

After the data collection, all the kinematic data was plotted and reviewed by the author for completeness and reasonability checks. When deemed complete, the data was filtered, using a 6 Hz Low-pass fourth order Butterworth filter that removed any high frequency noise from the data (Winter et al., 1974). For the FOB comparative analysis, both the FOB and Qualysis data were filtered using a 1 Hz Low-pass fourth order Butterworth filter. The Qualysis data was then windowed using the trigger data and time normalized for it to be comparable between participants. The now filtered, windowed and normalized data was used to calculate the absolute and relative joint angles of the upper extremity, as well as the linear displacement patterns of the load during the four tasks.

The primary data analysis was performed on the absolute angles calculated using the Flock of Bird and Qualysis systems with respect to the pelvis and trunk. The angles were calculated for both systems using the same angular conventions. The Visual 3D software by C-Motion calculated the absolute angles of the pelvis and trunk with respect to the GCS established in the lab, while a MATLAB[®] program was used to calculate the corresponding angles from the FOB system. These angles were calculated in accordance to the recommendation's put forth by the ISB for human upper and lower extremity joint coordinate systems (Wu et al., 2002, 2005) and plotted to show the movement patterns

for the population. The maximum angular displacement (MAD) was calculated in each of the X, Y & Z-axis' for the pelvis and trunk in each trial for both systems. This was performed by subtracting the lowest angular value from the highest value achieved within the trial. Statistical Package for the Social Sciences (SPSS) software was used to perform a series of Analysis of Variance (ANOVA) tests on the MAD data to assess the variability of the two systems, as well as the effect of instruction on angle variability. SPSS was also used to perform a series of Bland-Altman Analyses to assess the agreement of the two motion capture systems.

To address the second objective of calculating the relative angles of the trunk, and upper extremities, the Visual 3D software calculated the three-dimensional relative angles of thorax, both upper arms and both forearms with respect to their adjacent segments (Figure 5). The angular motion patterns for the group of participants were collectively plotted using the Visual 3D software. The results for each participant were not normalized to a standing bias.

The third objective of recording the linear motion patterns of the load was addressed through the creation of a number of linear displacement-time graphs of the path of the load in each of the three planes of motion. These graphs are a collective of each trial performed by the sample population to show the general pattern of the load in each of the 4 tasks. Visual 3D also calculated the respective time taken to complete each trial. This data was compared statistically using a series of paired t-tests to assess the

effect that instruction may have had on the time taken to complete the tasks. This analysis was performed using the SPSS software.

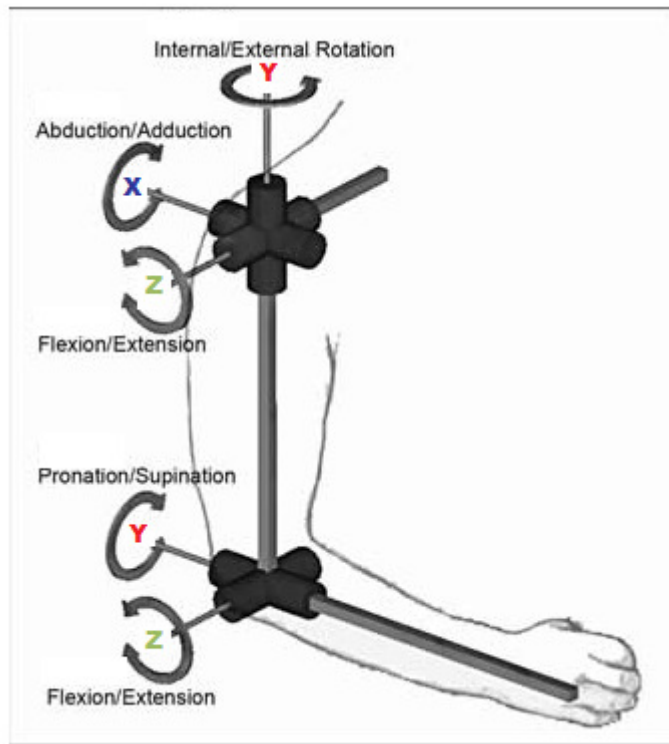


Figure 5. Proposed biomechanical model detailing the degrees of freedom being examined at both the shoulder and elbow joints. (Abdullah et al., 2007)

3.6 Summary and rationale for the methodology

The proposed study looked to improve the understanding of the linear and angular motion patterns present in the healthy population while performing four upper extremity lifting tasks. It aimed to build upon previous research that has shown the plausibility of accurately recording the kinematics of the upper extremity. This study laid the groundwork for future research to be performed looking at kinetic models of the four activities.

Chapter 4: Results

4.1 Qualysis & Flock of Birds Comparison

The 3-D motion of the trunk and pelvis rigid body segments were recorded simultaneously using the Qualysis and Flock of Birds (FOB) motion capture systems while participants performed a series of standardized tasks under two different conditions. The Qualysis data was processed using the Visual 3D software to calculate the absolute angles of the two segments with respect to a global coordinate system (GCS), along with the angle-time graphs shown in the subsequent figures. Matlab software was used to collect and calculate FOB absolute angles with reference to a similar GCS. The GCS' for both systems were aligned with each other in front of the participant on the experimental table.

Both Visual 3D and Matlab were used to calculate the maximum angular displacement for each angular dimension within each trial and these measures were used in the statistical comparison with all angular measures presented in degrees. To determine if there was a significant trial effect, a One-way ANOVA was performed on each data subset. No trial effect was found within participants across all angular measures; therefore, the data was collapsed to the mean of the three trials for each participant.

The remainder of this chapter will systematically present this comparative data by examining the trunk and pelvis segments in individual sub-sections. Within each sub-section, there will be tabular presentation of the MAD data for FOB and Qualysis systems, as well as graphic presentation of the angular displacement-time data collected

by Qualysis. Within each sub-section, a statistical comparison of the angular MAD of the two sensors (FOB vs. Qualysis) and condition (Freestyle vs. Standardized) was performed using a series of univariate General Linear Model analyses. The analyses were performed on both body segments (trunk & pelvis) in all 3 degrees of freedom for each of the 4 experimental tasks; therefore the test was performed 24 times. Prior to the GLM analysis, a Shapiro-Wilk test for normality was performed and when necessary corrections were made using a log transformation. The general form of the overall GLM model is described in equation 1:

$$\mu = \text{Constant} + \text{Subject} + \text{Sensor} + \text{Condition} + \text{Sensor} * \text{Condition} + \text{error} \quad [1]$$

For all tests the critical α was set to 0.05. Each ANOVA analysis is accompanied with a contrast graph between the experimental variables. These graphs present the results of each sensor in different lines with condition in two separate columns. The effect of condition*sensor was found to be not significant unless noted otherwise.

In addition to the GLM analysis, a Bland-Altman comparison was performed to assess the agreement of the angular data between the two systems. The difference between the two sensors was calculated by subtracting the Qualysis angular value from the FOB. This difference was then tested for normality using the Shapiro-Wilk Test and if necessary, corrections to the data were made using a log transformation. Post normality check, for each test, a one sample T-test was performed to determine whether the sample of angular differences differed from 0. If the difference was not significant, the two devices were

considered to be in agreement. Lastly the 95% confidence interval of the difference was determined and presented graphically.

The Y-axis is the calculated difference used in performing the one sample T-test. The X-Axis represents the mean MAD calculated by the two sensors. The graphs include a solid black line representing the mean of the differences calculated between the two systems. The dotted red lines represent the upper and lower limits of the 95% confidence interval. The dotted blue line represents “0” in each graph. All three trials for each participant were included in the graphs.

A summary of all of the results for both the ANOVA and Bland Altman analysis’ can be found at the end of the section (Section 4.1.9). Results for the Lift and Replace Normal Reach are shown below as an example; the results for the other 3 lifting tasks can be found in Appendix A.

4.1.1 Lift & Replace Normal Reach – Trunk

Figure 6 presents a representative graph of the angular displacement patterns for the trunk as collected by the Qualysis system for the lift and replace task in the normal reach and the two instructional conditions. This graph represents all trials for all participants in this task. While there were individual differences between the participants, there was minimal motion seen within the individual trials. Shown in Table 3 are the mean and the standard deviation of the MAD values for all trunk values for the two sensors, 3 degrees

of freedom and two lift styles in the normal lift and replace task. The MAD values ranged from 0.3(0.4) to 2.3(1.3) degrees across the values.

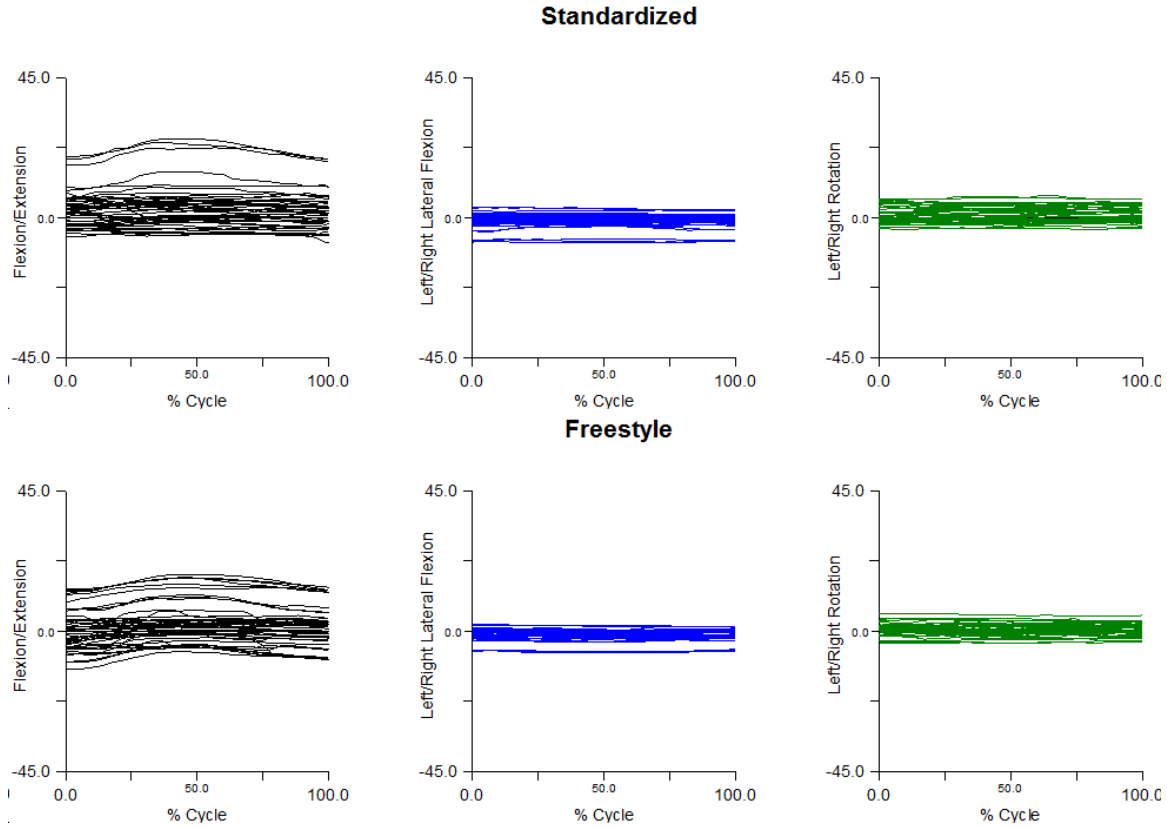


Figure 6. Angular displacement-time graphs showing the angular position of the trunk with reference to the GCS for both the standardized and freestyle conditions as recorded by the Qualysis system. Forward flexion and movements to the left are negative; Trunk extension and lateral bending to the right are positive values.

Table 3. Mean (standard deviation) maximum angular displacement (degrees) of the trunk in relation to the GCS during the normal reach lift and replace task.

	Standardized			Freestyle		
	Flex/Ext	Lat. Flex.	Axial Rot.	Flex/Ext	Lat. Flex.	Axial Rot.
FOB	2.2 (1.3)	0.7 (0.4)	1.6 (0.9)	3.1 (1.6)	0.7 (0.3)	1.5 (0.6)
Qualysis	0.8 (1.4)	0.5 (0.2)	0.6 (0.3)	2.1 (1.6)	0.4 (0.3)	0.7 (0.4)
Difference	1.2 (0.8)	0.3 (0.4)	1.0 (0.9)	1.0 (1.1)	0.3 (0.4)	0.8 (0.4)

Flexion - Extension

A univariate GLM was performed to assess the effect of condition and sensor on the MAD differences. The analysis considered the main effects as well as the interactions and the results are presented in Figure 7. There was a significant difference due to sensors ($F=19.69$, $df=1,48$, $p <0.001$). There was also a significant difference due conditions ($F=21.45$, $df=1,48$, $p= <0.001$). Overall, the means (and SE) varied from 0.9 (± 0.2) to 3.1 (± 0.2) with the freestyle condition having the greater difference in MAD values.

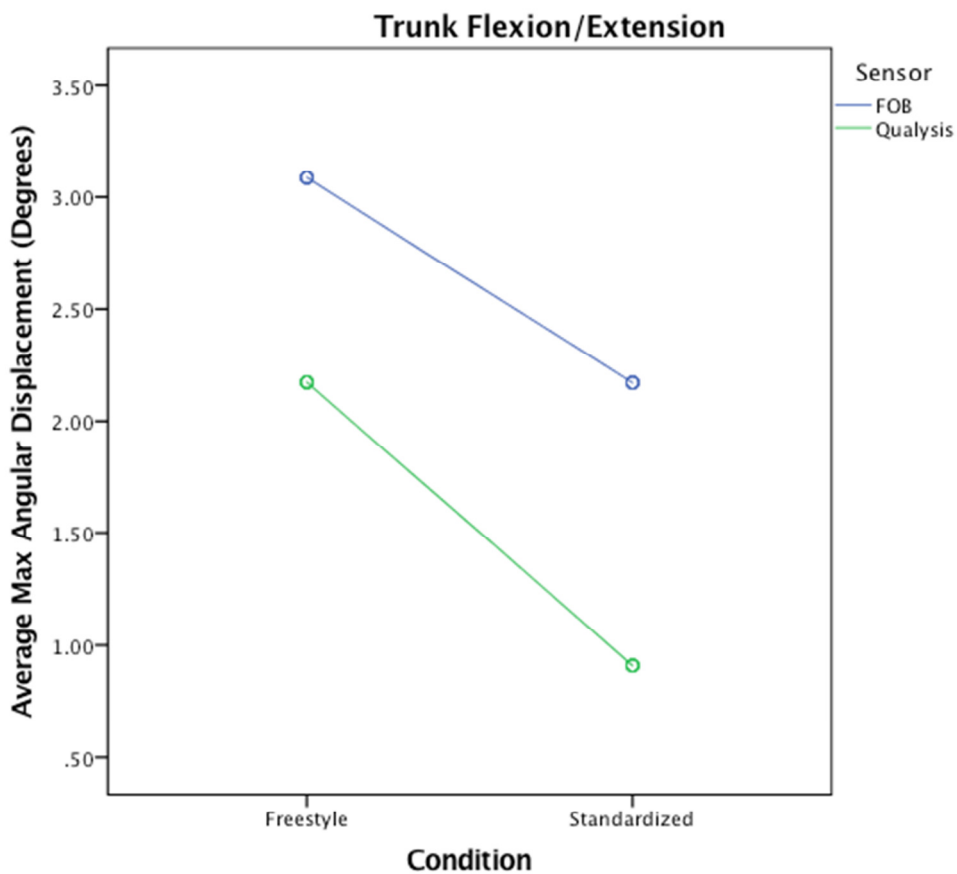


Figure 7. Graphical representation of the output from the univariate ANOVA results.

The graphical analysis of the Bland-Altman analysis is shown in Figure 8. The mean difference of 1.2 (1.0) was significant ($t= 6.75$, $df = 32$, $p<0.001$). The 95%ile confidence interval was ± 2.0 degrees.

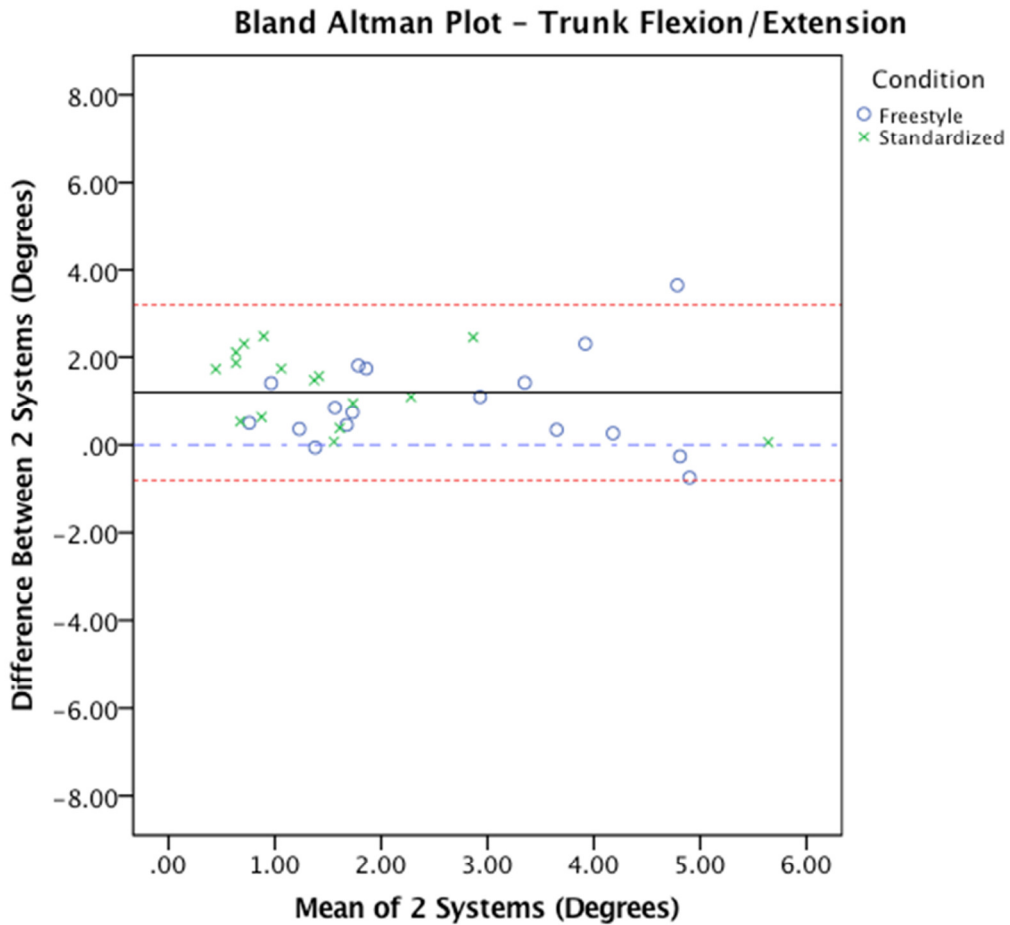


Figure 8. Bland-Altman Plot demonstrating the agreement between the FOB and Qualysis systems while recording trunk flexion/extension during the lifting task normal reach task.

Lateral Flexion

A univariate GLM was performed to assess the effect of condition and sensor on the output. The analysis considered the main effects as well as the interactions and the results are presented in Figure 9. There was a significant difference due to sensors ($F=23.14$, $df=1,49$, $p<0.001$). There was no significant difference due to condition ($F=0.137$, $df=1,49$, $p= 0.713$). Overall, the means (and SE) varied from $0.4 (\pm 0.1)$ to $0.7 (\pm 0.1)$ with the standardized condition having the greater difference.

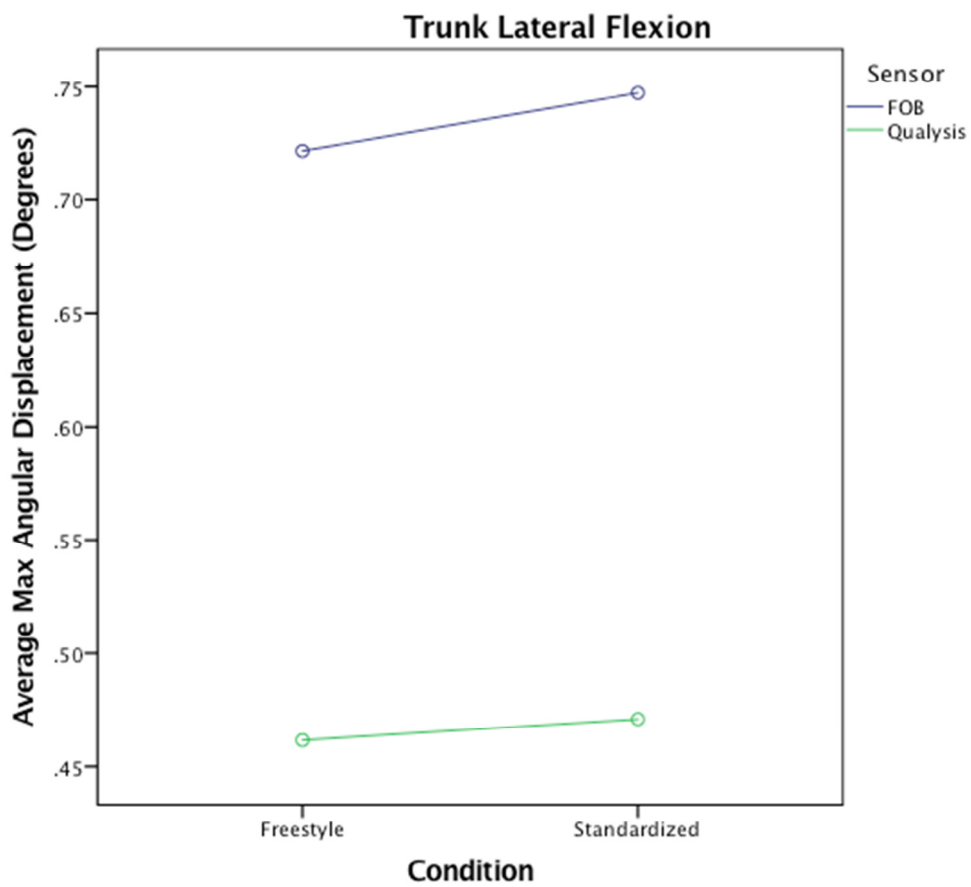


Figure 9. Graphical representation of the output from the univariate ANOVA results.

The graphical analysis of the Bland-Altman analysis is shown in Figure 10. The mean difference of 0.3 (0.4) was significant ($t = -9.4$, $df = 30$, $p < 0.001$). The 95%ile confidence interval was ± 0.8 degrees.

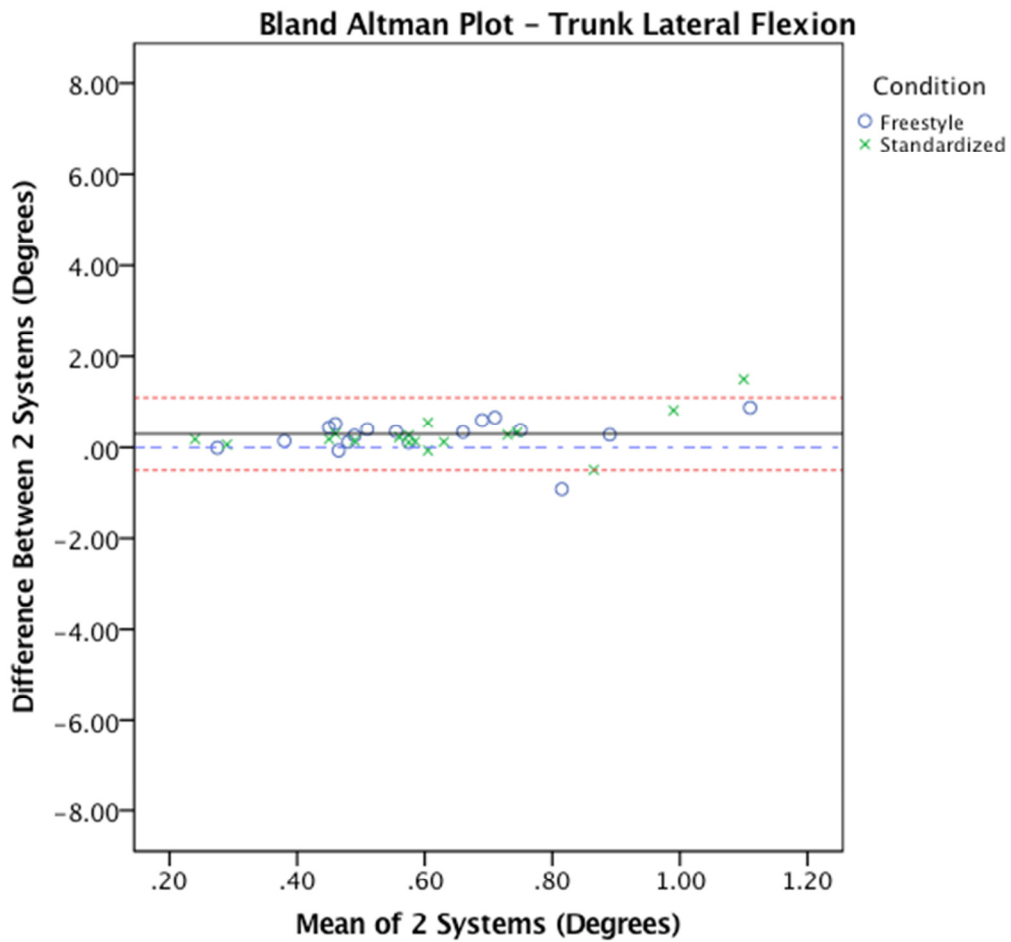


Figure 10. Bland-Altman Plot demonstrating the agreement between the FOB and Qualysis systems while recording trunk lateral flexion during the lifting task normal reach task. The dotted red lines represent the upper and lower limits of the 95% confidence interval. The solid black line represents the mean of the differences calculated between the two systems.

Axial Rotation

A univariate GLM was performed to assess the effect of condition and sensor on the output. The analysis considered the main effects as well as the interactions. Shown below in Figure 11 are the means for this data. There was a significant difference due to sensors ($F=88.59$, $df=1,48$, $p<0.001$) and no significant difference due to condition ($F=1.96$, $df=1,48$, $p= 0.167$). Overall, the means (and SE) varied from 0.6 (± 0.1) to 1.6 (± 0.1) with the freestyle condition having the greater difference.

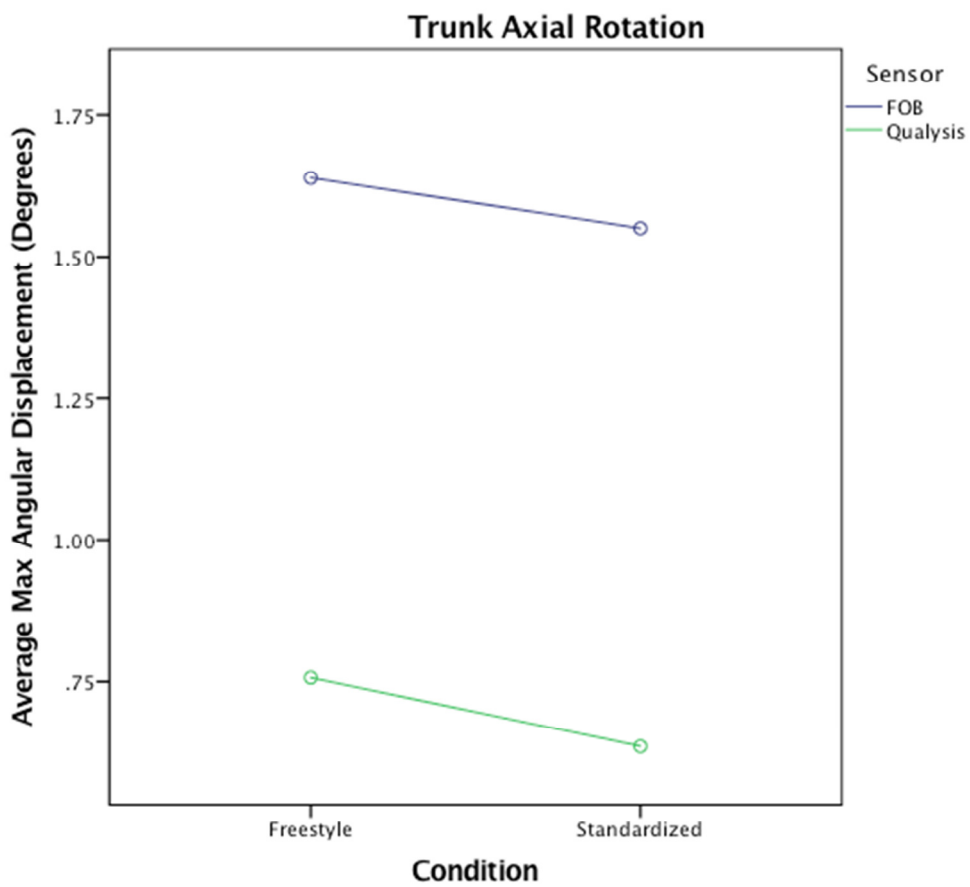


Figure 11. Graphical representation of the output from the univariate ANOVA results.

The graphical analysis of the Bland-Altman analysis is shown in Figure 12. The max angular displacement data was used once again for this comparison. The mean difference

of 0.9 (0.7) was not significant ($t = -2.7$, $df = 30$, $p=0.011$). The 95%ile confidence interval was ± 1.4 degrees.

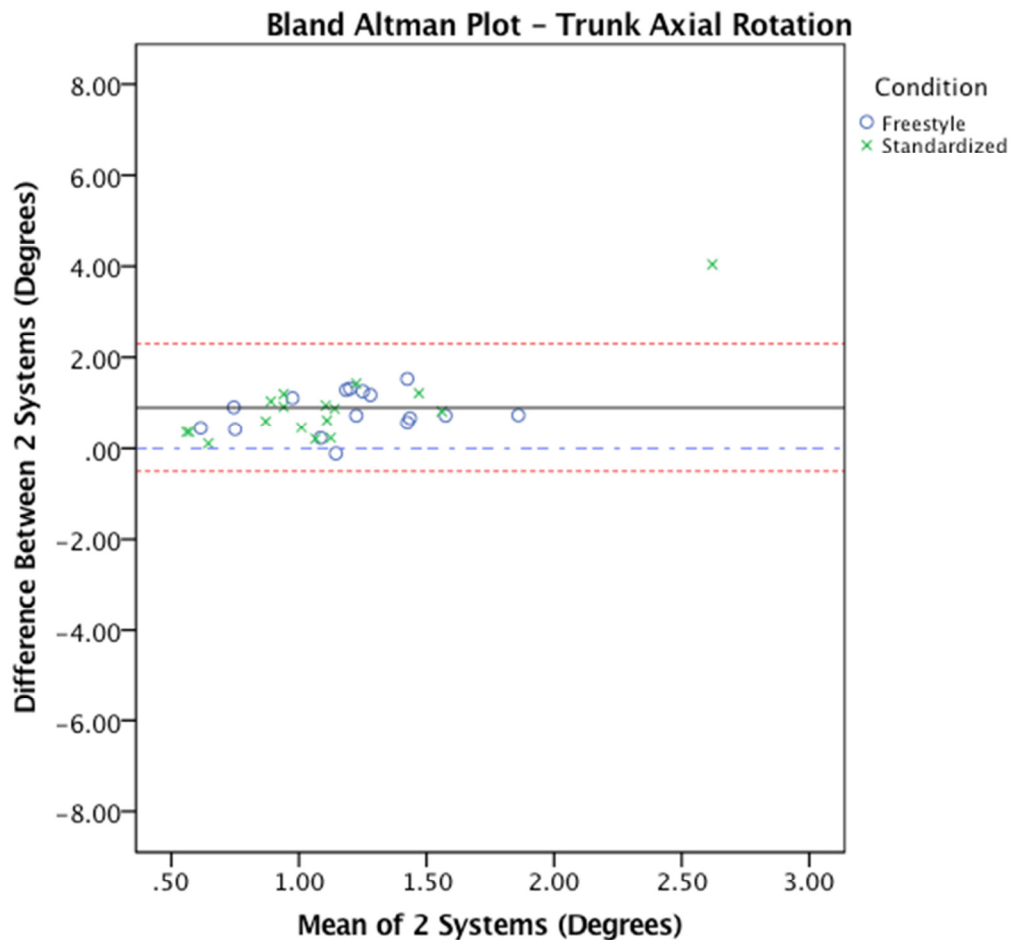


Figure 12. Bland-Altman Plot demonstrating the agreement between the FOB and Qualysis systems while recording trunk axial rotation during the lift and replace normal reach task.

4.1.2 Lifting Task Normal Reach – Pelvis

Shown in Figure 13 is a representative graph of the angular displacement patterns for the pelvis as collected by the Qualysis system for the lift and replace task in the normal reach and the two instructional conditions. This graph represents all trials for all

participants in this task. As can be visualized there was limited motion during the task. While there were individual differences between the participants, there was minimal motion seen within the individual trials.

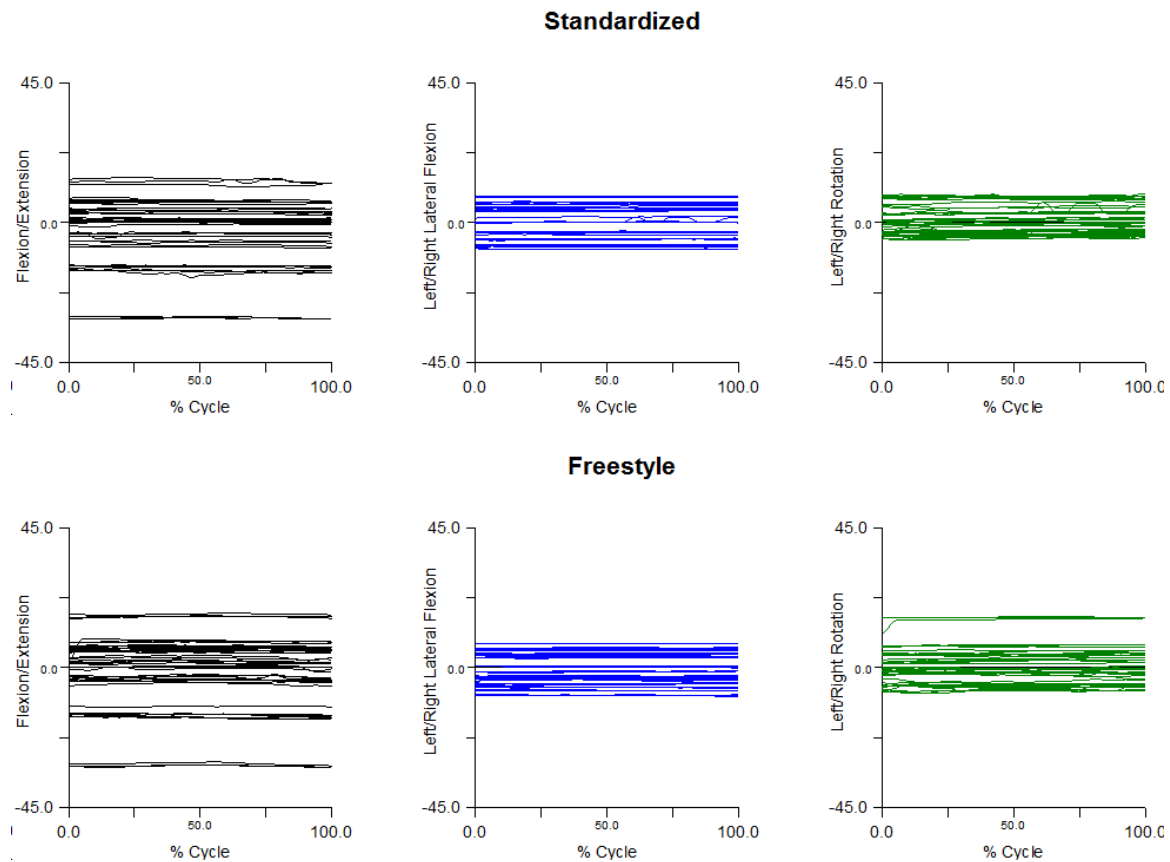


Figure 13. Angle-time graphs showing the angular position of the pelvis with reference to the GCS for both the standardized and freestyle conditions for the Qualysis system. Angles are measured in degrees. Forward flexion and movements in the left are negative values; extension and movements to the right are positive values.

The table below summarizes the MAD averages calculated by each system, separated into separate instructional conditions for comparison. The average difference between the two systems was also calculated. All units are in degrees.

Table 4. Average max angular displacement (Standard Deviation) of the pelvis in relation to the GCS during the normal reach lift and replace task. Standard deviation is included in brackets. Units are in degrees.

	Standardized			Freestyle		
	Flex/Ext	Lat. Tilt	Axial Rot.	Flex/Ext	Lat. Tilt	Axial Rot.
FOB	0.7 (0.4)	0.3 (0.1)	0.7 (0.3)	0.9 (0.5)	0.3 (0.2)	1.0 (0.6)
Qualysis	0.4 (0.2)	0.2 (0.1)	0.4 (0.2)	0.6 (0.4)	0.2 (0.1)	0.6 (0.3)
Difference	0.4 (0.4)	0.1 (0.2)	0.3 (0.3)	0.4 (0.3)	0.1 (0.2)	0.4 (0.5)

Flexion – Extension

A univariate GLM was performed to assess the effect of condition and sensor on the output. The analysis considered the main effects as well as the interactions. Shown below in Figure 14 are the means for this data. There was a significant difference due to sensors ($F=34.81$, $df=1,49$, $p<0.001$). There was no significant difference due to conditions ($F=0.125$, $df=1,49$, $p= 0.725$). There was a condition*sensor effect ($F=7.62$, $df=1$, $p= 0.008$). Overall, the means (and SE) varied from 0.4 (± 0.1) to 0.9 (± 0.1) with the freestyle condition having the greater differences.

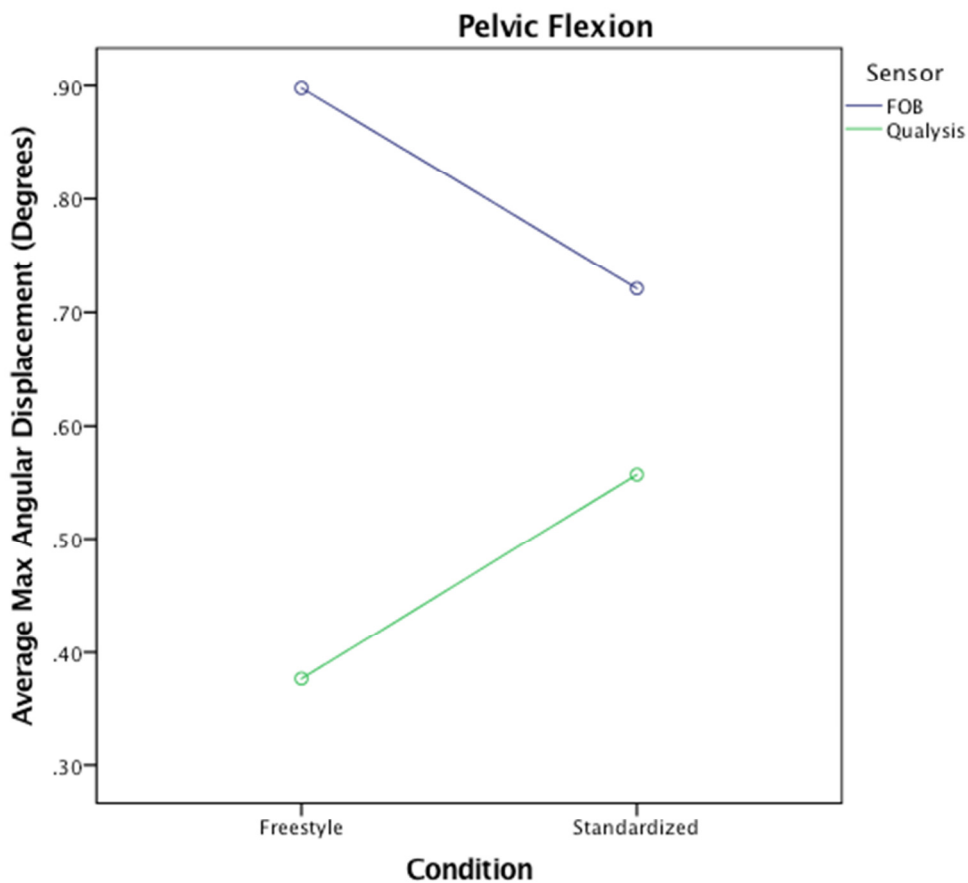


Figure 14. Graphical representation of the output from the univariate ANOVA results.

The graphical analysis of the Bland-Altman analysis is shown in Figure 15. The max angular displacement data was used once again for this comparison. The mean difference of 0.4 (0.3) was significant ($t= 6.48$, $df = 35$, $p<0.001$). The 95%ile confidence interval was ± 0.6 degrees.

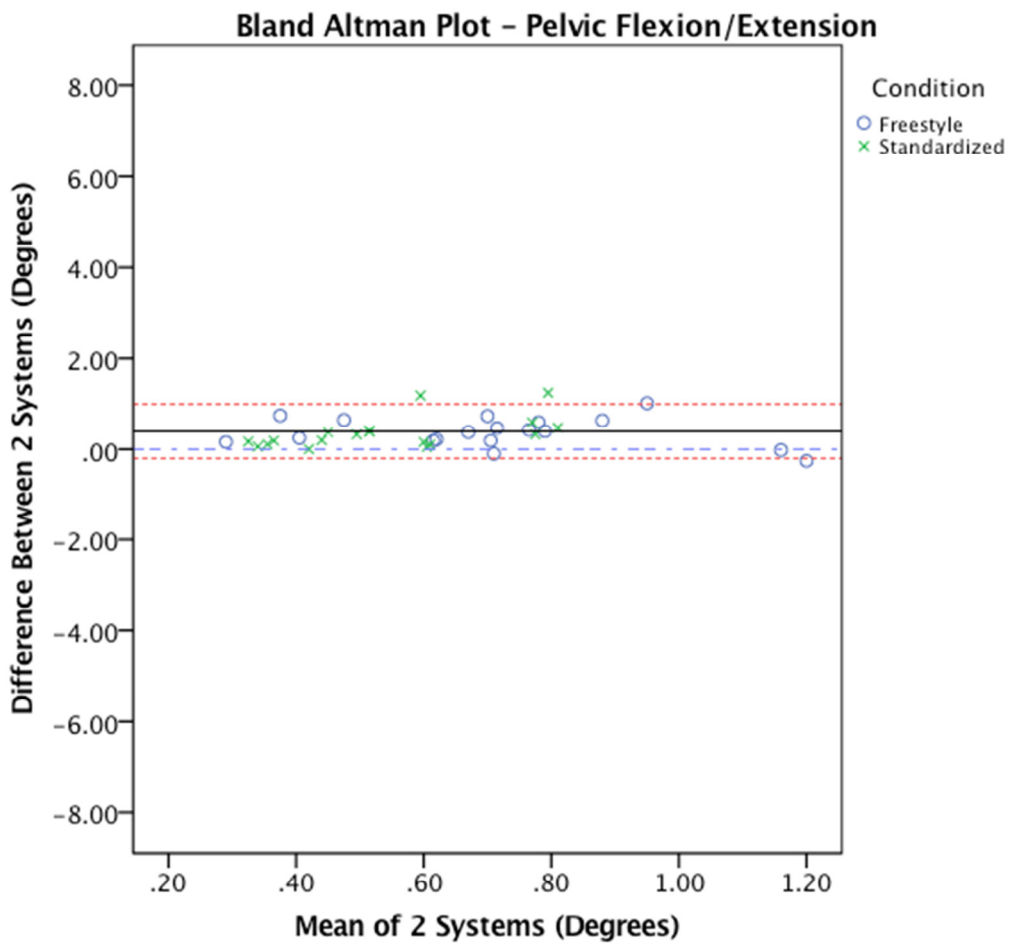


Figure 15. Bland-Altman Plot demonstrating the agreement between the FOB and Qualysis systems while recording pelvic flexion/extension during the lift and replace normal reach task.

Lateral Flexion

A univariate GLM was performed to assess the effect of condition and sensor on the output. The analysis considered the main effects as well as the interactions. Shown below in Figure 16 are the means for this data. There was a significant difference due to sensors ($F=29.48$, $df=1,48$, $p<0.001$). There was no significant difference due to condition ($F=3.18$, $df=1,48$, $p=0.081$). Overall, the means (and SE) varied from 0.2 (± 0.02) to 0.33 (± 0.02) with the freestyle condition having the greater difference.

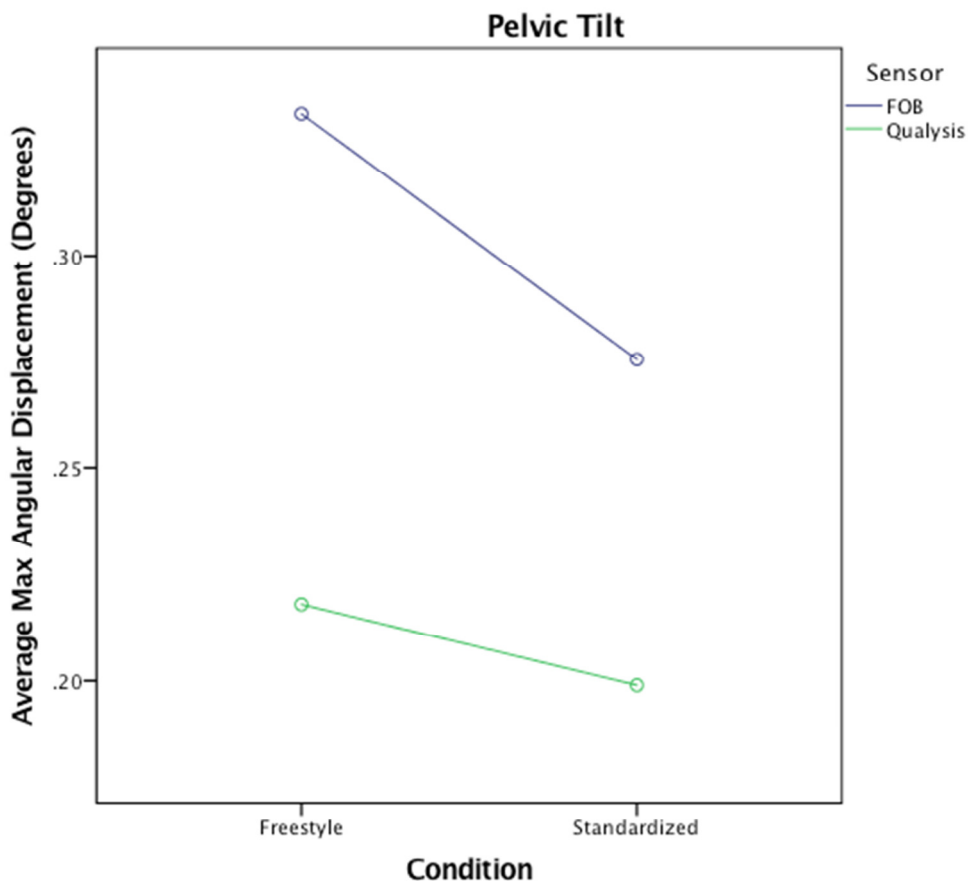


Figure 16. Graphical representation of the output from the univariate ANOVA results

The graphical analysis of the Bland-Altman analysis is shown in Figure 17. The max angular displacement data was used once again for this comparison. The mean difference of 0.1 (0.2) was significant ($t= 4.39$, $df = 29$, $p<0.001$). The 95%ile confidence interval was ± 0.4 degrees.

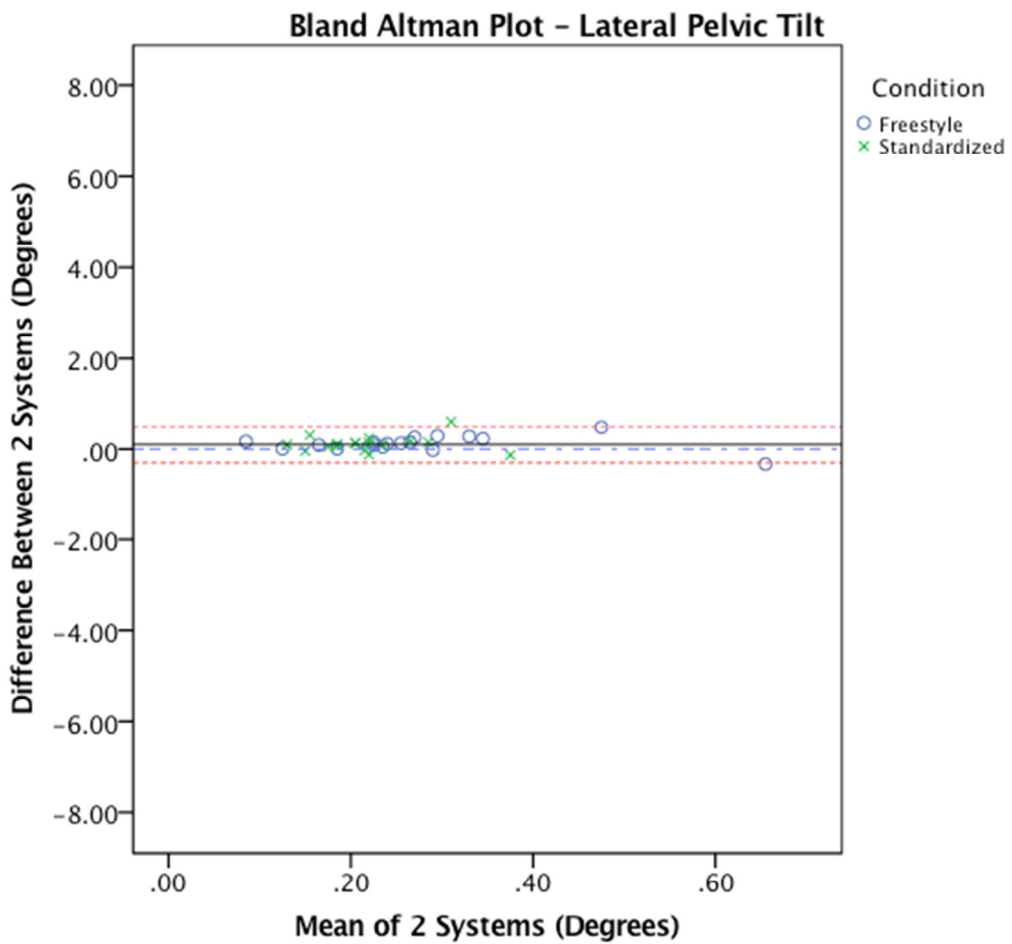


Figure 17. Bland-Altman Plot demonstrating the agreement between the FOB and Qualysis systems while recording pelvic lateral tilt during the lift and replace normal reach task.

Axial Rotation

A univariate GLM was performed to assess the effect of condition and sensor on the output. The analysis considered the main effects as well as the interactions. Shown below in Figure 18 are the means for this data. There was a significant difference due to sensors ($F=47.32$, $df=1,49$, $p<0.001$). There was a significant difference due to condition

($F=13.48$, $df=1,49$, $p=0.001$). Overall, the means (and SE) varied from $0.45 (\pm 0.06)$ to $1.0 (\pm 0.06)$ with the freestyle condition having the greater difference.

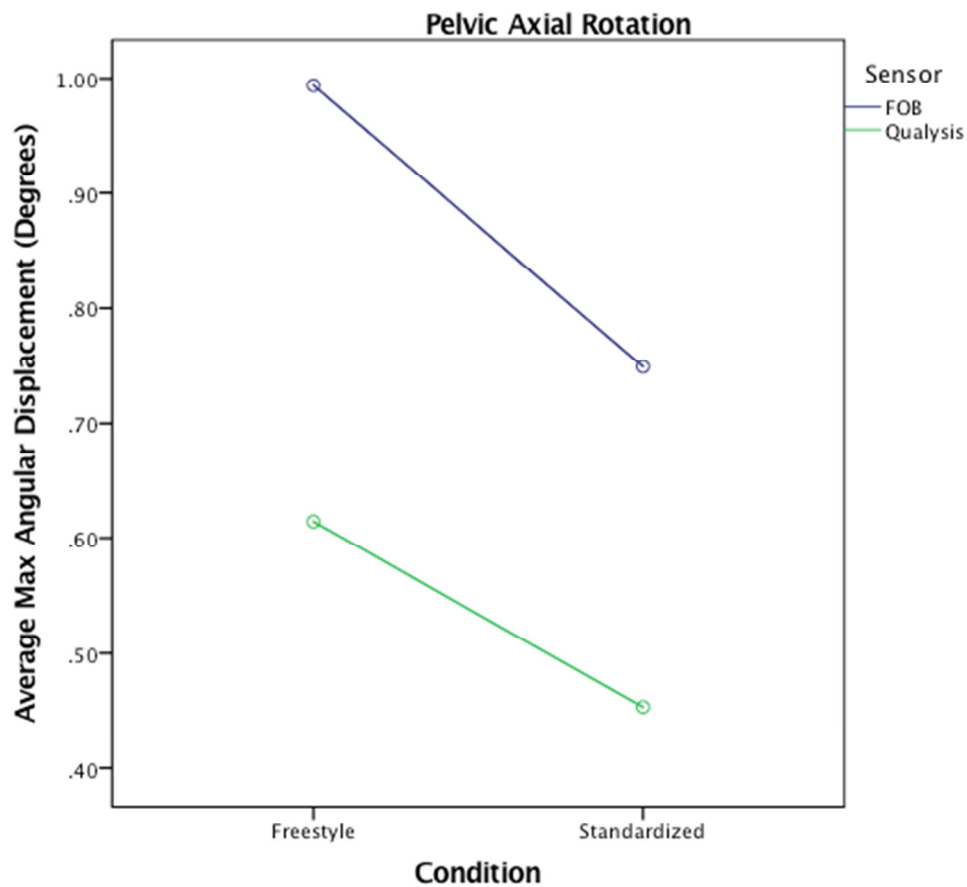


Figure 18. Graphical representation of the output from the univariate ANOVA results.

The graphical analysis of the Bland-Altman analysis is shown in Figure 19. The max angular displacement data was used once again for this comparison. The mean difference of $0.4 (0.4)$ was significant ($t= -7.1$, $df = 33$, $p<0.001$). The 95%ile confidence interval was ± 0.8 degrees.

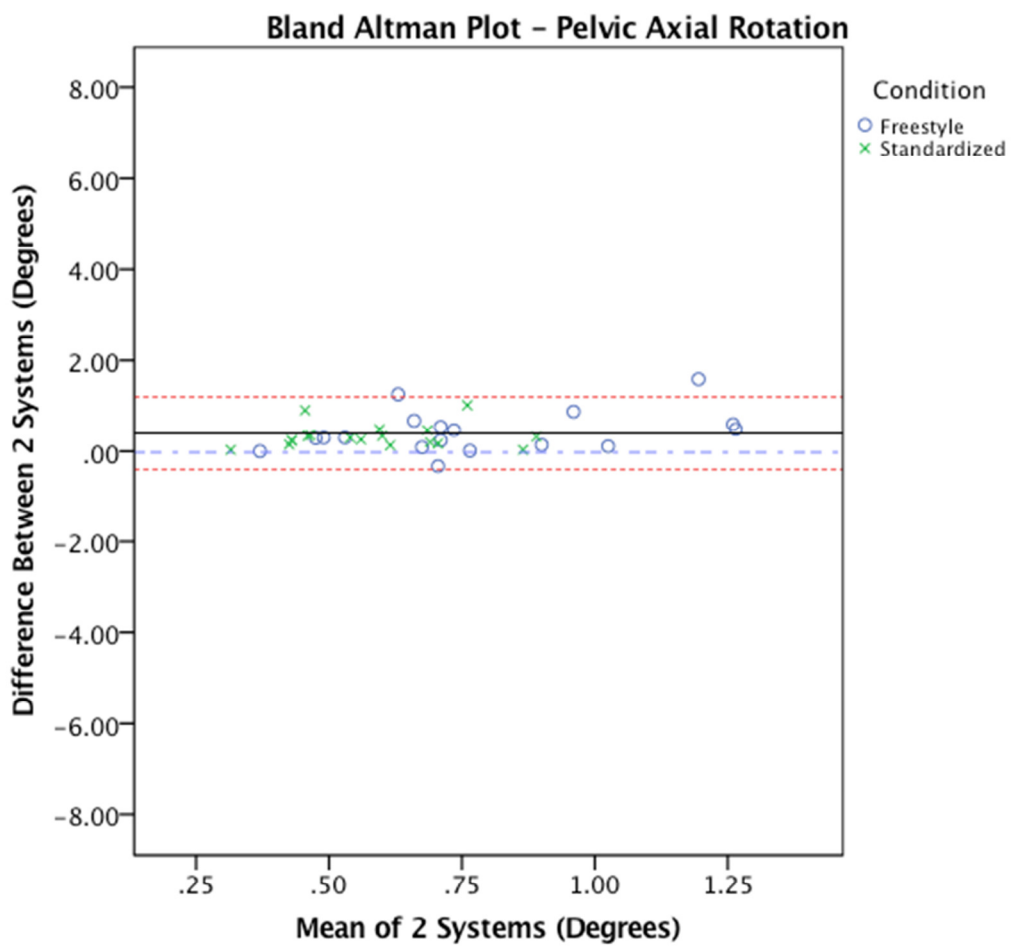


Figure 19. Bland-Altman Plot demonstrating the agreement between the FOB and Qualysis systems while recording axial rotation during the lift and replace normal reach task.

4.1.3 Summary Tables

Section 4.1.1 and 4.1.2 have presented the comparative analysis for the trunk and pelvis during the LTN task. This analysis was completed for both tasks in each of the two reach conditions. The results for the LTM, HTTN and HTTM comparison is presented in Appendix A. This section of the results will present the overall summary of the comparison of the two sensors across all the axes of measure by the different experimental conditions. In total 23 of the 24 comparisons found significant differences between the two systems. However, these differences were relatively small on the order of 0.1 to 2.3 degrees. The summarized results are presented in table format. The descriptions of the tasks and a symbol for each task are presented here as:

Lift & Replace Normal Reach – LTN

Lift & Replace Maximum Reach – LTM

Horizontal Transfer Task Normal Reach – HTTN

Horizontal Transfer Task Maximum Reach – HTTM

Table 5. The table below summarizes the Average (Standard Error) difference in maximum angular displacement measurements between the two systems. All units are in degrees.

Movement Type	Standardized			Freestyle		
	Flex/Ext	Lat. Tilt	Axial Rot.	Flex/Ext	Lat. Tilt	Axial Rot.
LTN Trunk	1.2 (0.8)	0.3 (0.4)	1.0 (0.9)	1.0 (1.1)	0.3 (0.4)	0.8 (0.4)
LTN Pelvis	0.4 (0.4)	0.1 (0.2)	0.3 (0.3)	0.4 (0.3)	0.1 (0.2)	0.4 (0.5)
LTM Trunk	1.5 (1.4)	0.2 (0.6)	0.8 (0.7)	1.8 (1.3)	0.1 (0.5)	0.7 (1.1)
LTM Pelvis	0.6 (0.4)	0.1 (0.1)	0.4 (0.3)	0.5 (0.3)	0.2 (0.1)	0.4 (0.4)
HTTN Trunk	2.0 (2.1)	0.5 (0.8)	1.5 (1.4)	1.8 (1.6)	0.8 (0.7)	1.4 (1.0)
HTTN Pelvis	1.2 (1.4)	0.9 (1.1)	1.4 (1.7)	1.2 (1.1)	0.8 (1.0)	0.9 (0.8)
HTTM Trunk	2.3 (1.8)	0.3 (1.6)	2.3 (2.6)	2.3 (0.9)	0.7 (0.9)	1.7 (1.1)
HTTM Pelvis	1.2 (1.2)	0.6 (0.5)	1.7 (1.6)	1.4 (1.5)	0.9 (1.2)	1.6 (1.1)

Table 6. The table below summarizes the results from the univariate ANOVA analysis with regards to a sensor effect.. A positive sign (+) means there was a significant effect, while a negative sign (-) means there was no effect (1/24).

Movement Type		Trunk			Pelvis	
	Flex/Ext	Lat. Flex.	Axial Rot.	Flex/Ext	Lat. Tilt	Axial Rot.
LTN	+	+	+	+	+	+
LTE	+	+	+	+	+	+
HTTN	+	+	+	+	+	+
HTTM	+	-	+	+	+	+

Table 7. The table below summarizes the results from the univariate ANOVA analysis with regards to an instructional condition effect. The analysis was performed to assess if the condition performed (Freestyle vs. Standardized) would have a statistically significant effect on the angular output collected. A positive sign (+) means there was a significant effect, while a negative sign (-) means there was no effect (16/24).

Movement Type		Trunk			Pelvis	
	Flex/Ext	Lat. Flex.	Axial Rot.	Flex/Ext	Lat. Tilt	Axial Rot.
LTN	+	-	-	-	-	+
LTE	+	-	-	+	-	+
HTTN	+	+	+	+	+	+
HTTM	+	-	+	+	+	+

Table 8. The table below summarizes the results from the Bland Altman analysis. This was performed to assess the agreement of the two motion capture systems, the Flock of Birds and the Qualysis, when it came to recording motion of the trunk and pelvis. A positive sign (+) means the two systems were in agreement (5/24). A negative sign (-) means the two systems were not in agreement.

Movement Type		Trunk			Pelvis	
	Flex/Ext	Lat. Flex.	Axial Rot.	Flex/Ext	Lat. Tilt	Axial Rot.
LTN	-	-	-	-	-	-
LTE	+	-	-	-	-	-
HTTN	-	-	-	+	-	-
HTTM	-	+	-	+	-	+

4.2 Body Segment Angular Motion Patterns

The relative joint angles for the trunk and left & right shoulder and elbow joints were calculated using the Visual 3D software. These angles were calculated in degrees and the angular patterns from the beginning to the end of the trials were normalized and presented in the following graphs. The red vertical markers found in the graphs for the horizontal transfer task trials represent the instant the load was transferred from right to left hands. Rotations follow a Cardan sequence (Z, X, Y) (Flex, Lateral, Rotation). The data for the upper limb was normalized to be from the start of the task to the moment of transfer for the right limb, and from the moment of transfer to the end of the task for the left. Therefore, there are no red markers to signify the moment the load was transferred between hands. The shoulder and elbow angular data on the left hand side of the body were multiplied by -1 so rotations about the left side of the body coincide with those on the right side. This was performed for all rotations except flexion/extension. The results were not normalized to account for standing posture, thus subject to subject differences are due to slight differences in the initial posture of the subjects. Results for the Lift and Similar to the results presented in section 4.2, only the results for LTN are shown below in the body of the results. The results for the other 3 lifting tasks can be found in Appendix A. The angular conventions repeated are consistent with the ISB recommendations which are:

Trunk:

Positive Rotations - Extension and movements (lateral bending and axial rotations) to the right

Negative Rotations - Forward flexion and movements (lateral bending and axial rotations) to the left

Upper Arm (Shoulder):

Positive Rotations - Flexion, Adduction & Internal Rotation

Negative Rotations - Extension, Abduction & External Rotation

Forearm (Elbow):

Positive Rotations - Flexion, Adduction & Internal Rotation

Negative Rotations - Extension, Abduction & External Rotation

4.2.1 Lift & Replace Normal Reach

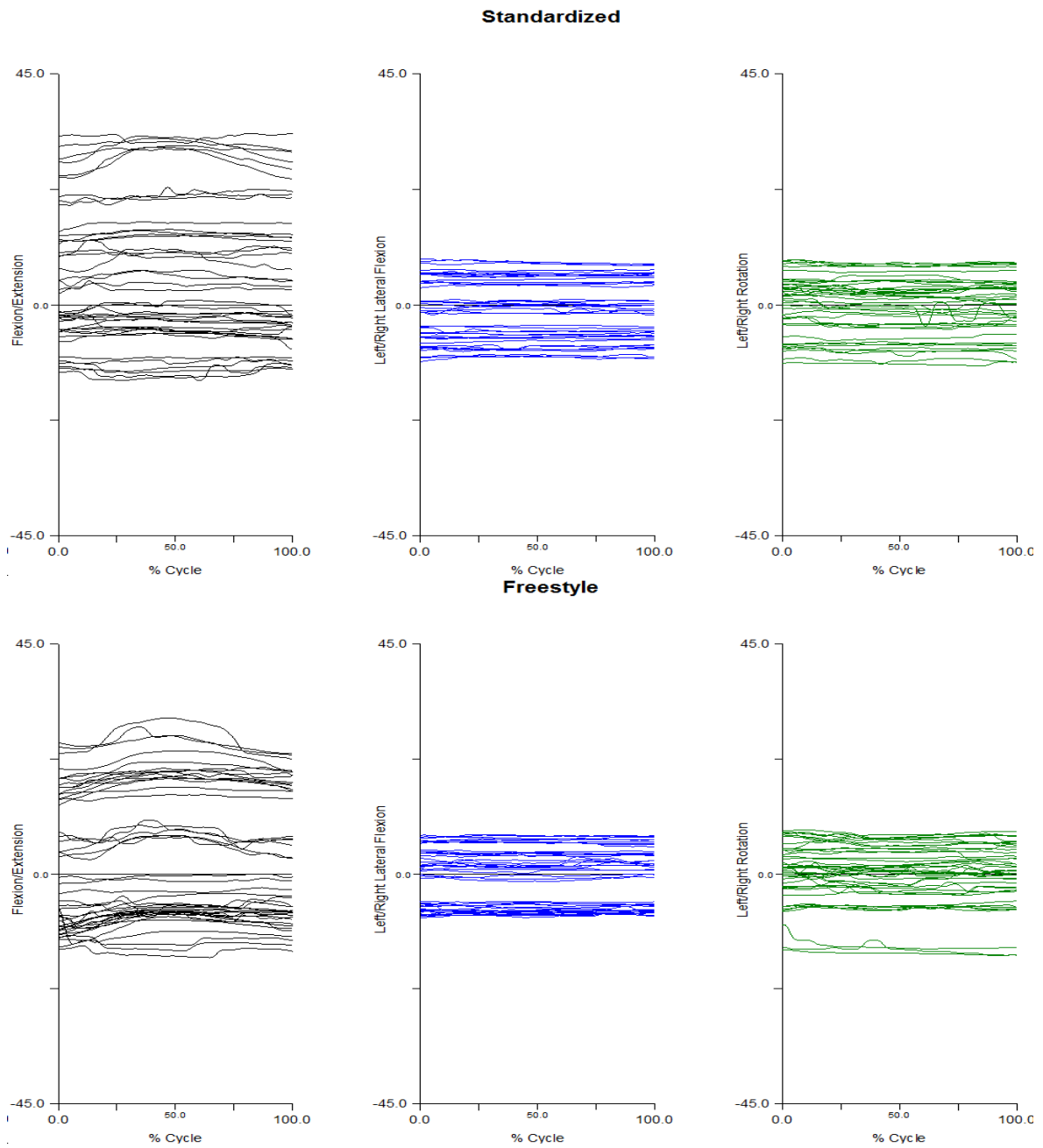


Figure 20. Angle-time graphs showing the angular position of the trunk with reference to the pelvis during the Lift & Replace Normal Reach task.

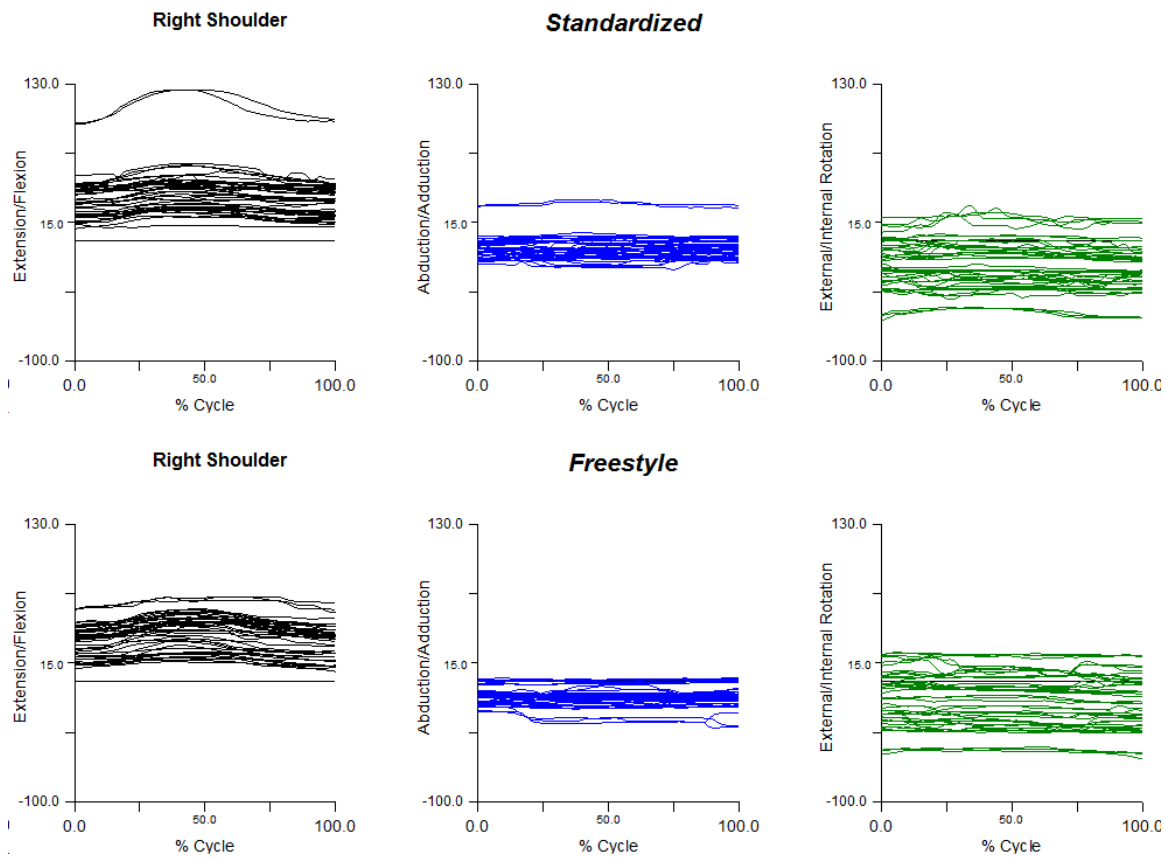


Figure 21. Angle-time graphs showing the angular position of the right upper arm with reference to the torso during the Lift & Replace Normal Reach task.

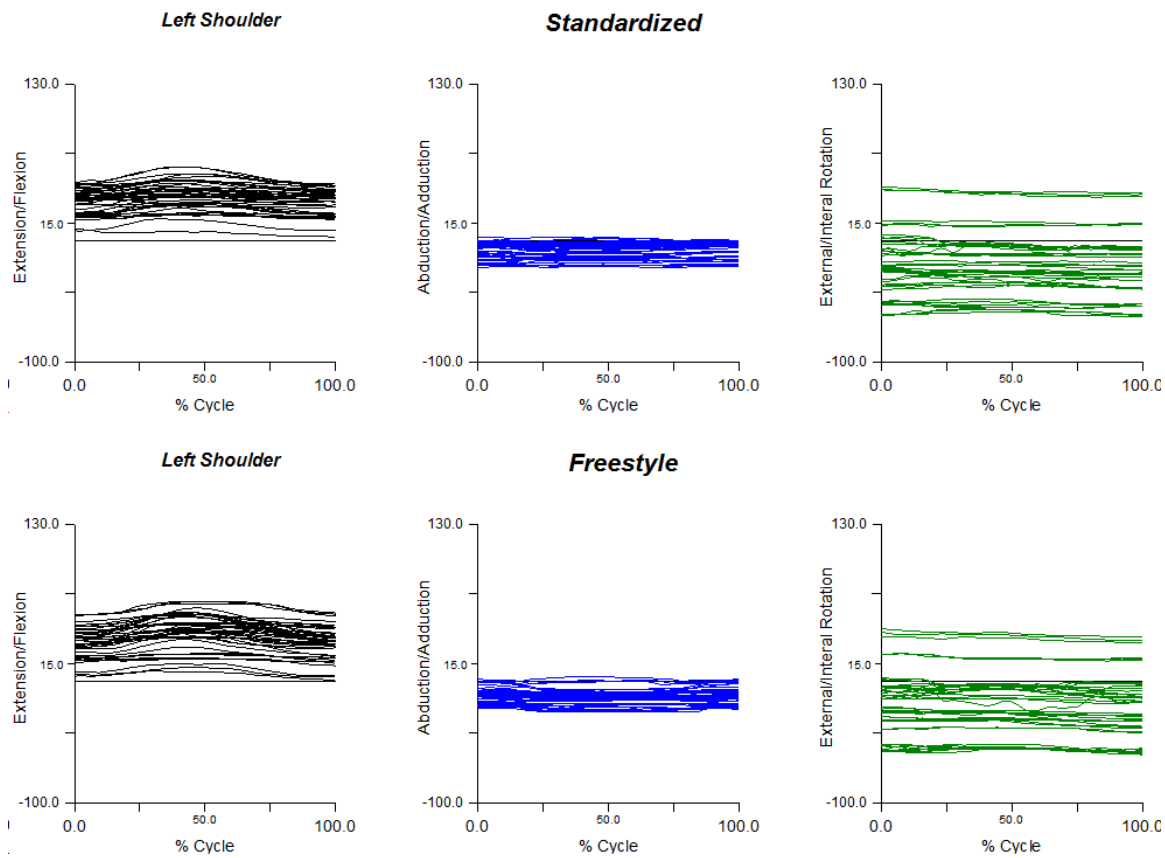


Figure 22. Angle-time graphs showing the angular position of the left upper arm with reference to the torso during the Lift & Replace Normal Reach task.

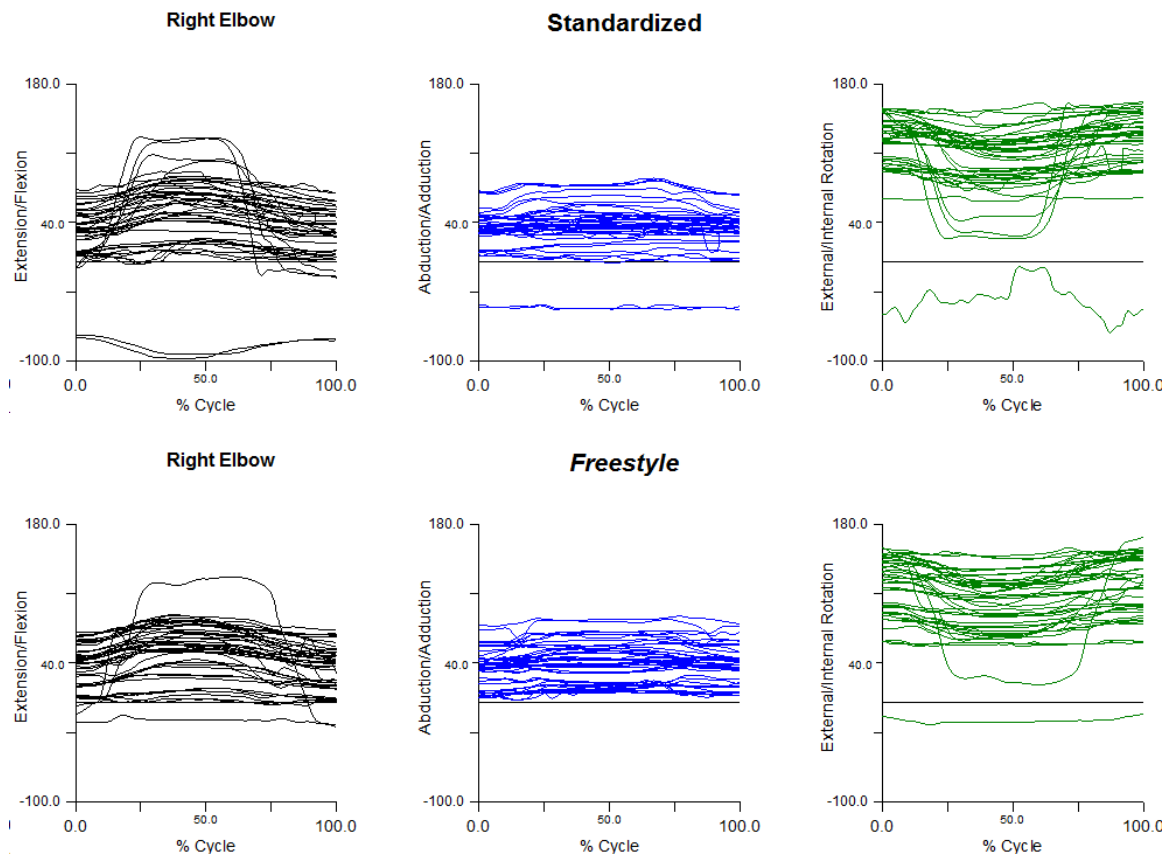


Figure 23. Angle-time graphs showing the angular position of the right lower arm with reference to the right upper arm during the Lift & Replace Normal Reach task.

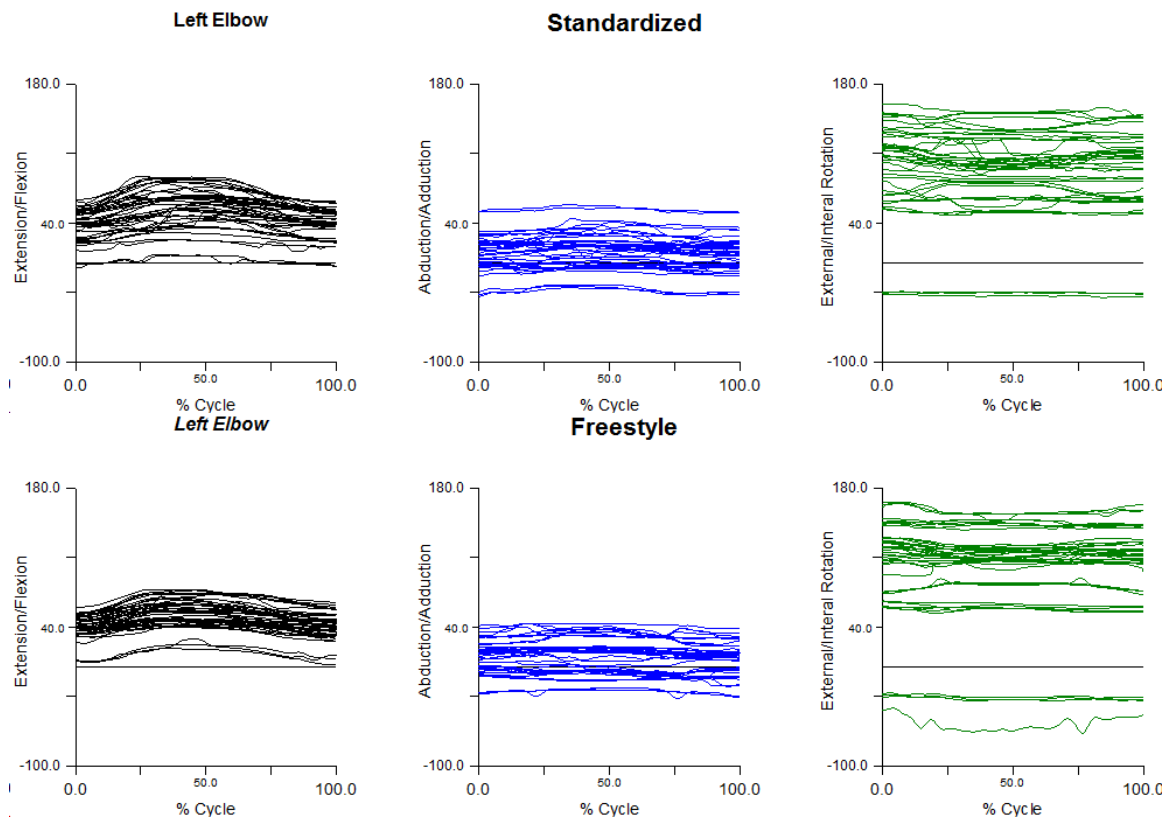


Figure 24. Angle-time graphs showing the angular position of the left lower arm with reference to the left upper arm during the Lift & Replace Normal Reach task.

4.3 Lifting Load Linear Motion Patterns & Time Comparison

The trajectory of the load was recorded by placing a reflective marker on the top surface of the load. The linear trajectory was recorded for each trial from start to finish, in all three directions. The graphs showing the cumulative results can be found in Figures 25-27, in their respective sub-section. Motion patterns recorded were relative to the GCS which was on top of the table, directly in front of each participant. Motion in the X axis takes place in the frontal plane of the participant and represents the left to right motion of the load. The Y axis is in the transverse plane and represents the motion in the anterior-posterior direction and lastly, the Z axis in the sagittal plane and represents the vertical position of the load during the trial. Units were collected and presented in meters. For the horizontal transfer task trials, the red dash represents the moment the lifting load was transferred from right to left hands. Sudden drop-offs are a result of the tracking marker leaving the field of view of the Qualysis system

The time taken to complete each trial from start to finish was collected and processed using the Visual 3D software. This was obtained using the pressure sensor data on the bottom of the load. SPSS software was used to test for normality (Shapiro-Wilkes) and to compare the time results between standardized and freestyle techniques using a series of paired t-tests. A Shapiro Wilk test for normality was performed on each data sub-set and a two-step transformation to normality (Templeton, 2011) was performed if the data was deemed not normal.

X = Subject Frontal Plane, Y= Subject Transverse Plane, Z = Subject Sagittal Plane.

4.3.1 Lift & Replace Normal Reach

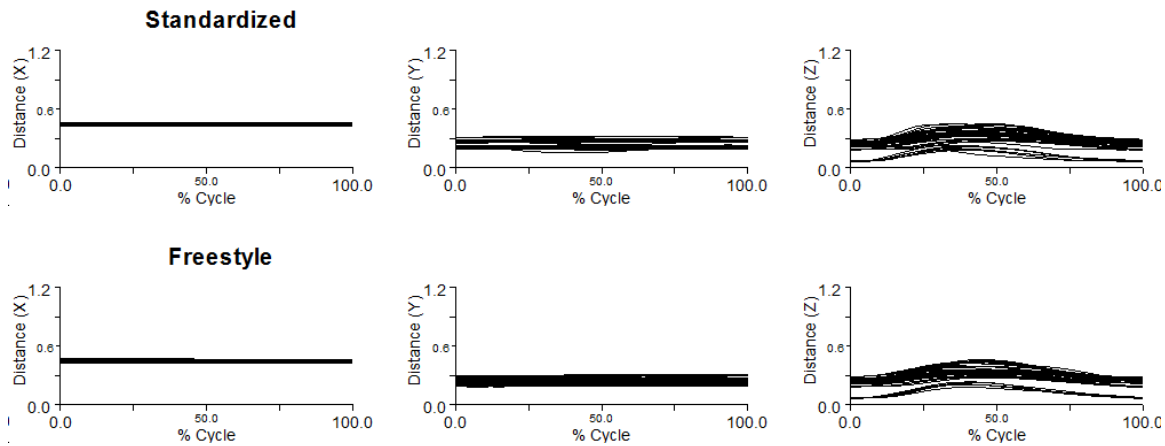


Figure 25. Linear movement patterns for the lifting load during the lift and replace normal reach condition. Distance units are in meters (m). X = Subject Frontal Plane, Y= Subject Transverse Plane, Z = Subject Sagittal Plane.

The mean and standard deviation times of the free style and standardized conditions were 1.75 (0.28) and 1.85 (0.37), respectively. Using a paired t-test, these differences were found to be significantly different ($t = -3.609$, $df = 49$, $p = 0.01$).

4.3.2 Lift & Replace Maximum Reach

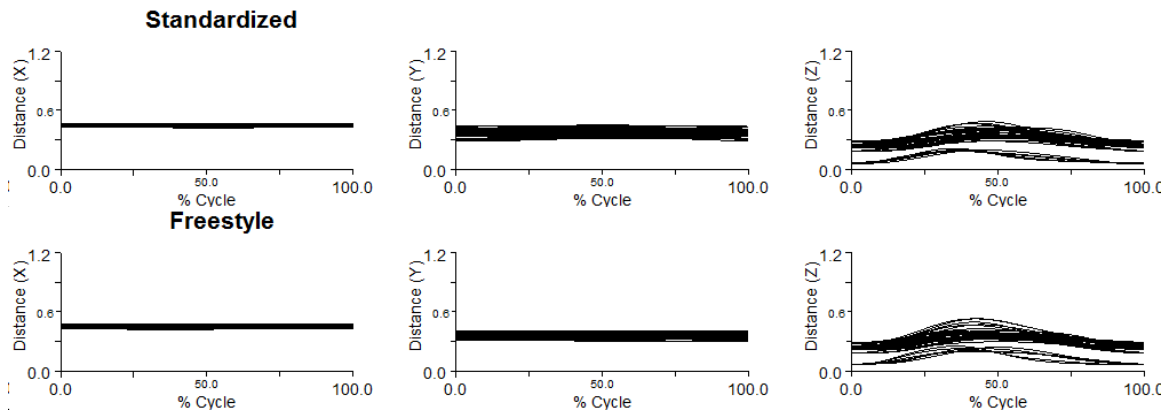


Figure 26. Linear movement patterns for the lifting load during the lift and replace extended reach condition. Distance units are in meters (m). X = Subject Frontal Plane, Y= Subject Transverse Plane, Z = Subject Sagittal Plane.

The mean and standard deviation times of the free style and standardized conditions were 1.8 (0.29) and 1.9 (0.27), respectively. Using a paired t-test, these differences were found to be not significantly different ($t= 1.67$, $df= 49$, $p= 0.101$).

4.3.3 Horizontal Transfer Task Normal Reach

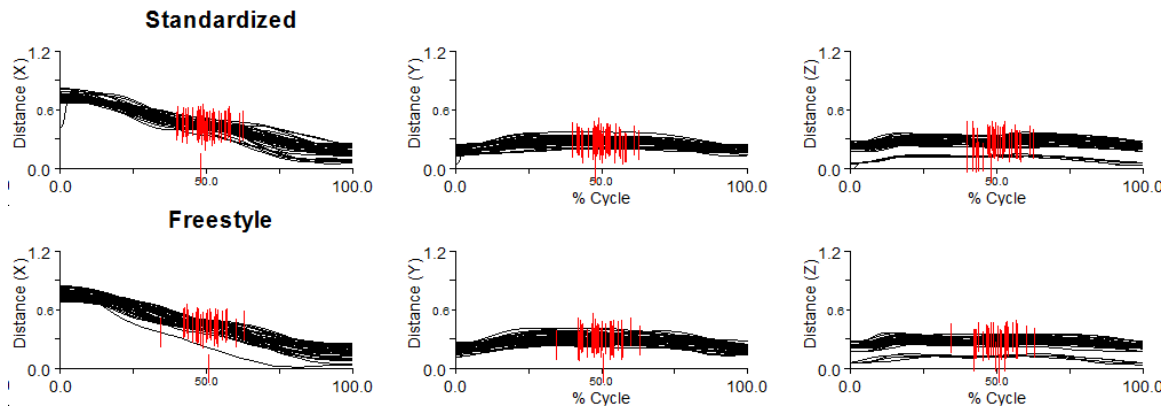


Figure 27. Linear movement patterns for the lifting load during the normal reach variant of the horizontal transfer task condition. The red line signifies the moment the load was transferred between hands. Distance units are in meters (m). X = Subject Frontal Plane, Y= Subject Transverse Plane, Z = Subject Sagittal Plane.

The mean and standard deviation times of the free style and standardized conditions were 3.99 (0.51) and 3.99 (0.43), respectively. Using a paired t-test, these differences were found to be not significantly different ($t= 0.235$, $df= 49$, $p= 0.815$).

4.3.4 Horizontal Transfer Task Maximum Reach

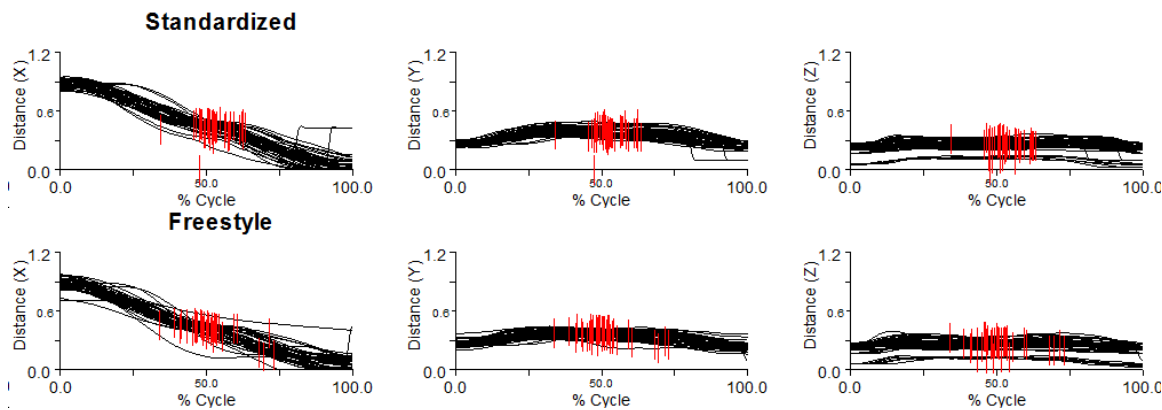


Figure 28. Linear movement patterns for the lifting load during the extended reach variant of the horizontal transfer task condition. The red line signifies the moment the load was transferred between hands. Distance units are in meters (m). X = Subject Frontal Plane, Y = Subject Transverse Plane, Z = Subject Sagittal Plane.

The mean and standard deviation times of the free style and standardized conditions were 4.13 (0.47) and 4.22 (0.45), respectively. Using a paired t-test, these differences were found to be not significantly different. ($t = -1.83$, $df = 49$, $p = 0.074$).

4.3.5 Time Summary

A summary of the statistical analyses performed in the previous sections 4.3.1 - 4.3.4 can be found in the following table.

Table 5. Results from the paired t-tests performed to assess the effect of instruction on the time needed to perform each task. A positive result (+) indicates a significant difference between standardized and freestyle instructive conditions. All units are in seconds.

	LTN	LTM	HTTN	HTTM
Standardized	1.85 (0.37)	1.86 (0.27)	3.99 (0.43)	4.22 (0.45)
Freestyle	1.75 (0.28)	1.8 (0.29)	3.99 (0.51)	4.13 (0.47)
Stat. Diff.	+	-	-	-

Chapter 5: Discussion

The purpose of this study was to develop a process for using motion capture technology (Qualysis) to record the 3-D kinematics of the pelvis, trunk and upper limb during the experimental protocol used for a series of studies related the lumbar spine performed at the Neuromuscular Functioning Laboratory at the Dalhousie School of Physiotherapy (5-7, 16). This information was used to address a series of questions, most importantly to compare the angular kinematic measures between the current (FOB) system and the Qualysis system for the pelvis and trunk. Other objectives involved the collection and analysis of the motion patterns of the upper extremities during the differing conditions of instruction. These objectives are summarized below.

1. Compare the FOB and Qualysis motion tracking systems as they record the motion of the trunk and pelvis.
2. Measure and document the angular displacement time graphs about the trunk, shoulder and elbow for the healthy population throughout the four lifting tasks.
3. Document the linear movement patterns of the load during the four tasks.
4. Examine the effect that instruction has on the four experimental tasks.

(Preferred Lifting Style vs. Standardized)

5.1 Qualysis - FOB System Comparison

The first primary objective of the study was to compare the Qualysis and Flock of Bird (FOB) systems with respect to their ability to record pelvic and trunk three-dimensional motion. This was done by performing a series of two separate statistical tests on the MAD data collected, a univariate ANOVA and the Bland Altman. The ANOVA compared the means for each subset of data while the Bland Altman tested for the agreeability of the two systems.

The results from the ANOVA (Table 11) revealed a significant difference between the systems in 23 out of the 24 tests performed. The two systems were only in agreement when recording trunk lateral flexion during the maximum reach horizontal transfer task. The FOB system obtained a higher average recorded MAD in each subset examined.

The two systems were further examined by comparing the same MAD using a series of Bland-Altman Analysis'. The results revealed that the two systems were only in agreement in 5 of the 24 tests performed. This further supports the notion that the FOB system provides an overestimate of recorded motion compared to the Qualysis when recording the same activity. This difference is however small, with only a sole occurrence of an outcome having over 10 degrees of MAD (Results; Figure 54). The average difference between recorded MAD ranged from 0.1 to 2.3 degrees in each of the comparisons.

The differences between the two systems could be due to a number of reasons. First, the angular resolution of the two systems is different with the Qualysis having a higher resolution. While the differences in the pelvic data may be too small to compare and therefore may be within the range where angular resolution may explain their differences, the differences from the trunk would be considered outside this range. The FOB system consistently overestimated the MAD when compared to the Qualysis and differences that lie outside the explanation of angular resolution may be explained by a systematic error in the placement of the sensors or with the processing of the motion data as the FOB data was processed using Matlab and the Qualysis data by Visual 3D.

5.2 Angular Motion Patterns

The second primary objective of the study was to establish the three dimensional movement patterns about the torso, shoulder and elbow for each of the four lifting conditions. This motion was tracked using the Qualysis movement tracking system and processed using the Qualysis Track Manager and Visual 3D software packages.

5.2.1 Lift & Replace Normal Reach

The results for the Lifting Task Normal Reach condition were as expected for each of the segments. There was minimal change in movement about all three axes of the trunk. There was variability from participant to participant in the relative measure of the starting position from flexion and extension but this would be expected, as each participant would have a different starting posture and initial relative angle between the sensors and therefore different trunk position relative to the pelvis. The within subject movement motion about the transverse axis is below 10 degrees however, with the

motion about the other in the other 2 axes less than 5 degrees. There were no obvious differences between the freestyle and standardized conditions.

Bi-lateral, kinematic patterns were also recorded for both shoulders. Similar to the trunk there was no correction for the initial start position from a neutral control posture. Once again motion mainly in the sagittal plane, flexion and extension. The patterns show that there was about 10-20 degrees of flexion in this plane and it appears that the participants were using shoulder flexion to lift the load from the table. Minimal motion was recorded in the other two axes, which is what was expected. There were no obvious differences between the freestyle and standardized conditions.

Results for the elbow were expected but not consistent for both elbows, which would have been expected seeing as the participants performed a bilateral lift and you would expect both arms to move symmetrically. Flexion and extension patterns were normal for the majority of participants but there appears to be a few trials that have significantly more flexion than the rest. This anomaly appears to be coming from a single participant and could be explained by excessive flexion during both freestyle and standardized conditions, but it is not present in the graphs for the left elbow. If it were due to the subject, you would expect the anomaly to be present in both arms, but seeing as it is only found in one, a more reasonable explanation for it may be an error during the data collection. This anomaly was also present in internal external rotation and once again only found in the right elbow, again supporting the theory of marker error. There was once again no obvious difference between freestyle and standardized conditions.

5.2.2 Lift & Replace Maximum Reach

The results for the Lifting Task Extended Reach condition were as expected for each of the segments. There was minimal movement in all three axis' of the trunk. Standing posture once again caused starting position variability for flexion/extension. There appears to be more trunk extension occurring in the extended reach condition when compared to the normal reach, with freestyle having more than standardized. The increased force required to lift the load off the table due to the longer moment arm could explain this. Having the proprioceptive aid could account for the difference due instruction. Motion in the other two axes of motion was minimal. No noticeable differences can be observed between freestyle and standardized conditions for these two axes.

The results from both shoulders were near identical and followed the patterns expected for the nature of the activity. Motion was mainly in the form of flexion and this would be expected because the subjects were directed to maintain a straight arm while lifting, therefore forcing them to flex at the shoulder to lift the load the required height. This instruction was only given for the standardized condition but there doesn't appear to be any noticeable differences between standardized and freestyle. Therefore one could assume that the starting position of the load and resulting start position of the arms has an effect on how the load is lifted and it may not be essential to direct future participants to maintain this extended position throughout the trial, they may do this naturally. Motion in

the other 2 axes was minimal with no evident differences between freestyle and standardized conditions.

Results for the elbows were also representative of the activity being performed. One would expect there to be minimal motion in all three axes because the participants were positioned with their arms fully extended and told to lift the load in this position. This instruction was left out during the freestyle condition and there doesn't appear to be any difference between with condition and the standardized. This further supports the fact that instruction had little effect on how the load was lifted; most likely due to the starting position and intuitive lifting style of those asked to lift from this position. There does appear to be some gimbal lock occurring at the upper limits of internal rotation (Abdullah et al. 2007; Van Andel et al., 2008).

5.2.3 Horizontal Transfer Task Normal Reach

The results for the Lifting Task Normal Reach Task were as expected for each of the segments. Increased motion was found in all three axes of the trunk when compared the lifting task conditions. The increased motion of the load in the transfer tasks could explain this, as the load needs to move in all three planes of motion instead of one. This added motion would require the activation of more musculature to compensate for the added load, and this added activation could result in more motion in the trunk. There does not appear to be an effect due to instruction.

Results for the shoulders represented the expected motion patterns for the nature of this behavior. There was flexion in the right arm during the initial stage, like during the

normal reach lifting task, therefore supporting the fact that the participants used shoulder flexion instead of elbow flexion to lift the load from the table. This was true for both instruction conditions as there were no noticeable differences between the two conditions. This was further supported by the patterns of the left shoulder that showed a slight extension of the shoulder joint as the load was transferred to the left side of the table and put down. Rotations in the other two axes also show expected patterns. For the right arm, the arm adducted and internally rotated as the right arm moved medially toward the left. Once the left arm received the load at the participant's midline, the left arm abducted and externally rotated as the load was transferred to the left side of the table.

Elbow patterns were expected but inconsistent for both elbows. Once again, the left elbow gave results that differed from the right, with the results from the right showing the presumed patterns. There was very little motion in all three axes with exception to three trials that can be presumed to have been performed by the same subject as the three trials are near identical and involve a sigmoid pattern of flexion/extension and internal/external rotation. Minimal motion is what would be expected, especially as it has already been shown in the shoulder results that shoulder flexion was present in the right arm during the lifting phase for all the subjects. Results for the left elbow were unclear and were hard to decipher for a specific pattern. The most interesting pattern is the one found in the flexion axis as there appears to be a lot of variability as to what participants did in the second half of the task in order to place the load on the marked point on the table. Most had a slight amount of flexion but many also extended slightly. Certain participants had much more motion than others, resulting in a very wide range of

patterns. There is gimbal lock from flexion and internal rotation as there was in the Lifting Task Extended Reach results for the same joint. This would support the notion that there was an issue with the marker or camera setup on that part of the body, as it was never found on the right side. The marker triad used to record the forearm motion was too small and caused issues with marker cross talk when processing with QTM. These issues were present for both instruction conditions.

5.2.4 Horizontal Transfer Task Maximum Reach

The results for the Horizontal Transfer Task Normal Reach condition were as expected for each of the segments. Increased motion was once again found in all three axes of the trunk when compared with the lifting task conditions, further supporting the fact that the nature of the transfer task results in more trunk muscle activation and therefore more motion. Reach condition did not seem to have an effect on motion even though the moment arm was longer in this task. For the first time, gimbal lock was found in a single trial in each of the axes during the standardized condition. The amount of motion involved in each axis seems to be in excess and therefore this would lead one to believe there was a possible error with the marker or camera (field of view) during collection. The most likely reason for this is having the marker triad for the trunk being displaced from its original position when the calibration trial was performed, effort was made to avoid this but it would not be unlikely that is occurred during a singe participant.

Results for the shoulders represented the expected motion patterns for the nature of this behavior. The results followed a very similar pattern to those collected during the normal reach condition for the same joints. There was flexion in the right arm during the

initial stage, therefore supporting the fact that the participants used shoulder flexion to lift the load from the table, as would be expected. This was true for both instruction conditions as there were no noticeable differences between the two conditions. This was further supported by the patterns of the left shoulder that showed a slight extension of the shoulder joint as the load was transferred to the left side of the table and put down. Rotations in the other two axes also show expected patterns. For the right arm, the arm adducted and internally rotated as the right arm moved medially toward the left. Once the left arm received the load at the participant's midline, the left arm abducted and externally rotated as the load was transferred to the left side of the table. There were also no noticeable differences due to instruction.

Results for the elbows once again followed expected patterns and further support the notion that the lift is not bilaterally symmetric between both arms. Results for the right arm are consistent and show a very clear pattern. The starting position of the can appears to influence the lifting style by causing the participants to maintain a stable elbow joint during the first half of the trials. These patterns portray very little motion in all three axes and there are no noticeable differences due to instruction condition. The results vary greatly for the left elbow however, with a number of patterns present. The majority of the variability can be found in the flexion extension axis, as there appears to be no distinct pattern. This was also the case during the normal reach condition for the transfer task. Participants did a combination of flexion, extension and no movement in order to place the load on the table. No pattern was more prevalent. For the other two axes the pattern is indistinct with gimbal lock once again appearing in both instruction conditions for

internal rotation, this further supports the notion that there may have been an issue collecting the kinematics of the lower left arm. There appears to be little difference between instruction conditions.

5.3 Lifting Load Trajectory

Another objective of the study was to document the linear motion patterns of the lifting load in three dimensions. This was accomplished by tracking a single marker located on the dorsal surface of the load. The Qualysis motion capture system was used to track the three-dimensional motion of this marker as the trials were performed. Each trial performed was included in the graphs found in Chapter 4 for collective representation of the motion of the four experimental tasks performed.

The results for the two lift & replace conditions (normal & maximum) were as expected in all three dimensions. For the frontal plane (X), there was very little, if any, motion in either direction. Little to no motion was also recorded in the transverse plane (Y) as well, however there was a evident difference between normal and extended conditions distance because the load started farther away from the participants body when they had they arms extended. Minimal motion in the X & Y planes was expected as the participants were asked to lift the load up and down off the table; therefore motion should only be expected in the sagittal plane (Z). There appear to be minimal difference between the freestyle and standardized conditions.

The results for the two transfer task conditions (normal & extended) also followed the expected patterns. For the frontal plane (X), the sigmoid pattern would be the expected result as the participants transferred the weight across the table from right to left and briefly stopped to transfer the load between hands. It is worth noting that there is marker drop off in the extended reach condition because the marker went out of the field of view of the Qualysis cameras. This was due to the load being held farther from the body, which was used as the center reference for the field of view for each participant. Motion was also recorded in the transverse plane (Y) because the can was moving away from the participant & GCS in a semi-circumferential pattern in front of the participants. Motion in the sagittal plane (Z) was similar to the lifting conditions, except the load did not go as high off the table in the transfer task because the participants were instructed to keep the load below the sensor in order to trigger it. There once again appeared to be very little difference between the standardized and freestyle conditions.

5.4 Effect of Instruction on Trial Time & Pelvic/Trunk Motion

The final secondary objective of the study examines the effect that instruction had on the time it took to complete the experimental tasks, as well as its effect on the motion of the pelvis and trunk. Each of the four tasks were performed twice, first with minimal instruction and without a proprioceptive aid and again once more with more instruction and the proprioceptive aid to assist with preventing trunk and pelvic motion. This was done to assess the necessity of these variables in future studies.

The first comparison performed examining the effect of instruction was performed on the time needed to perform the tasks. The pressure trigger on the plantar surface of the

lifting load allowed the Labview software to record the time required to perform each trial from the moment the load left the table to the moment it landed. Participants were given a cadence to perform the task and told to perform the task in a set amount of time. For the trials without instruction, participants were told to perform the task in a set amount of time but trials weren't redone if they did not come close to the time. For the second set of trials that involved instruction, participants were instructed to meet the time requirement or the trials were performed once again. For the transfer tasks, they were specifically told to transfer the load halfway through the trial.

The timing results were examined in each of the four experimental tasks using a series of paired t-tests. There were no significant differences found between three of the four tasks, with lifting task normal reach being the sole task that showed a difference. This difference was however small, with Standardized and Freestyle conditions having an average of 1.85 (0.37) & 1.75 (0.28) seconds, respectively. The difference could be due to the fact that this task was the first to be performed during the experimental testing and there may have been a learning effect.

For the other three tasks there was no significant difference found between instructional conditions. There were similarly small differences found. The greatest difference between conditions was 0.1 seconds during the lifting task normal reach. These results show that the need to redo trials moving forward isn't absolutely necessary as participants perform the activity in generally the same amount of time.

The second comparison to examine the effect of instruction was performed on the movement data collected from the pelvis and trunk. A series of univariate ANOVAs were performed on the ROM data collected using both motion capture systems. A total of 24 tests were performed and a total of 16 showed a significant difference due to instructional condition. There were a total of seven significant outcomes with the trunk data and nine with the pelvis. Trunk flexion and pelvic axial rotation were the only two sections that had a significant result in each of the four experimental tasks. This speaks to the need for future studies to use the proprioceptive aid if they wish to reduce motion. Consideration must be made to the amount of movement occurring however, as there was only a degree or two separating the two instructional conditions. This is important in its relevance to the EMG study (Hubley-Kozey et al., 2007, 2013) in that less motion has been the goal in order to control added forces being applied to the spinal-pelvic juncture.

5.5 Conclusion

This study builds upon previous research performed at Dalhousie's School of Physiotherapy (5-7, 16). Its experimental protocol revealed the patterns of motion present during their tests while also answering questions regarding how the tests are performed and monitored. The primary objective of the study was to compare the previously used Flock of Bird motion capture system with the Qualysis. The FOB was used in the previous studies to measure the amount of motion occurring in the trunk and pelvis during the experimental protocol. This motion was controlled through instruction and trials were redone if there was ≥ 10 degrees of motion in any plane. The main goal of this research is to one day become part of a clinical test that would help in the assessment of lower back injury. For this to happen, clinical testers would also need to ensure that there

isn't excess motion and this can be very expensive. While the Qualysis system was proven to record significantly less motion than the FOB, the motion of the FOB system still averaged less than 10 degrees in total motion in the majority of conditions examined. The measure from the Qualysis is considered the “gold standard” and would be assumed to be the correct value, meaning the FOB system is overestimating the motion and this would make sense because its resolution is less than the Qualysis'. Therefore, one could replicate the experimental protocol in a clinical setting without motion capture and as long as they include the controls, they can be fairly certain that the motion is minimal and experimenter observation should suffice to monitor any access motion.

Secondary objectives from this study established the kinematic motion patterns of the upper extremity during the experimental protocol. The models created using the Visual 3D software will allow for the easy calculation of the kinetics of the activities in question. Future models can include anthropometric data in order to gain further insight into the moments present, specifically those acting upon the torso and being compensated for by the musculature. These future studies should reduce the number of degrees of freedom for the elbow as it has been shown in this study to be unreliable in any other plan than flexion/extension.

The final objectives of the study examined the effect that control had on the motion of the trunk and pelvis. It was revealed that there was a significant effect on overall motion of the pelvis and trunk when control was introduced, consistently resulting in less motion. This further supports the notion that motion capture technology might not

be necessary, especially if you ensure that you have the controls in place during testing. Control had no effect, however, on the amount of time it took for participants to complete the tasks. This study has established further understanding of the kinematics of the upper extremity during four functional experimental tasks and has established the groundwork for future research that will help this project continue to develop.

References

1. Abdullah, H. A., Tarry, C., Datta, R., Mittal, G.S., & Mohamed, A. (2007). Dynamic biomechanical model for assessing and monitoring robot-assisted upper-limb therapy, *Journal of rehabilitation research and development*, 44(1), 43.
2. Al-Zahrani, K. S., & Bakheit, M. O. (2008). A historical review of gait analysis.*Neurosci (Riyadh)*, 13(2), 105-108.
3. Bodenheimer, B., Rose, C., Rosenthal, S., & Pella, J. (1997). *The process of motion capture: Dealing with the data* (pp. 3-18). Springer Vienna.
4. Burnett, A. F., Cornelius, M. W., Dankaerts, W., & O'Sullivan, P. B. (2004). Spinal kinematics and trunk muscle activity in cyclists: a comparison between healthy controls and non-specific chronic low back pain subjects—a pilot investigation. *Manual Therapy*, 9(4), 211-219.
5. Butler, H. L., Hubley-Kozey, C. L., & Kozey, J. W. (2007). Changes in trunk muscle activation and lumbar-pelvic position associated with abdominal hollowing and reach during a simulated manual material handling task. *Ergonomics*, 50(3), 410-425.
6. Butler, H. L., Hubley-Kozey, C. L., & Kozey, J. W. (2009). Electromyographic assessment of trunk muscle activation amplitudes during a simulated lifting task using pattern recognition techniques. *Journal of Electromyography and Kinesiology*, 19(6), e505-e512.
7. Butler, H. L., Hubley-Kozey, C. L., & Kozey, J. W. (2013). Changes in electromyographic activity of trunk muscles within the sub-acute phase for individuals deemed recovered from a low back injury. *Journal of Electromyography and Kinesiology*, 23(2), 369-377.
8. Callaghan, J. P., & McGill, S. M. (2001). Low back joint loading and kinematics during standing and unsupported sitting. *Ergonomics*, 44(3), 280-294.
9. Cholewicki, J., & McGill, S. M. (1996). Mechanical stability of the in vivo lumbar spine: implications for injury and chronic low back pain. *Clinical biomechanics*, 11(1), 1-15.

10. DiFranco, D. E., Cham, T. J., & Rehg, J. M. (2001). Reconstruction of 3D figure motion from 2D correspondences. In *Computer Vision and Pattern Recognition, 2001. CVPR 2001. Proceedings of the 2001 IEEE Computer Society Conference on* (Vol. 1, pp. I-307). IEEE.
11. Gage, J. R., & Novacheck, T. F. (2001). An update on the treatment of gait problems in cerebral palsy. *Journal of Pediatric Orthopaedics B*, 10(4), 265-274.
12. Garg, A., & Saxena, U. (1985). Physiological Stresses in Warehouse Operations with Special Reference to Lifting Technique and Gender: a case study. *American Industrial Hygiene Association Journal*, 46, 2. 53-59.
13. Gebhardt, K., Kormendy, J., Ho, L. C., Bender, R., Bower, G., Dressler, A., ... & Tremaine, S. (2000). Black hole mass estimates from reverberation mapping and from spatially resolved kinematics. *The Astrophysical Journal Letters*, 543(1), L5.
14. Hodges, P. W., & Richardson, C. A. (1999). Altered trunk muscle recruitment in people with low back pain with upper limb movement at different speeds. *Archives of physical medicine and rehabilitation*, 80(9), 1005-1012.
15. Hubley-Kozey, C. L., & Vezina, M. J. (2002). Muscle activation during exercises to improve trunk stability in men with low back pain. *Archives of physical medicine and rehabilitation*, 83(8), 1100-1108.
16. Hubley-Kozey, C., Moreside, J. M., & Quirk, D. A. (2014). Trunk neuromuscular pattern alterations during a controlled functional task in a low back injured group deemed ready to resume regular activities. *Work: A Journal of Prevention, Assessment and Rehabilitation*, 47(1), 87-100.
17. Kozey, J., & Das, B. (1997). The determination of the maximum reach envelope for wheelchair mobile adults. *ADVANCES IN OCCUPATIONAL ERGONOMICS AND SAFETY*, 315-318.
18. Maletsky, L. P., Sun, J., & Morton, N. A. (2007). Accuracy of an optical active-marker system to track the relative motion of rigid bodies. *Journal of biomechanics*, 40(3), 682-685.
19. Marras, Marras, W. S., Knapik, G. G., & Ferguson, S. (2009). Lumbar spine forces during manoeuvring of ceiling-based and floor-based patient transfer devices. *Ergonomics*, 52(3), 384-397.
20. McClure, P. W., Esola, M., Schreier, R., & Siegler, S. (1997). Kinematic analysis of lumbar and hip motion while rising from a forward, flexed position in patients with and without a history of low back pain. *Spine*, 22(5), 552-558.

21. Mercer, J. L., Boninger, M., Koontz, A., Ren, D., Dyson-Hudson, T., & Cooper, R. (2006). Shoulder joint kinetics and pathology in manual wheelchair users. *Clinical Biomechanics*, 21(8), 781-789.
22. Meskers, C. G. M., Fraterman, H., Van der Helm, F. C. T., Vermeulen, H. M., & Rozing, P. M. (1999). Calibration of the “Flock of Birds” electromagnetic tracking device and its application in shoulder motion studies. *Journal of biomechanics*, 32(6), 629-633.
23. Panjabi, M. M. (2006). A hypothesis of chronic back pain: ligament subfailure injuries lead to muscle control dysfunction. *European Spine Journal*, 15(5), 668-676.
24. Park, K., & Chaffin, D. (1974). A biomechanical evaluation of two methods of manual load lifting. *AIIE Transactions*, 3, 105-113.
25. Pozrikidis, C. (2009). Introduction to Kinematics. In *Fluid Dynamics* (pp. 1-53). Springer US.
26. Rowe, P. J., Myles, C. M., Hillmann, S. J., & Hazlewood, M. E. (2001). Validation of flexible electrogoniometry as a measure of joint kinematics. *Physiotherapy*, 87(9), 479-488.
27. Roy, S. H., De Luca, C. J., Emley, M., & Buijs, R. J. (1995). Spectral Electromyographic Assessment of Back Muscles in Patients With Low Back Muscles in Patients With Low Back Pain Undergoing Rehabilitation. *Spine*, 20(1), 38-48.
28. Stanic, U., Bajd, T., Valencic, V., Kljajić, M., & Acimović, R. (1976). Standardization of kinematic gait measurements and automatic pathological gait pattern diagnostics. *Scandinavian journal of rehabilitation medicine*, 9(3), 95-105.
29. Templeton, G.F. (2011) A Two-Step Approach for Transforming Continuous Variables to Normal: Implications and Recommendations for IS Research. Communications of the AIS, Vol. 28, Article 4.
30. van Andel, C. J., Wolterbeek, N., Doorenbosch, C. A., Veeger, D. H., & Harlaar, J. (2008). Complete 3D kinematics of upper extremity functional tasks. *Gait & posture*, 27(1), 120-127.
31. Veeger, H., & Yu, B. (1996, March). Orientation of axes in the elbow and forearm for biomechanical modelling. In *Biomedical Engineering Conference, 1996., Proceedings of the 1996 Fifteenth Southern* (pp. 377-380). IEEE.

32. Vezina, M. J., & Hubley-Kozey, C. L. (2000). Muscle activation in therapeutic to improve trunk stability. *Archives of physical medicine and rehabilitation*, 81(10), 1370-1379.
33. Wang, G., Zhu, Z., Ding, H., Dang, X., Tang, J., & Zhou, Y. (2009, January). Using virtual markers to explore kinematics of articular bearing surfaces of knee joints. In *13th International Conference on Biomedical Engineering* (pp. 1037-1041). Springer Berlin Heidelberg.
34. Waters, T. R., Putz-Anderson, V., Garg, A., & National Institute for Occupational Safety and Health. (1994). *Applications manual for the revised NIOSH lifting equation* (pp. 94-110). US Department of Health and Human Services, Public Health Service, Centers for Disease Control and Prevention, National Institute for Occupational Safety and Health, Division of Biomedical and Behavioral Science.
35. Whiting, W. C., Gregor, R. J., & Finerman, G. A. (1988). Kinematic analysis of human upper extremity movements in boxing. *The American journal of sports medicine*, 16(2), 130-136.
36. Winter, D. A., Sidwall, H. G., & Hobson, D. A. (1974). Measurement and reduction of noise in kinematics of locomotion. *Journal of biomechanics*, 7(2), 157-159.
37. Workers' Compensation Board of Nova Scotia. (2011). Compensable time-loss claims by body part. Retrieved 11/06, 2014, from <http://www.worksafeforlife.ca/Home/GettingStarted/InjuryStatistics/PartofBody.aspx>
38. Wrigley, A. T., Albert, W. J., Deluzio, K. J., & Stevenson, J. M. (2005). Differentiating lifting technique between those who develop low back pain and those who do not. *Clinical Biomechanics*, 20(3), 254-263.
39. Wu, C. Y., Lin, K. C., Chen, H. C., Chen, I. H., & Hong, W. H. (2007). Effects of modified constraint-induced movement therapy on movement kinematics and daily function in patients with stroke: a kinematic study of motor control mechanisms. *Neurorehabilitation and neural repair*, 21(5), 460-466.
40. Wu, G., Siegler, S., Allard, P., Kirtley, C., Leardini, A., Rosenbaum, D., ... & Stokes, I. (2002). ISB recommendation on definitions of joint coordinate system of various joints for the reporting of human joint motion—part I: ankle, hip, and spine. *Journal of biomechanics*, 35(4), 543-548.

41. Wu, G., Van Der Helm, F. C., Veeger, H. E. J., Makhous, M., Van Roy, P., Anglin, C., ... & Buchholz, B. (2005). ISB recommendation on definitions of joint coordinate systems of various joints for the reporting of human joint motion—Part II: shoulder, elbow, wrist and hand. *Journal of biomechanics*, 38(5), 981-992.
42. Zatsiorsky, V. M. (1998). *Kinematics of human motion*. Human Kinetics.

Appendix A: Results Continued

Qualysis & Flock of Birds Comparison: LTM, HTTN, HTTM

Lifting Task Maximum Reach - Trunk

Shown in Figure 20 is a representative graph of the angular displacement patterns for the trunk as collected by the Qualysis system for the lift and replace task in the extended reach and the two instructional conditions. This graph represents all trials for all participants in this task. As can be visualized there was limited motion during the task. While there were individual differences between the participants, there was minimal motion seen within the individual trials.

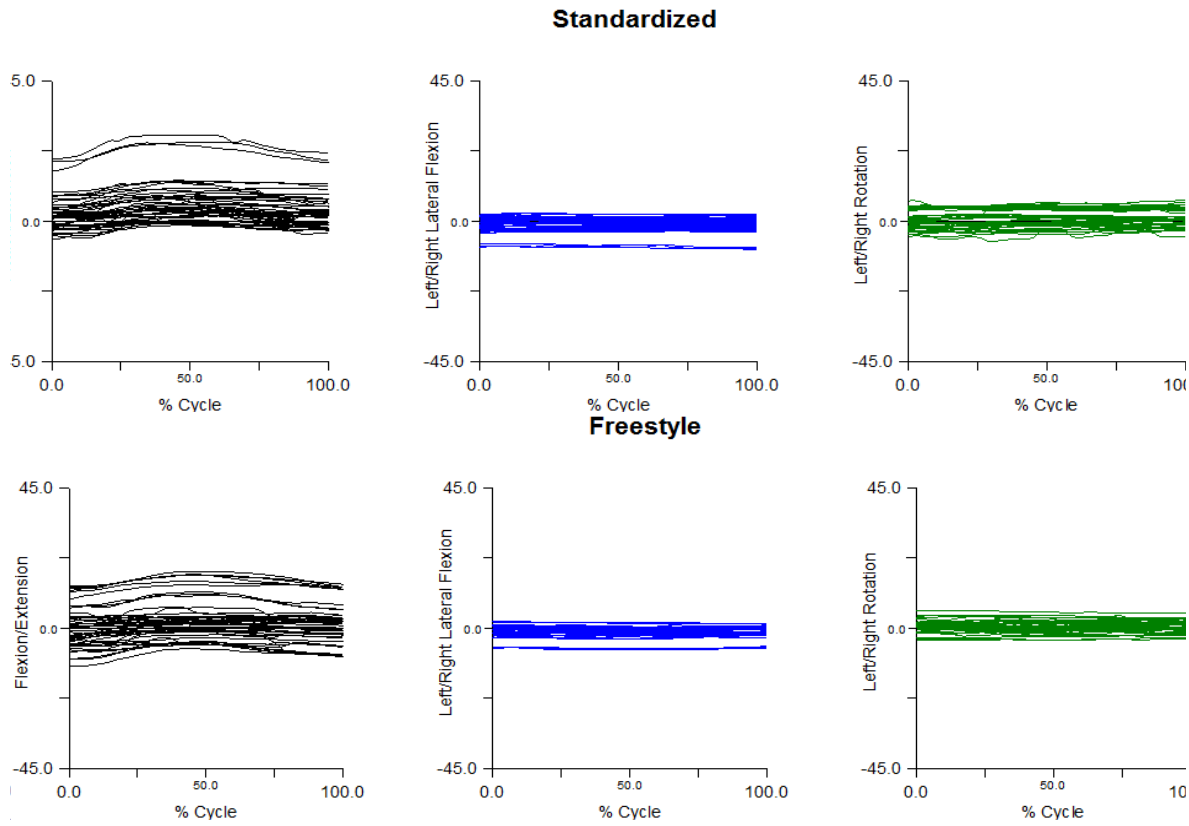


Figure 29. Angle-time graphs showing the angular position of the trunk with reference to the GCS for both the standardized and freestyle conditions as recorded by the Qualysis system. Angles are measured in degrees. Forward flexion and movements in the left are negative; Trunk extension and movements to the right are positive.

Table 6. Average (Standard Deviation) max angular displacement of the trunk in relation to the GCS during the maximum reach lift and replace task. Standard deviation is included in brackets. Units are in degrees.

	Standardized			Freestyle		
	Flex/Ext	Lat. Flex	Axial Rot.	Flex/Ext	Lat. Flex	Axial Rot.
FOB	4.0 (2.3)	1.0 (0.5)	1.6 (1.2)	5.7 (2.6)	0.9 (0.4)	1.7 (1.2)
Qualysis	2.5 (1.8)	0.8 (0.5)	0.9 (0.5)	4.1 (2.3)	0.8 (0.5)	1.1 (0.6)
Difference	1.5 (1.4)	0.2 (0.6)	0.8 (0.7)	1.8 (1.3)	0.1 (0.5)	0.7 (1.1)

Flexion - Extension

A univariate ANOVA was performed to assess the effect of condition and sensor on the output. The analysis considered the main effects as well as the interactions. Shown below in Figure 21 are the means for this data. There was a significant difference due to sensors ($F=27.91$, $df=1,48$, $p<0.001$). There was also a significant difference due to condition ($F=36.78$, $df=1,48$, $p<0.001$). Overall, the means (and SE) varied from 2.4 (± 0.3) to 5.8 (± 0.06) with the freestyle condition having the greater difference.

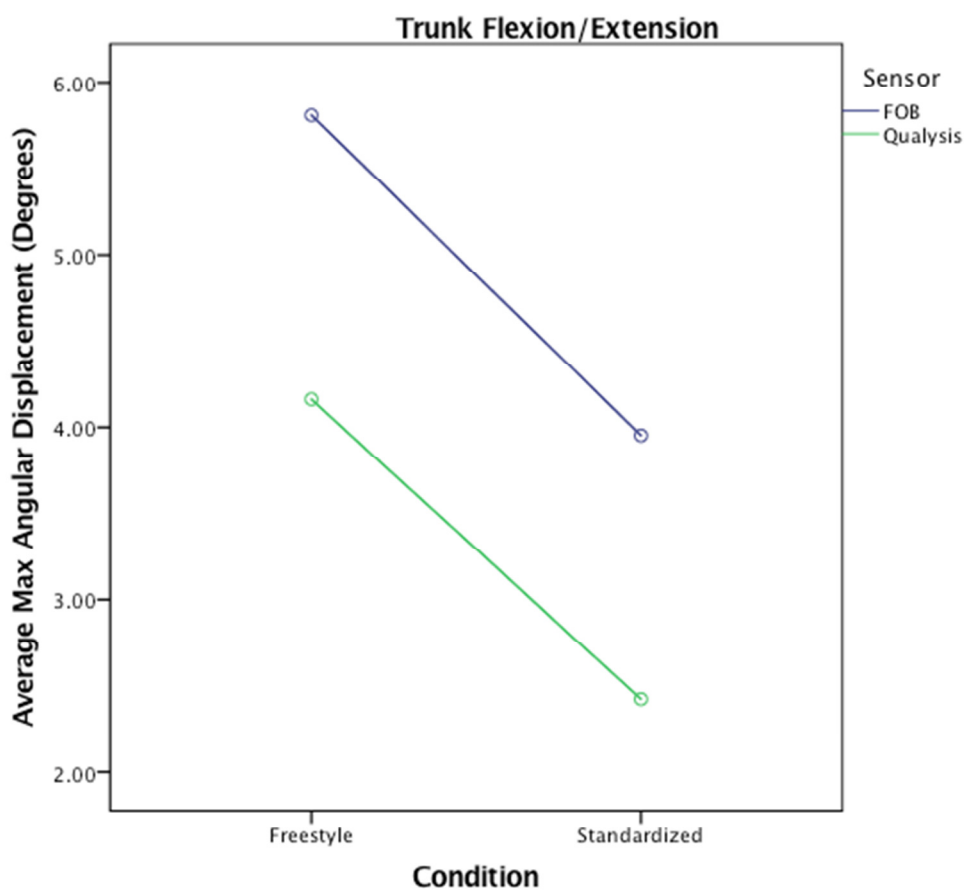


Figure 30: Graphical representation of the output from the univariate ANOVA results.

A Bland-Altman analysis was also performed to assess the agreement between the measures taken from the FOB and Qualysis systems. The max angular displacement data was used once again for this comparison. The mean difference of 1.7 (1.4) was insignificant ($t= 0.68$, $df = 33$, $p=0.497$). The 95%ile confidence interval was ± 2.8 degrees.

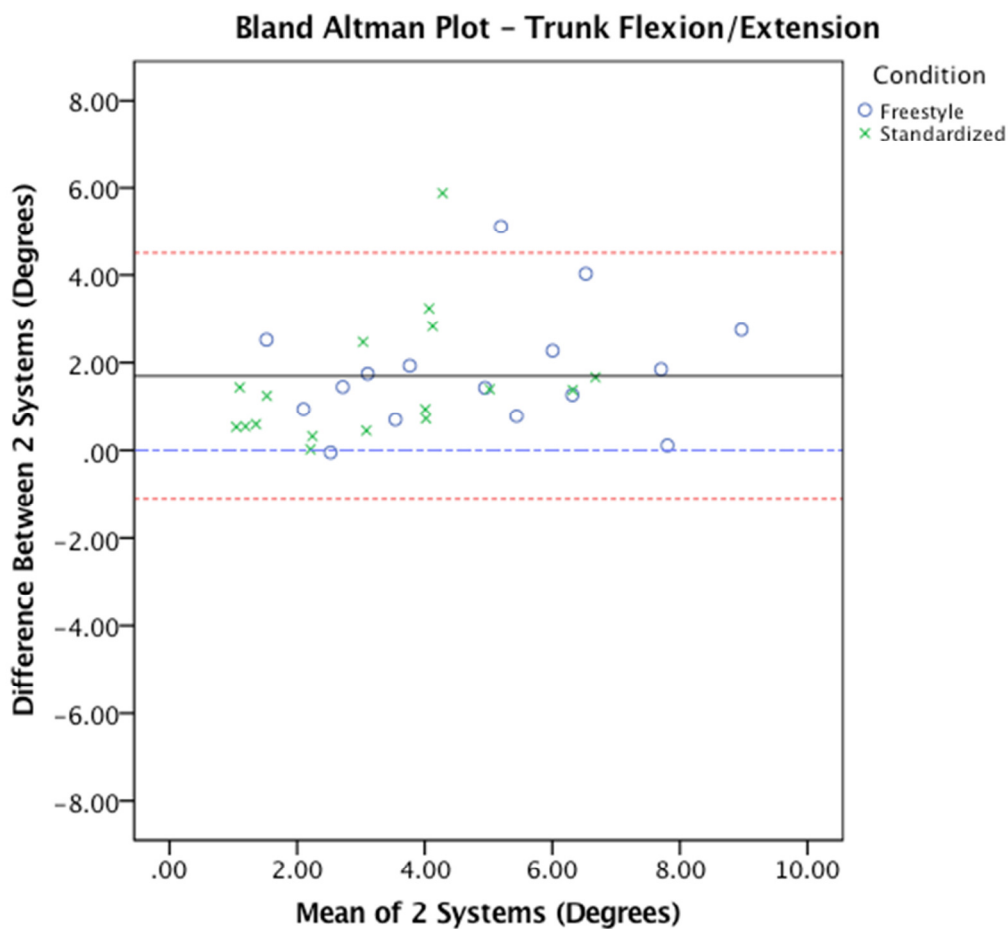


Figure 31: Bland-Altman Plot demonstrating the agreement between the FOB and Qualysis systems while recording trunk flexion/extension during the lift and replace maximum reach task.

Lateral Flexion

A univariate ANOVA was performed to assess the effect of condition and sensor on the output. The analysis considered the main effects as well as the interactions. Shown below in Figure 23 are the means for this data. There was a significant difference due to sensors ($F=5.87$, $df=1,49$, $p= 0.019$). There was no significant difference due to condition ($F=0.004$, $df=1,49$, $p= 0.949$). Overall, the means (and SE) varied from 0.75 (± 0.1) to 0.95 (± 0.1) with the standardized condition having the greater difference.

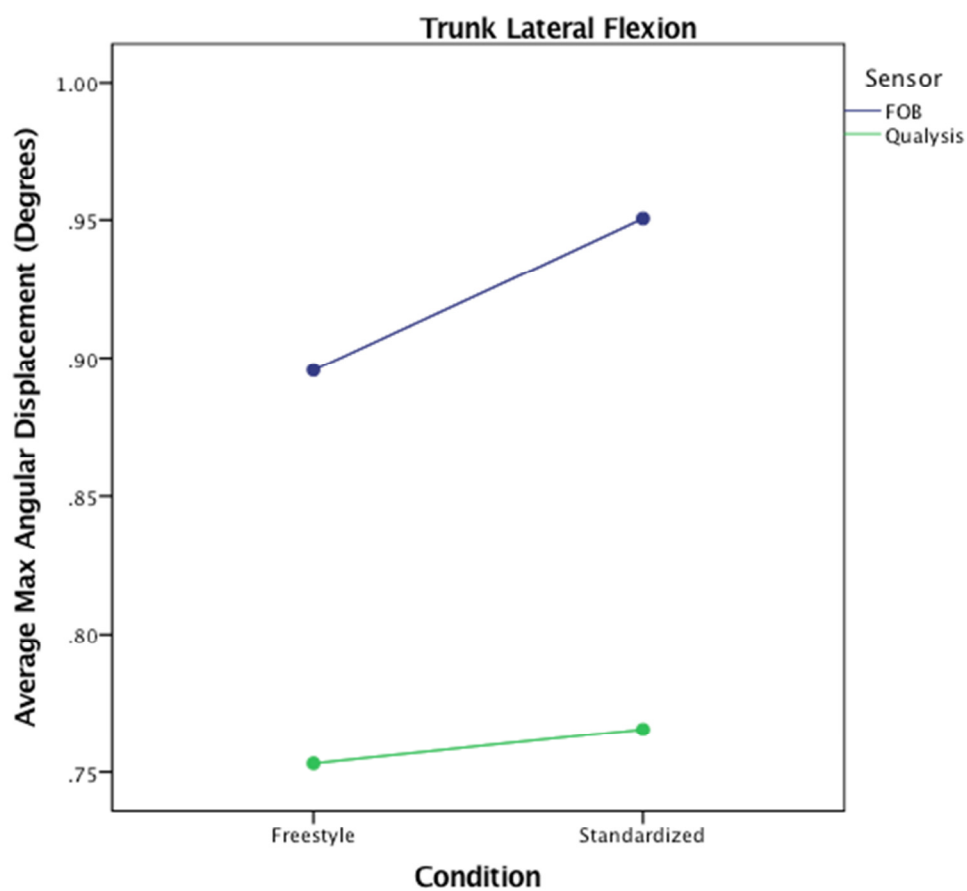


Figure 32: Graphical representation of the output from the univariate ANOVA results.

A Bland-Altman analysis was also performed to assess the agreement between the measures taken from the FOB and Qualysis systems. The max angular displacement data was used once again for this comparison. The mean difference of 0.2 (0.5) was significant ($t = -8.3$, $df = 26$, $p < 0.001$). The 95%ile confidence interval was ± 1.0 degrees.

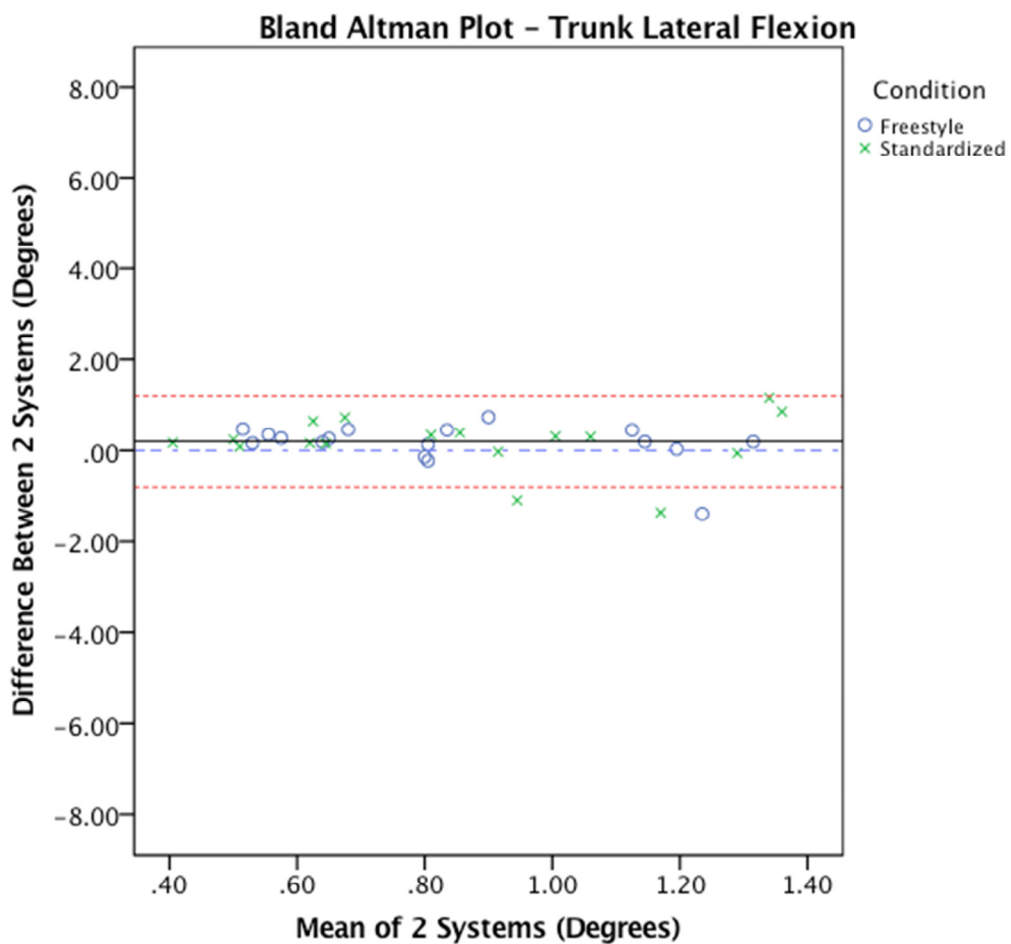


Figure 33: Bland-Altman Plot demonstrating the agreement between the FOB and Qualysis systems while recording lateral tilt during the lift and replace maximum reach task.

Axial Rotation

A univariate ANOVA was performed to assess the effect of condition and sensor on the output. The analysis considered the main effects as well as the interactions. Shown below in Figure 25 are the means for this data. There was a significant difference due to sensors ($F=38.55$, $df=1,49$, $p<0.001$). There wasn't a significant difference due to condition ($F=3.71$, $df=1,49$, $p=0.060$). Overall, the means (and SE) varied from 0.8 (± 0.15) to 1.7 (± 0.15) with the freestyle condition having the greater difference.

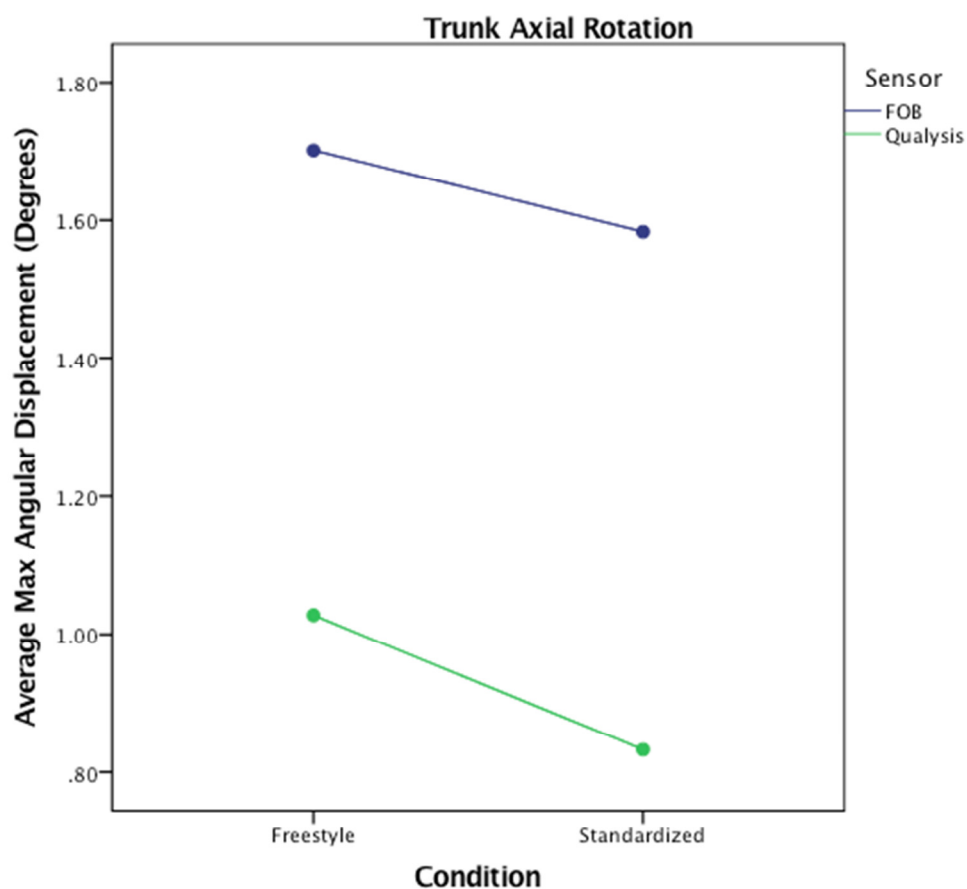


Figure 34: Graphical representation of the output from the univariate ANOVA results.

A Bland-Altman analysis was also performed to assess the agreement between the measures taken from the FOB and Qualysis systems. The max angular displacement data was used once again for this comparison. The mean difference of 0.7 (0.9) was significant ($t = -3.5$, $df = 30$, $p < 0.001$). The 95%ile confidence interval was ± 1.8 degrees.

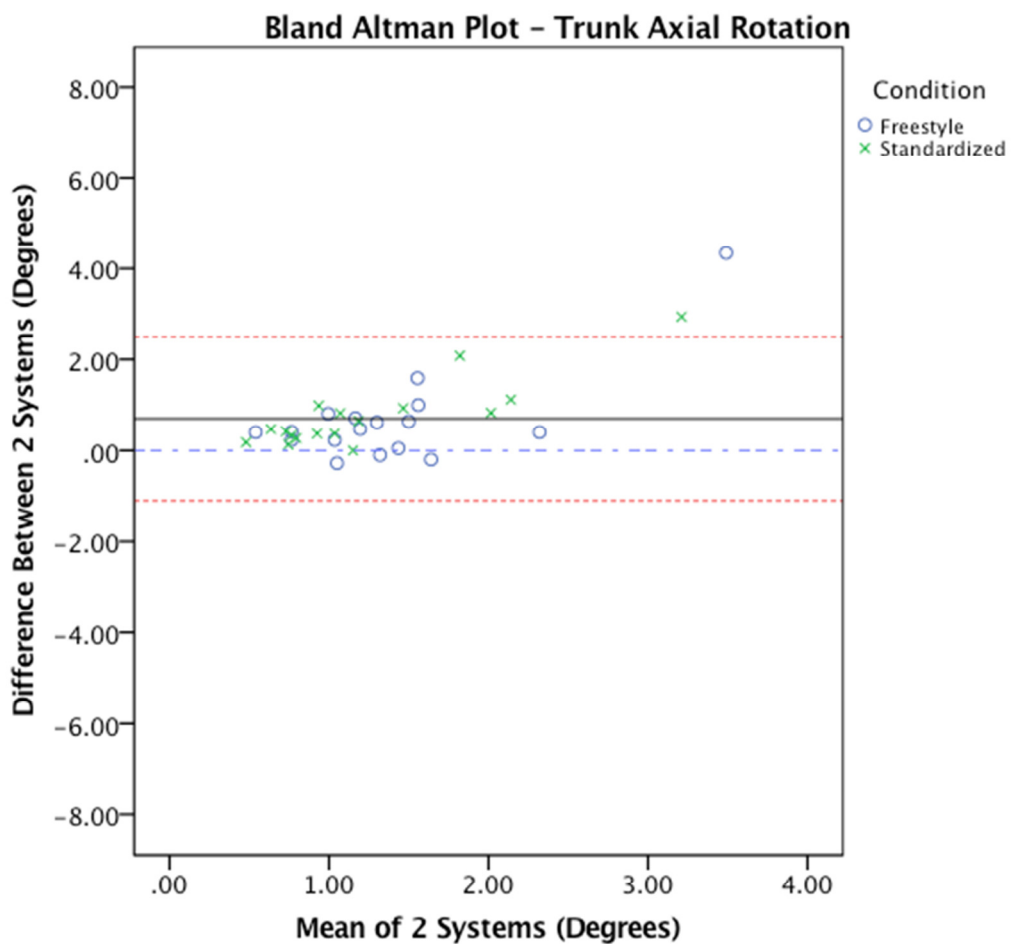


Figure 35: Bland-Altman Plot demonstrating the agreement between the FOB and Qualysis systems while recording axial rotation during the lift and replace extended reach task.

Lifting Task Extended Reach – Pelvis

Shown in Figure 27 is a representative graph of the angular displacement patterns for the pelvis as collected by the Qualysis system for the lift and replace task in the extended reach and the two instructional conditions. This graph represents all trials for all participants in this task. As can be visualized there was limited motion during the task. While there were individual differences between the participants, there was minimal motion seen within the individual trials.

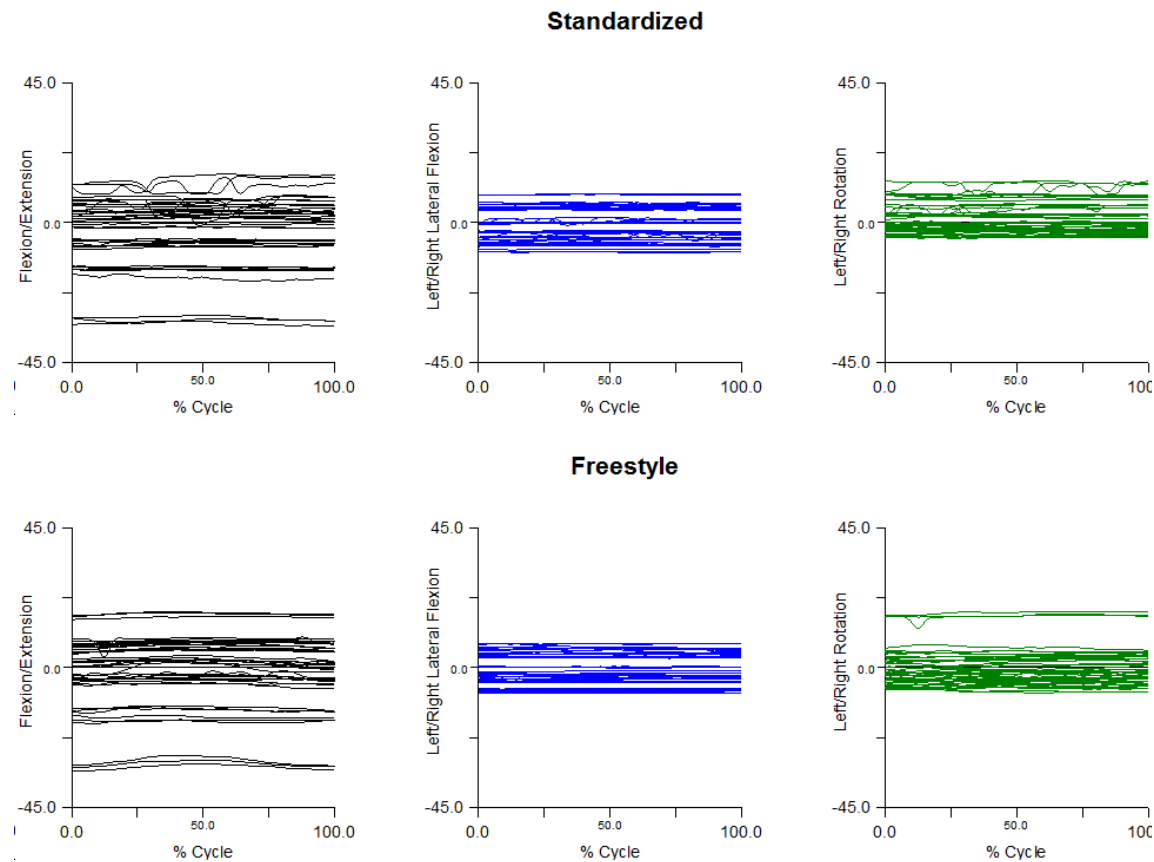


Figure 36. Angle-time graphs showing the angular position of the pelvis with reference to the GCS for both the standardized and freestyle conditions as recorded by the Qualysis system. Angles are measured in degrees. Forward flexion and movements in the left are negative; Trunk extension and movements to the right are positive.

Table 7. Average (Standard Deviation) max angular displacements of the pelvis in relation to the GCS during the maximum reach lift and replace task. Standard deviation is included in brackets. Units are in degrees.

	Standardized			Freestyle		
	Flex/Ext	Lat. Tilt	Axial Rot.	Flex/Ext	Lat. Tilt	Axial Rot.
FOB	1.3 (1.3)	0.3 (0.3)	1.1 (0.9)	1.5 (0.6)	0.4 (0.1)	1.2 (0.5)
Qualysis	0.4 (0.3)	0.2 (0.2)	0.5 (0.3)	1.0 (0.6)	0.2 (0.1)	0.8 (0.5)
Difference	0.6 (0.4)	0.1 (0.1)	0.4 (0.3)	0.5 (0.3)	0.2 (0.1)	0.4 (0.4)

Flexion - Extension

A univariate ANOVA was performed to assess the effect of condition and sensor on the output. The analysis considered the main effects as well as the interactions. Shown below in Figure 28 are the means for this data. There was a significant difference due to sensors ($F=31.65$, $df=1,49$, $p<0.001$). There was also a significant difference due to condition ($F=37.94$, $df=1,49$, $p<0.001$). Overall, the means (and SE) varied from 0.4 (± 0.1) to 1.5 (± 0.1) with the freestyle condition having the greater difference.

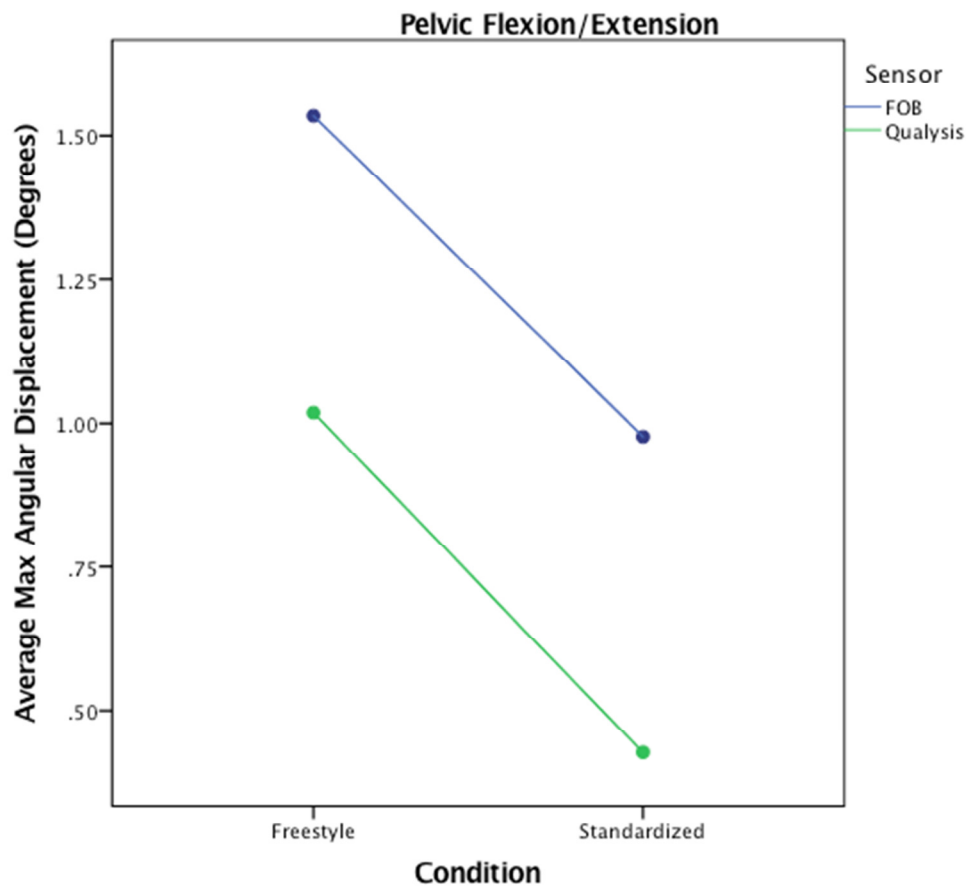


Figure 37: Graphical representation of the output from the univariate ANOVA results.

A Bland-Altman analysis was also performed to assess the agreement between the measures taken from the FOB and Qualysis systems. The max angular displacement data was used once again for this comparison. The mean difference of 0.5 (0.4) was significant ($t = -4.9$, $df = 31$, $p < 0.001$). The 95%ile confidence interval was ± 0.8 degrees.

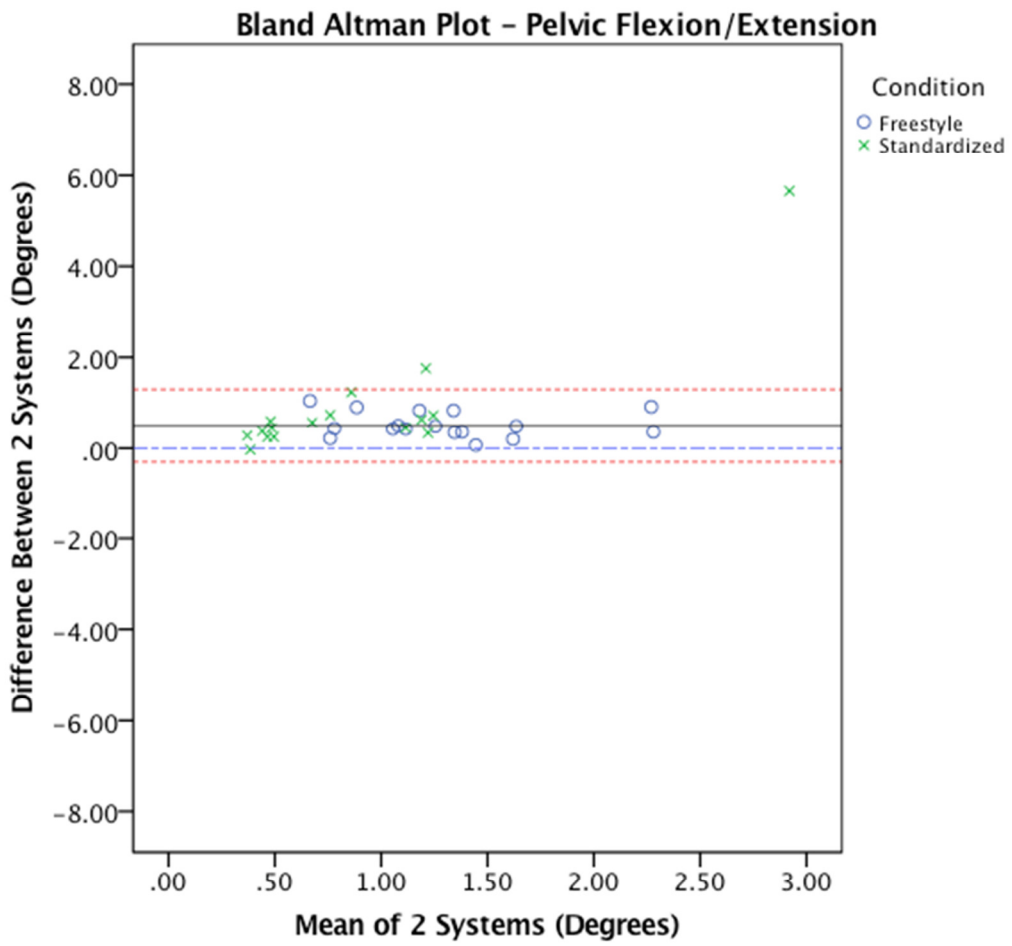


Figure 38: Bland-Altman Plot demonstrating the agreement between the FOB and Qualysis systems while recording pelvic flexion/extension during the lift and replace maximum reach task.

Lateral Flexion

A univariate ANOVA was performed to assess the effect of condition and sensor on the output. The analysis considered the main effects as well as the interactions. Shown below in Figure 30 are the mean and the standard errors for this data. There was a significant difference due to sensors ($F=28.86$, $df=1,49$, $p<0.001$). There was no a significant difference due to condition ($F=1.99$, $df=1,49$, $p= 0.164$). Overall, the means

(and SE) varied from 0.2 (± 0.05) to 0.4 (± 0.05).

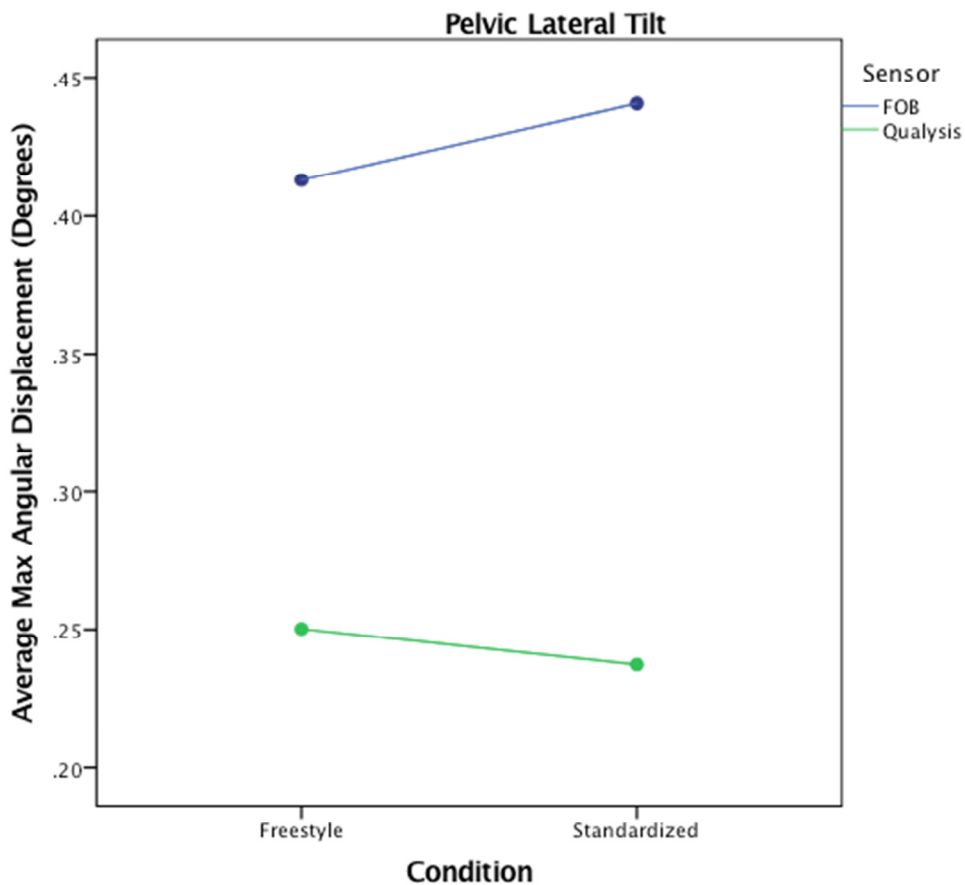


Figure 39: Graphical representation of the output from the univariate ANOVA results

A Bland-Altman analysis was also performed to assess the agreement between the measures taken from the FOB and Qualysis systems. The max angular displacement data was used once again for this comparison. The mean difference of 0.2 (0.3) was significant ($t= 3.7$, $df = 34$, $p<0.001$). The 95%ile confidence interval was ± 0.6 degrees.

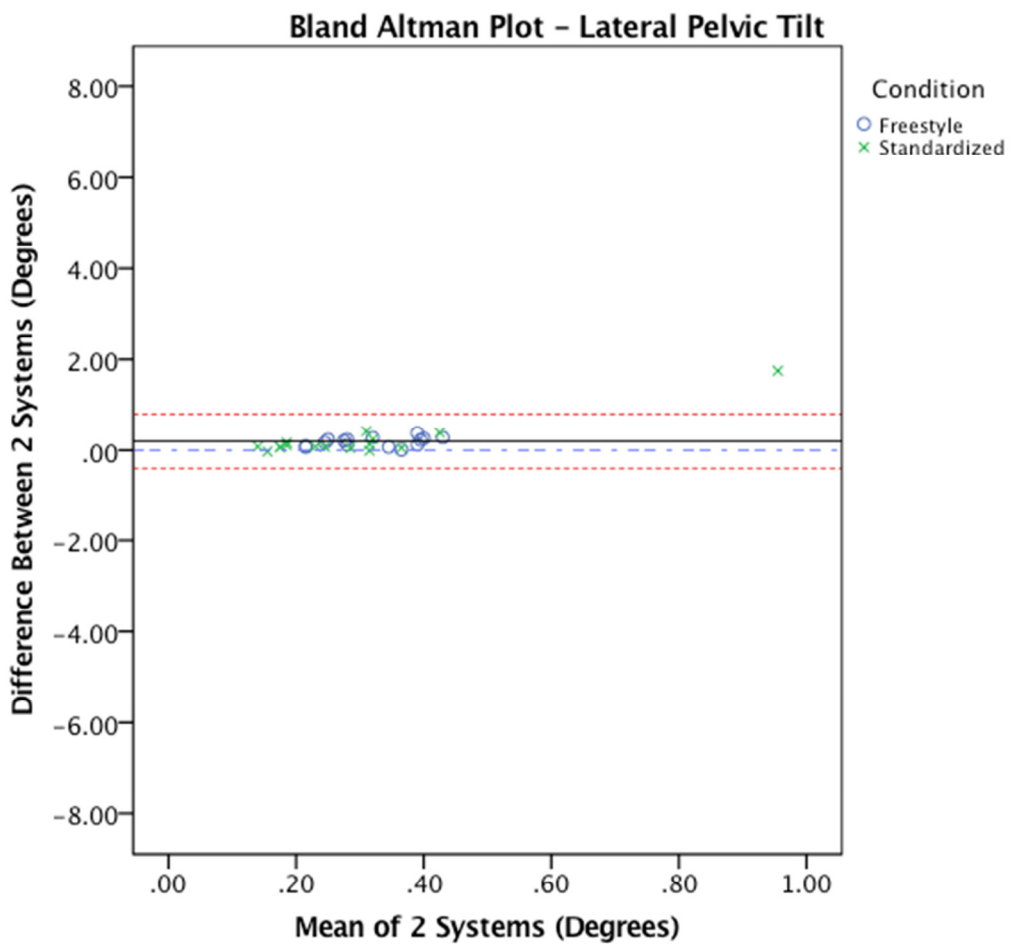


Figure 40: Bland-Altman Plot demonstrating the agreement between the FOB and Qualysis systems while recording lateral pelvic tilt during the lift and replace maximum reach task.

Axial Rotation

A univariate ANOVA was performed to assess the effect of condition and sensor on the output. The analysis considered the main effects as well as the interactions. Shown below in Figure 32 are the means for this data. There was a significant difference due to sensors ($F=44.00$, $df=1,48$, $p<0.001$). There was also a significant difference due to condition ($F=16.36$, $df=1,48$, $p<0.001$). Overall, the means (and SE) varied from 0.5 (± 0.1) to 1.2 (± 0.1) with the freestyle condition having the greater difference.

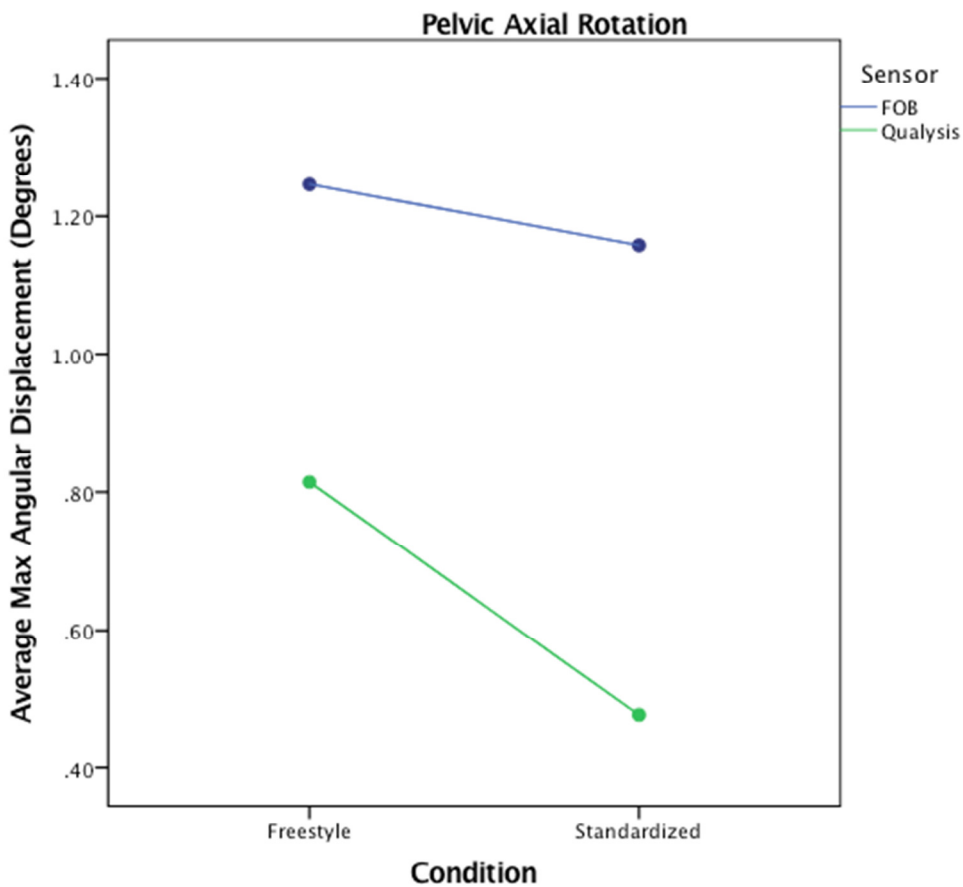


Figure 41: Graphical representation of the output from the univariate ANOVA results

A Bland-Altman analysis was also performed to assess the agreement between the measures taken from the FOB and Qualysis systems. The max angular displacement data was used once again for this comparison. The mean difference of 0.6 (0.7) was significant ($t= 4.8$, $df = 33$, $p<0.001$). The 95%ile confidence interval was ± 1.4 degrees.

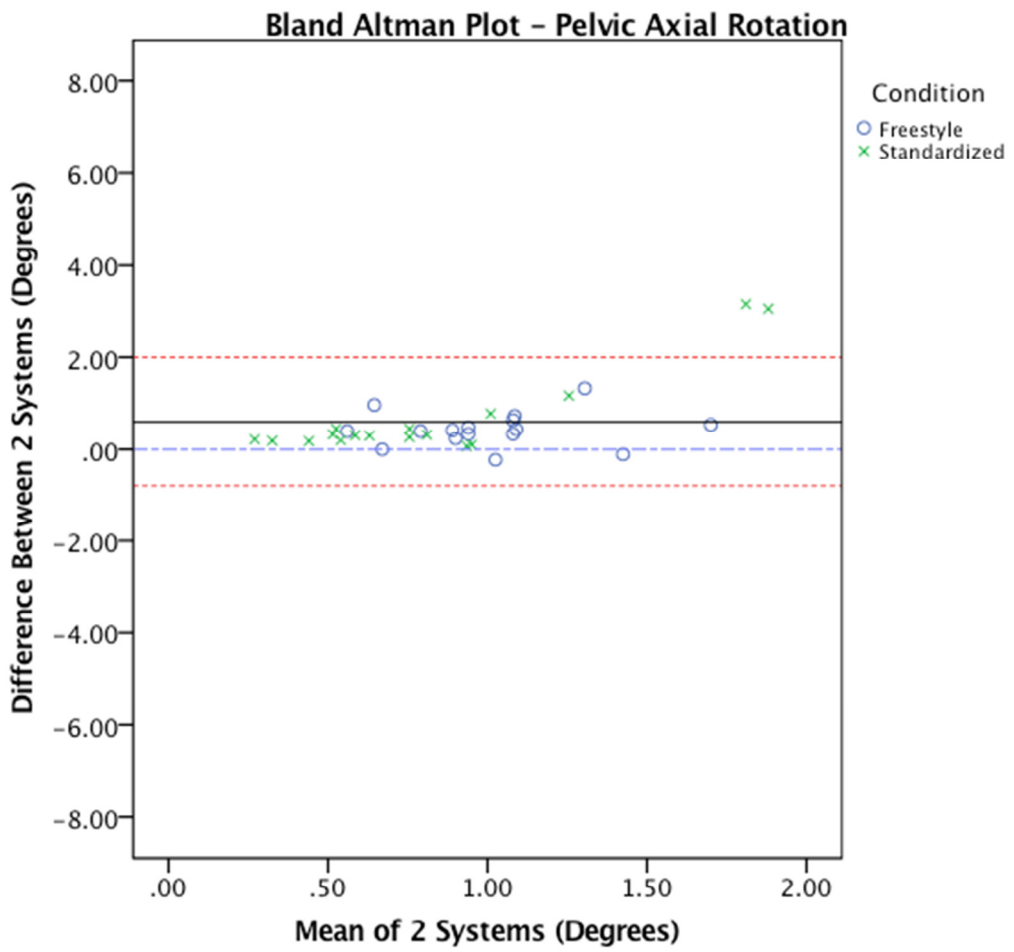


Figure 42: Bland-Altman Plot demonstrating the agreement between the FOB and Qualysis systems while recording pelvic axial rotation during the lift and replace maximum reach task.

Horizontal Transfer Task Normal Reach - Trunk

Shown in Figure 34 is a representative graph of the angular displacement patterns for the trunk as collected by the Qualysis system for the horizontal transfer task in the normal reach and the two instructional conditions. This graph represents all trials for all participants in this task. As can be visualized there was limited motion during the

task. While there were individual differences between the participants, there was minimal motion seen within the individual trials.

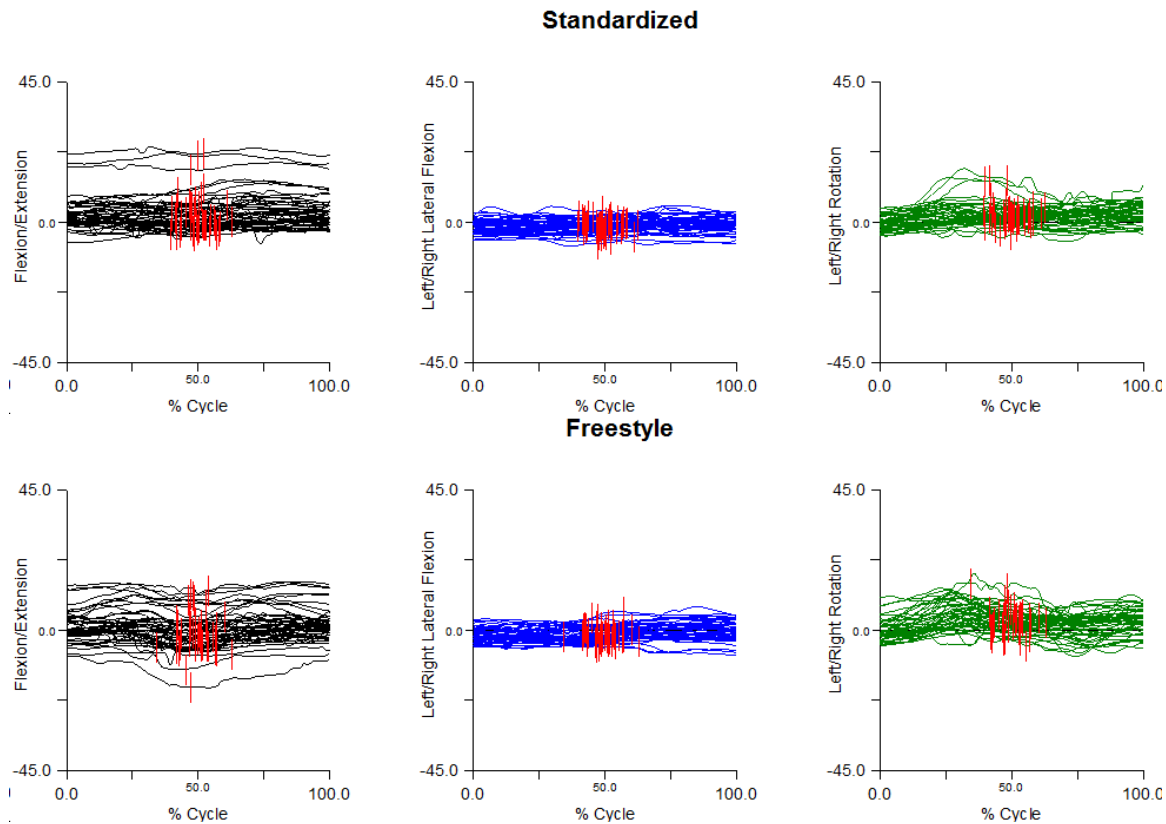


Figure 43. Angle-time graphs showing the angular position of the trunk with reference to the GCS for both the standardized and freestyle conditions as recorded by the Qualysis system. Angles are measured in degrees. Forward flexion and movements in the left are negative; Trunk extension and movements to the right are positive. The red lines represent the moment the lifting load was transfer from right to left hands.

Table 8. Average (Standard Deviation) max angular displacements of the trunk in relation to the GCS during the normal reach lift and horizontal transfer task. Standard deviation is included in brackets. Units are in degrees.

	Standardized			Freestyle		
	Flex/Ext	Lat. Flex.	Axial Rot.	Flex/Ext	Lat. Flex.	Axial Rot.
FOB	5.1 (2.6)	2.7 (1.5)	6.6 (2.8)	6.1 (2.4)	3.9 (1.7)	10.0 (4.1)
Qualysis	3.1 (1.8)	2.2 (1.3)	5.1 (2.5)	4.0 (1.8)	3.2 (1.6)	8.4 (4.0)
Difference	2.0 (2.1)	0.5 (0.8)	1.5 (1.4)	1.8 (1.6)	0.8 (0.7)	1.4 (1.0)

Flexion – Extension

A univariate ANOVA was performed to assess the effect of condition and sensor on the output. The analysis considered the main effects as well as the interactions. Shown below in Figure 35 are the means for this data. There was a significant difference due to sensors ($F=43.62$, $df=1,49$, $p<0.001$). There was also a significant difference due to condition ($F=13.17$, $df=1,49$, $p= 0.001$). Overall, the means (and SE) varied from 3.2 (± 0.3) to 6.1 (± 0.3) with the freestyle condition having the greater difference.

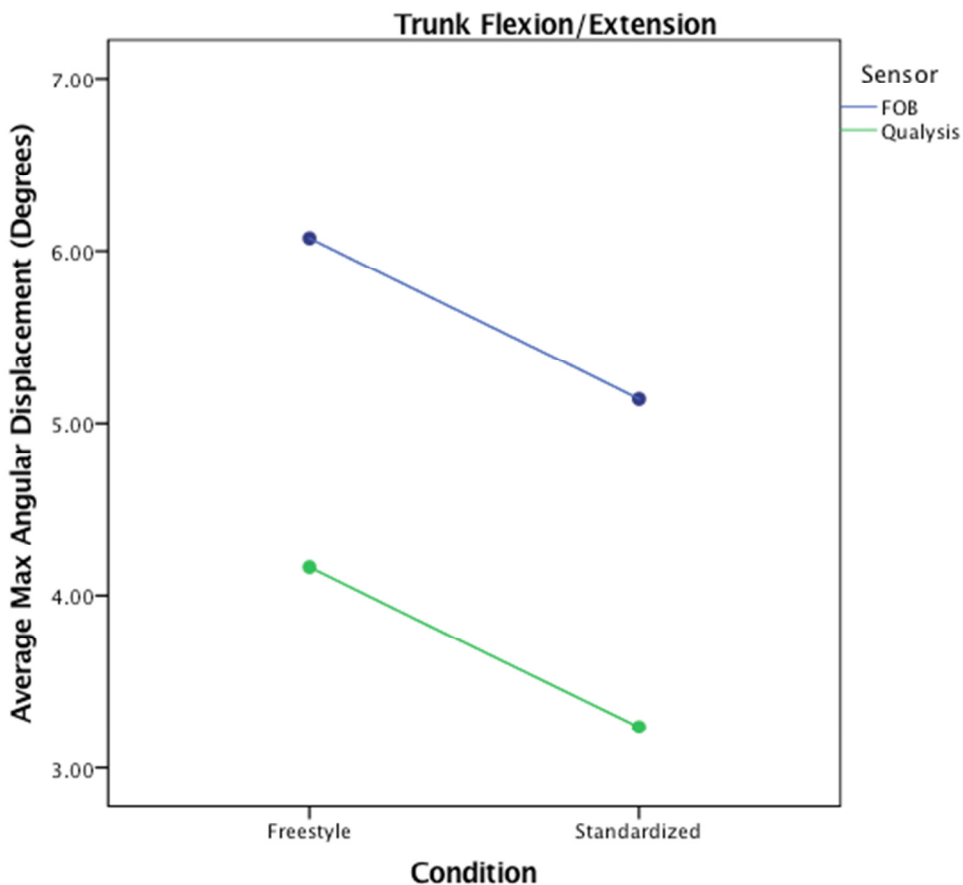


Figure 44: Graphical representation of the output from the univariate ANOVA results.

A Bland-Altman analysis was also performed to assess the agreement between the measures taken from the FOB and Qualysis systems. The max angular displacement data was used once again for this comparison. The mean difference of 1.9 (1.9) was significant ($t= 2.1$, $df = 33$, $p=0.042$). The 95%ile confidence interval was ± 3.8 degrees.

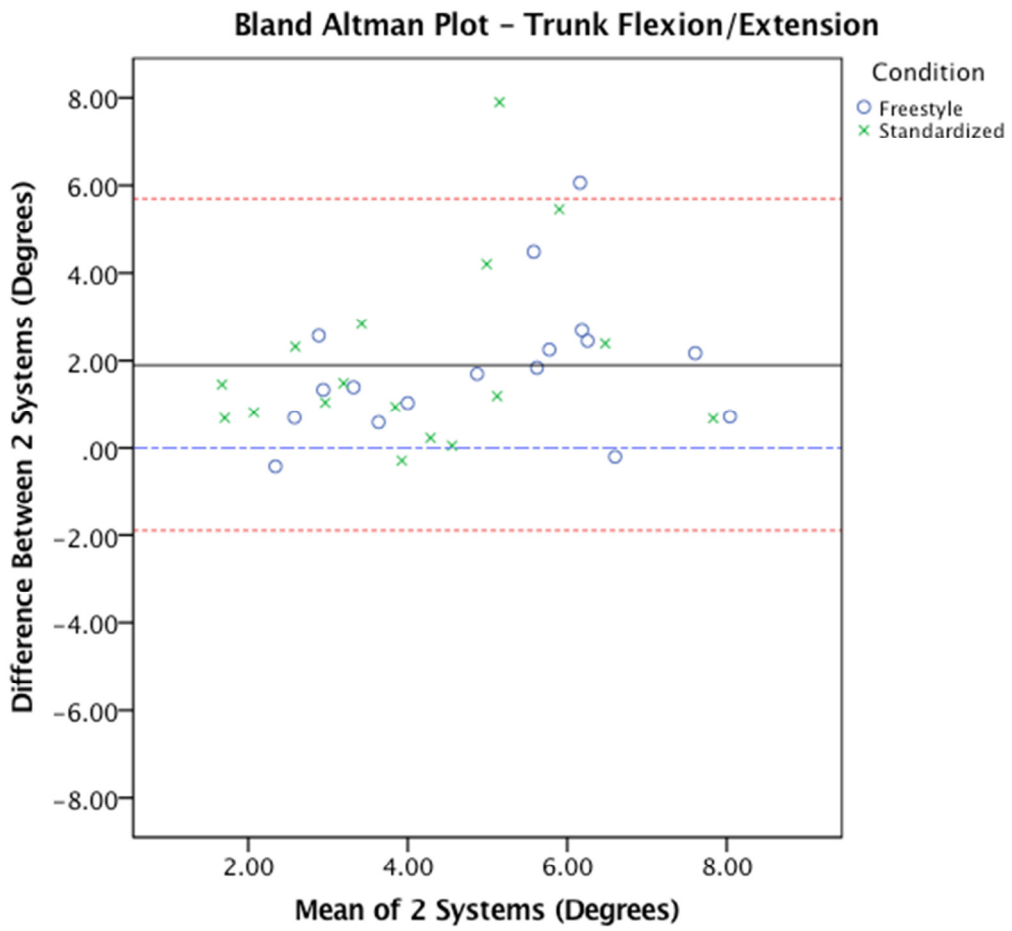


Figure 45: Bland-Altman Plot demonstrating the agreement between the FOB and Qualysis systems while recording trunk flexion/extension during the horizontal transfer task normal reach task.

Lateral Flexion

A univariate ANOVA was performed to assess the effect of condition and sensor on the output. The analysis considered the main effects as well as the interactions. Shown below in Figure 38 are the means for this data. There was a significant difference due to sensors ($F=14.91$, $df=1,49$, $p<0.001$). There was also a significant difference due to condition ($F=42.72$, $df=1,49$, $p<0.001$). Overall, the means (and SE) varied from 2.1

(± 0.2) to 3.9 (± 0.2) with the freestyle condition having the greater difference.

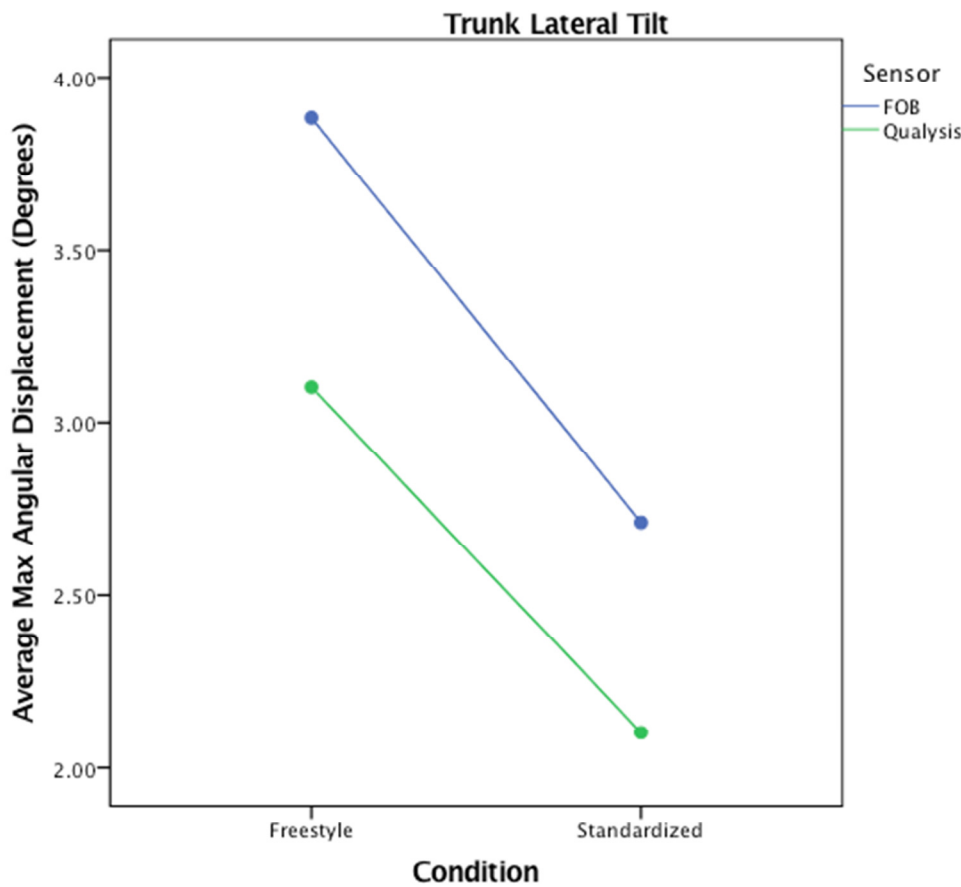


Figure 46: Graphical representation of the output from the univariate ANOVA results.

A Bland-Altman analysis was also performed to assess the agreement between the measures taken from the FOB and Qualysis systems. The max angular displacement data was used once again for this comparison. The mean difference of 0.6 (0.8) was significant ($t= 5.1$, $df = 30$, $p<0.001$). The 95%ile confidence interval was ± 1.6 degrees.

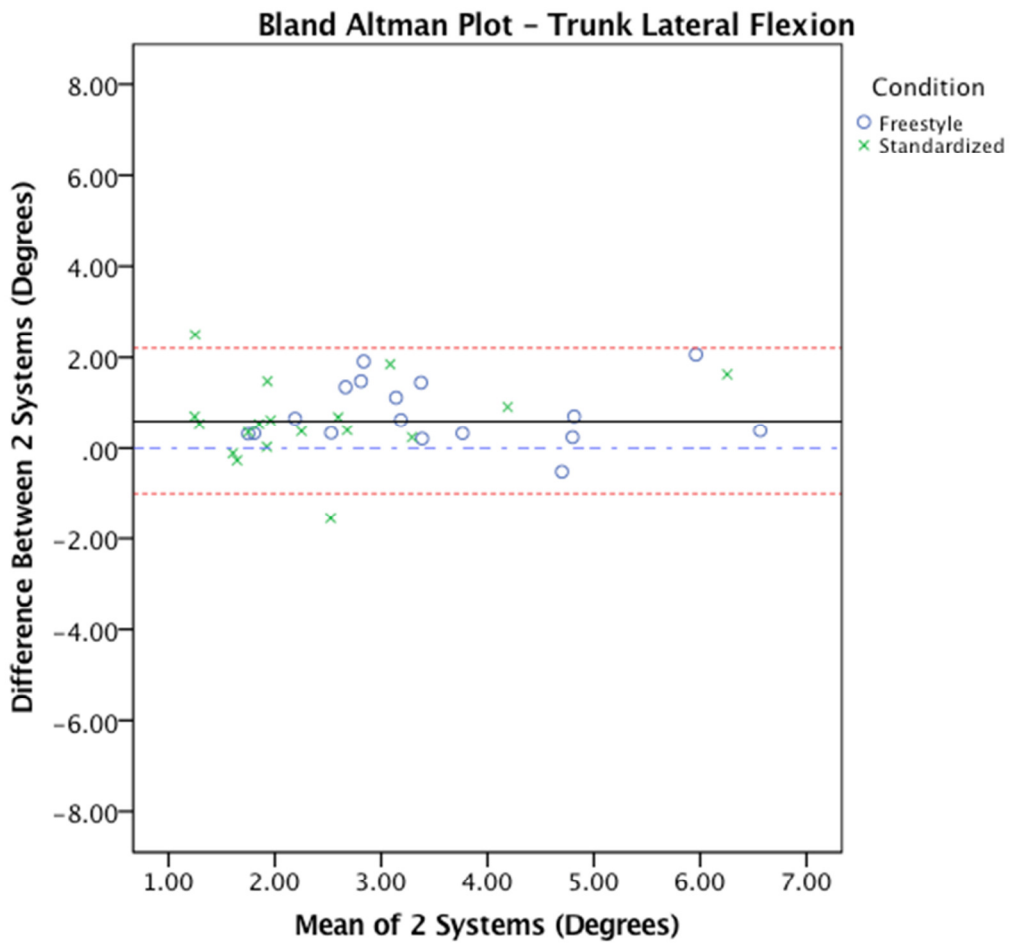


Figure 47: Bland-Altman Plot demonstrating the agreement between the FOB and Qualysis systems while recording trunk lateral flexion during the horizontal transfer task normal reach task.

Axial Rotation

A univariate ANOVA was performed to assess the effect of condition and sensor on the output. The analysis considered the main effects as well as the interactions. Shown below in Figure 40 are the means for this data. There was a significant difference due to sensors ($F=14.39$, $df=1,49$, $p<0.001$). There was also a significant difference due to condition ($F=55.34$, $df=1,49$, $p<0.001$). Overall, the means (and SE) varied from 5.2

(± 0.5) to 10.0 (± 0.5) with the freestyle condition having the greater difference.

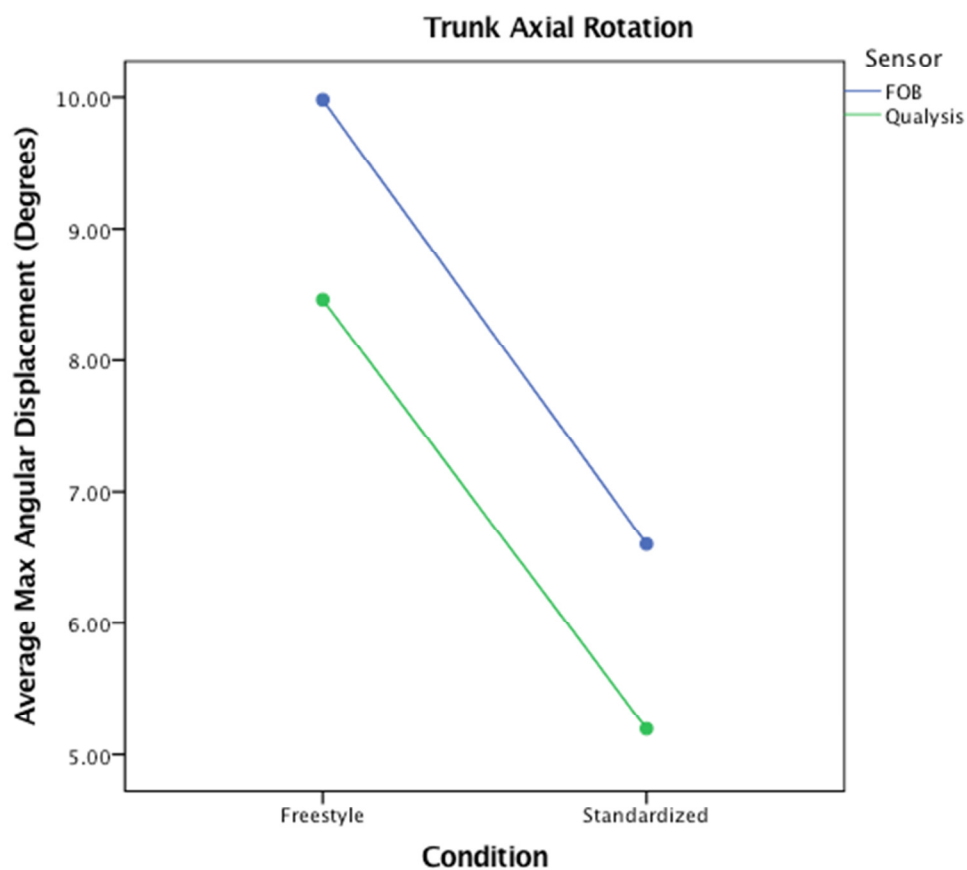


Figure 48: Graphical representation of the output from the univariate ANOVA results

A Bland-Altman analysis was also performed to assess the agreement between the measures taken from the FOB and Qualysis systems. The max angular displacement data was used once again for this comparison. The mean difference of 1.5 (1.3) was significant ($t= 2.4$, $df = 32$, $p=0.033$). The 95%ile confidence interval was ± 2.6 degrees.

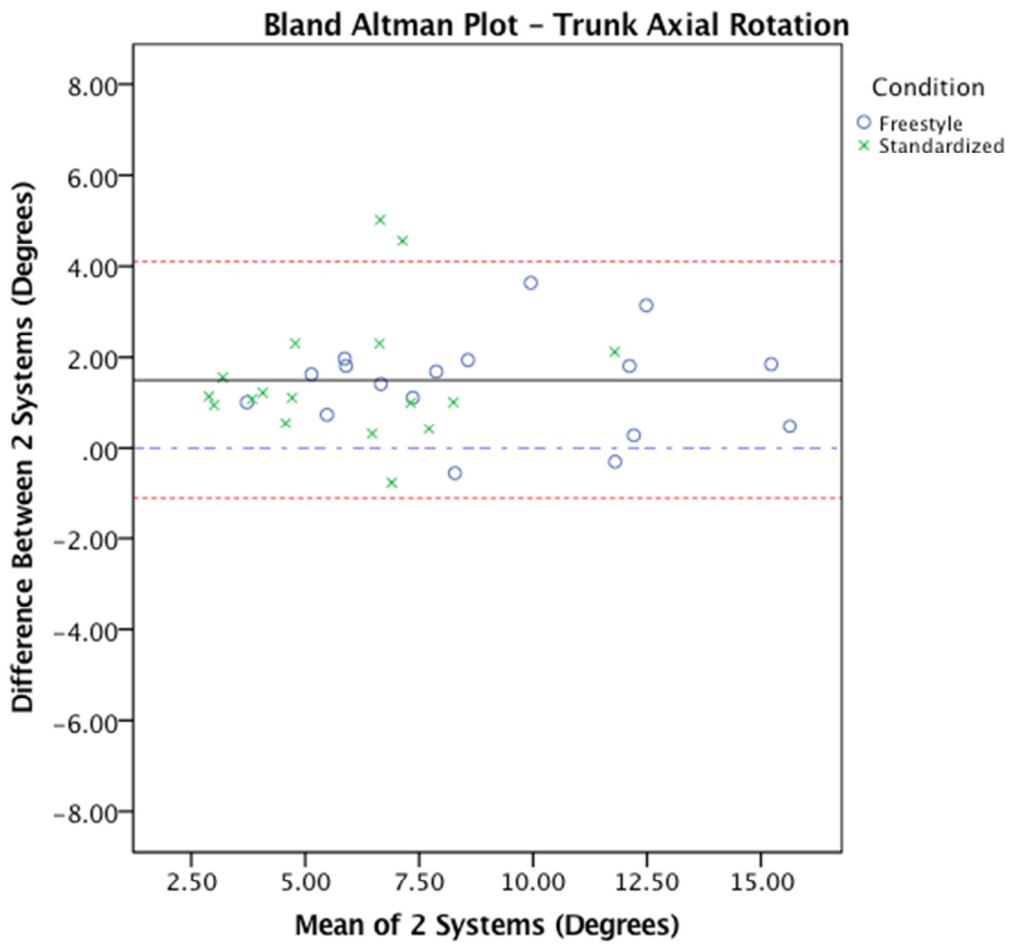


Figure 49: Bland-Altman Plot demonstrating the agreement between the FOB and Qualysis systems while recording trunk axial rotation during the horizontal transfer task normal reach task.

Horizontal Transfer Task Normal Reach – Pelvis

Shown in Figure 42 is a representative graph of the angular displacement patterns for the pelvis as collected by the Qualysis system for the horizontal transfer task in the normal reach and the two instructional conditions. This graph represents all trials for all participants in this task. As can be visualized there was limited motion during the task. While there were individual differences between the participants, there was minimal motion seen within the individual trials.

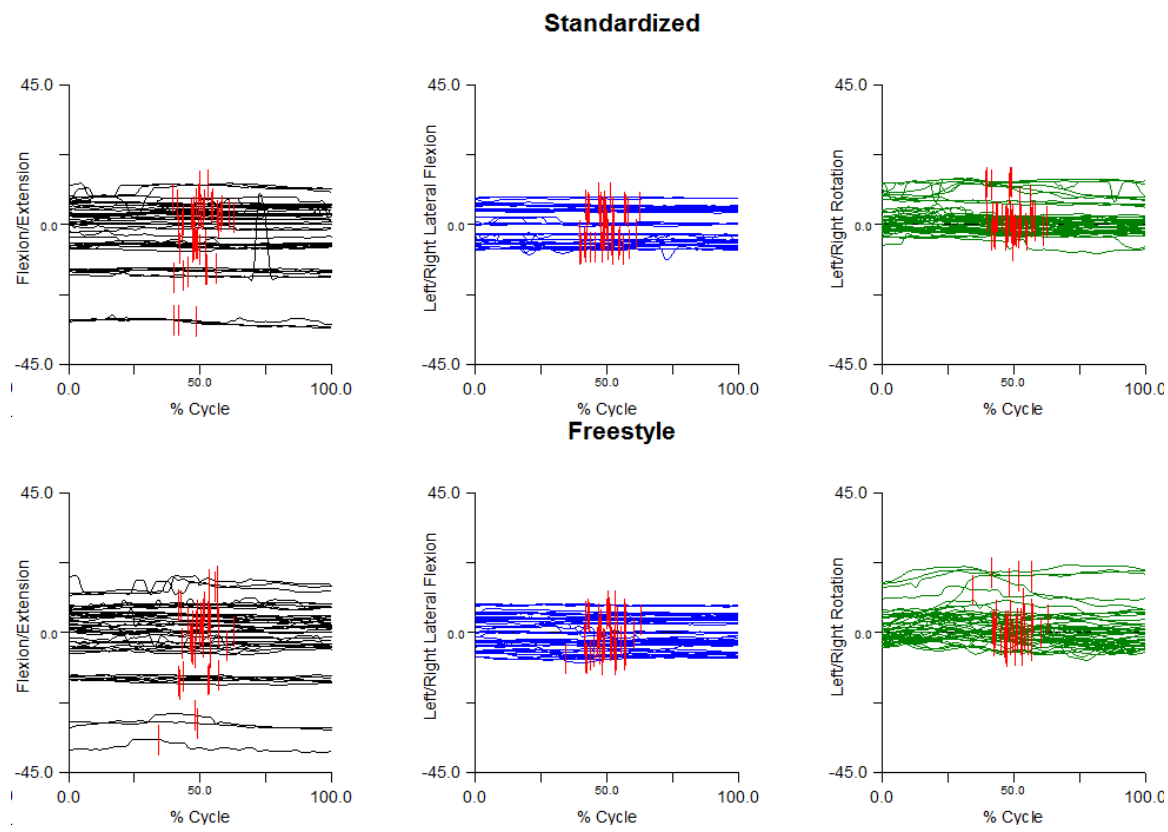


Figure 50. Angle-time graphs showing the angular position of the pelvis relative to the GCS as recorded by the Qualysis system. Angles are measured in degrees. Forward flexion and movements in the left are negative; Trunk extension and movements to the right are positive. The red lines represent the moment the lifting load was transferred from right to left hands.

Table 9. Average (Standard Deviation) max angular displacements of the pelvis in relation to the GCS during the normal reach lift and horizontal transfer task. Standard deviation is included in brackets. Units are in degrees.

	Standardized			Freestyle		
	Flex/Ext	Lat. Tilt	Axial Rot.	Flex/Ext	Lat. Tilt	Axial Rot.
FOB	2.0 (1.5)	1.3 (1.3)	3.8 (2.0)	2.8 (1.4)	1.5 (1.3)	6.0 (3.0)
Qualysis	0.8 (0.5)	0.5 (0.3)	2.4 (1.6)	1.4 (0.6)	0.7 (0.4)	5.0 (2.6)
Difference	1.2 (1.4)	0.9 (1.1)	1.4 (1.7)	1.2 (1.1)	0.8 (1.0)	0.9 (0.8)

Flexion – Extension

A univariate ANOVA was performed to assess the effect of condition and sensor on the output. The analysis considered the main effects as well as the interactions. Shown below in Figure 43 are the means for this data. There was a significant difference due to sensors ($F=46.05$, $df=1,49$, $p<0.001$). There was also a significant difference due to condition ($F=23.49$, $df=1,49$, $p<0.001$). Overall, the means (and SE) varied from 0.9 (± 0.2) to 2.8(± 0.2) with the freestyle condition having the greater difference.

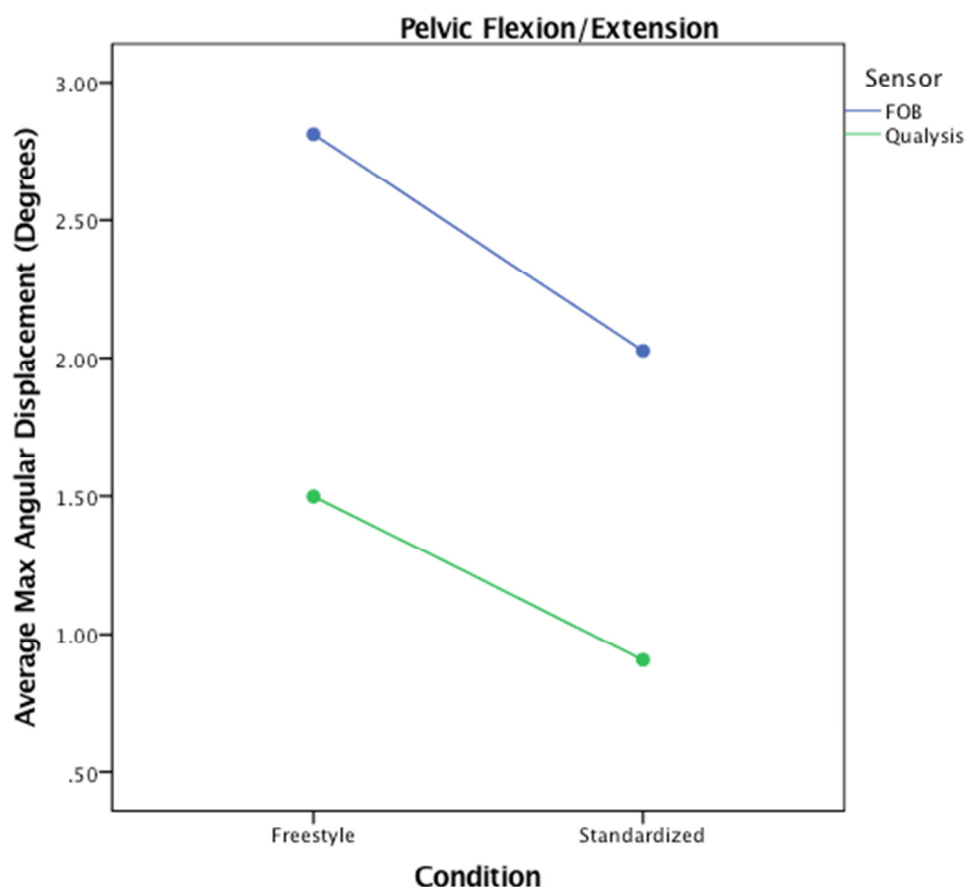


Figure 51: Graphical representation of the output from the univariate ANOVA results

A Bland-Altman analysis was also performed to assess the agreement between the measures taken from the FOB and Qualysis systems. The max angular displacement

data was used once again for this comparison. The mean difference of 1.2 (1.2) was insignificant ($t = -0.8$, $df = 31$, $p=0.394$). The 95%ile confidence interval was ± 2.4 degrees. There appears to be a linear trend in the graphic output.

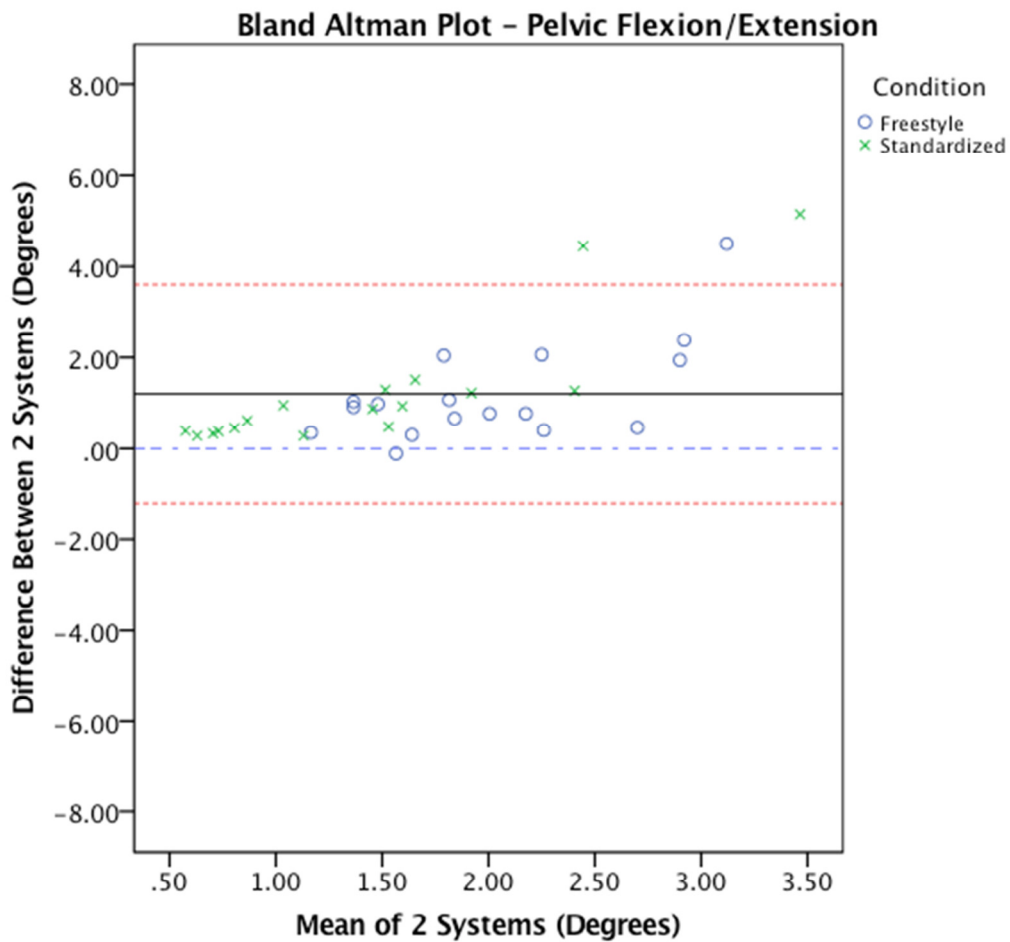


Figure 52: Bland-Altman Plot demonstrating the agreement between the FOB and Qualysis systems while recording pelvic flexion/extension during the horizontal transfer task normal reach task.

Lateral Flexion

A univariate ANOVA was performed to assess the effect of condition and sensor on the output. The analysis considered the main effects as well as the interactions. Shown below in Figure 45 are the means for this data. There was a significant difference due to sensors ($F=53.53$, $df=1,48$, $p<0.001$). There was also a significant difference due to condition ($F=7.03$, $df=1,48$, $p=0.01$). Overall, the means (and SE) varied from 0.5 (± 0.1) to 1.3(± 0.15).

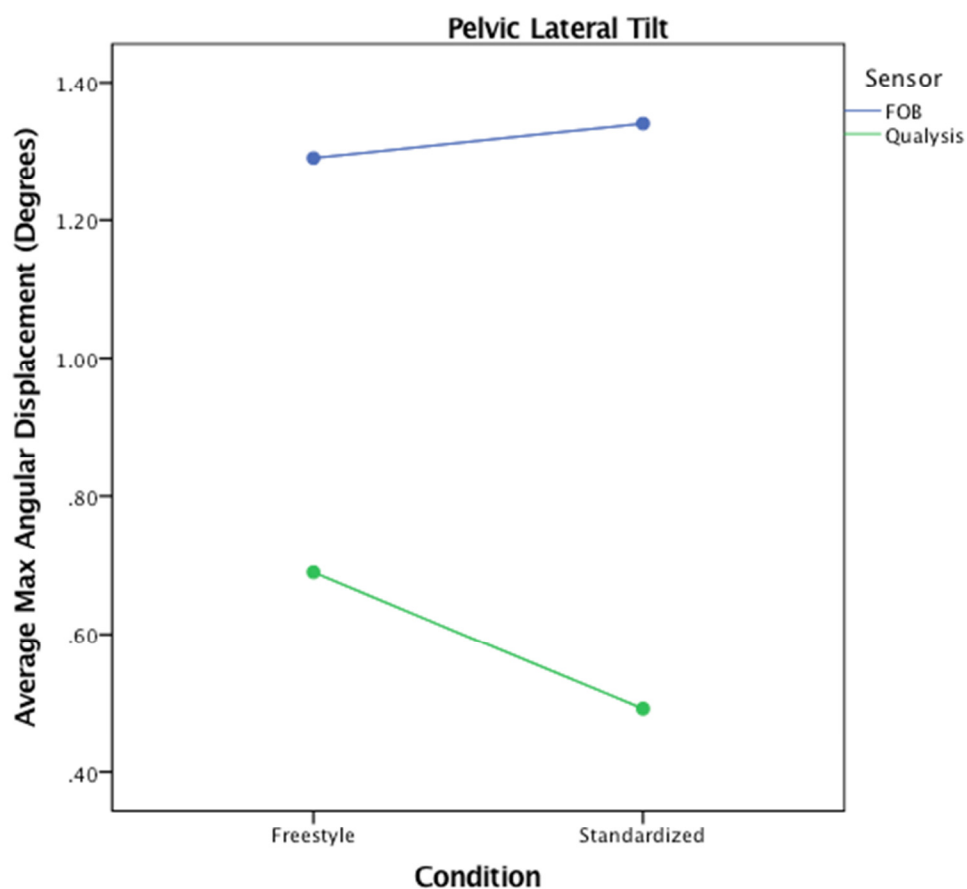


Figure 53: Graphical representation of the output from the univariate ANOVA results.

A Bland-Altman analysis was also performed to assess the agreement between the measures taken from the FOB and Qualysis systems. The max angular displacement data was used once again for this comparison. The mean difference of 0.9 (1.0) was significant ($t = -3.2$, $df = 29$, $p=0.003$). The 95%ile confidence interval was ± 2.0 degrees.

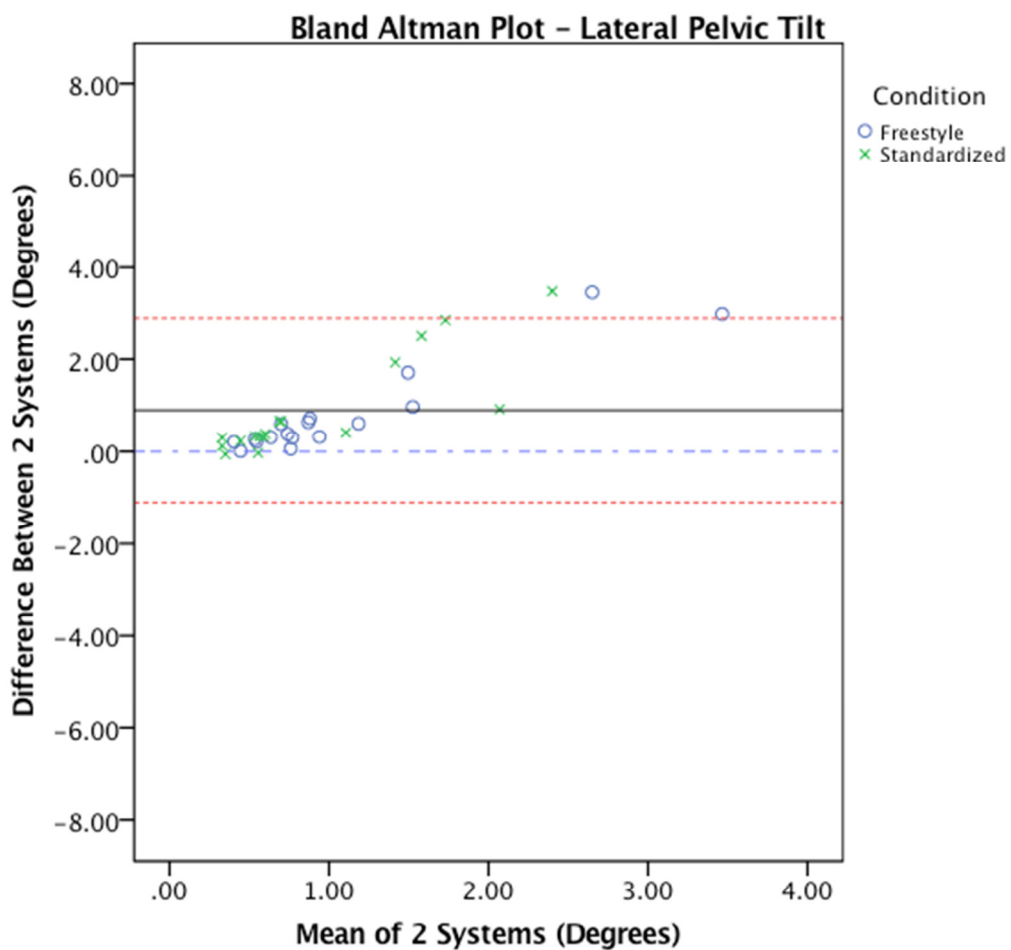


Figure 54: Bland-Altman Plot demonstrating the agreement between the FOB and Qualysis systems while recording pelvic lateral tilt during the horizontal transfer task normal reach task.

Axial Rotation

A univariate ANOVA was performed to assess the effect of condition and sensor on the output. The analysis considered the main effects as well as the interactions. Shown below in Figure 47 are the means for this data. There was a significant difference due to sensors ($F=18.37$, $df=1,49$, $p<0.001$). There was also a significant difference due to condition ($F=78.54$, $df=1,49$, $p<0.001$). Overall, the means (and SE) varied from 2.5 (± 0.3) to 6.2(± 0.3) with the freestyle condition having the greater difference.

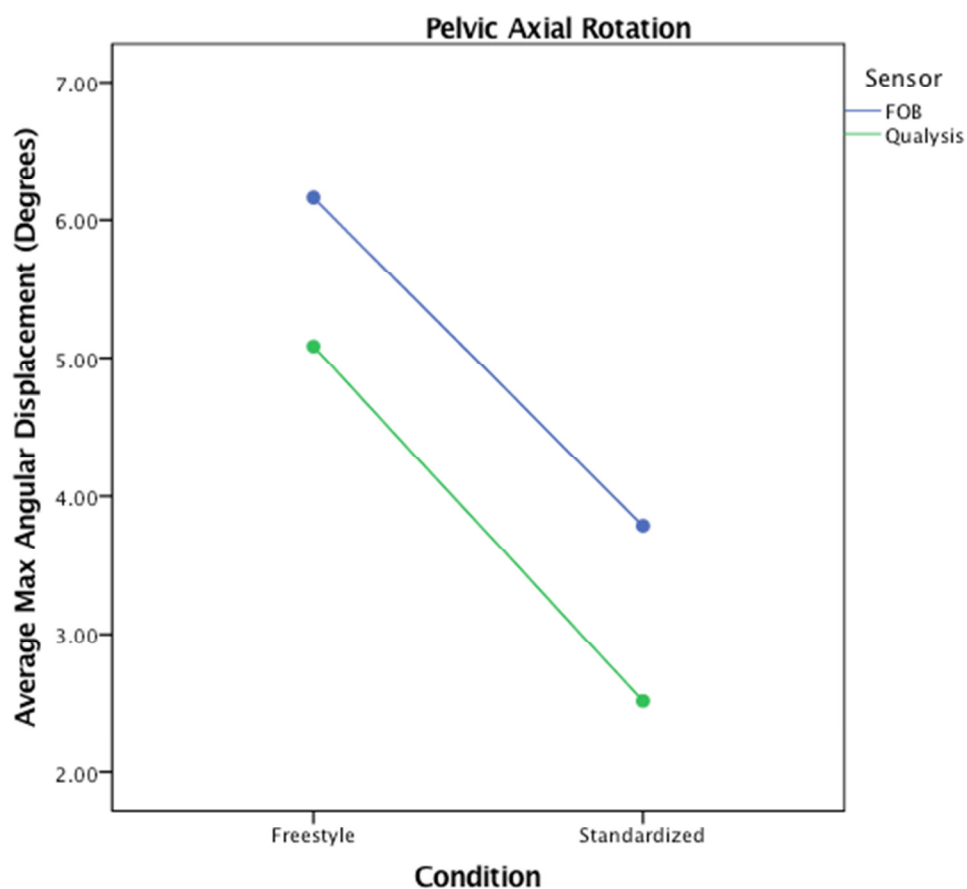
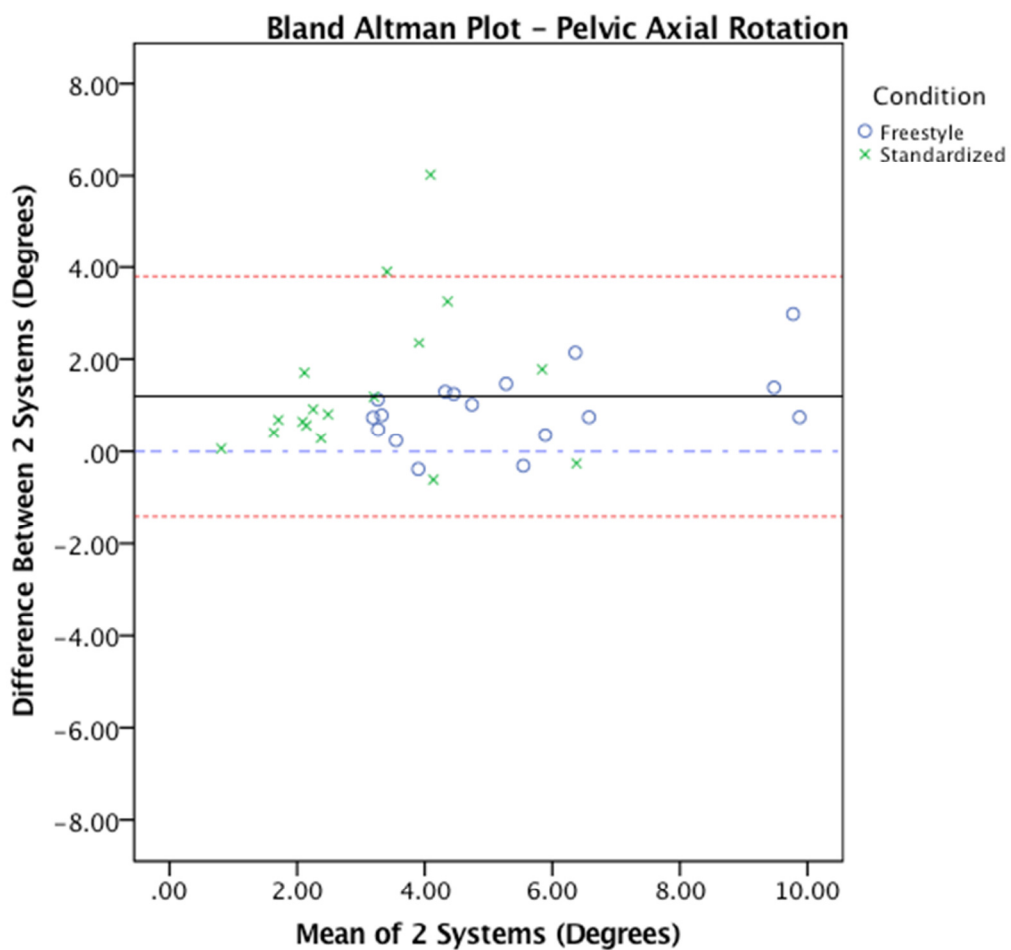


Figure 55: Graphical representation of the output from the univariate ANOVA results.

A Bland-Altman analysis was also performed to assess the agreement between the measures taken from the FOB and Qualysis systems. The max angular displacement data was used once again for this comparison. The mean difference of 1.2 (1.3) was insignificant ($t = -0.2$, $df = 33$, $p=0.812$). The 95%ile confidence interval was ± 2.6 degrees.



Horizontal Transfer Task Maximum Reach - Trunk

Shown in Figure 49 is a representative graph of the angular displacement patterns for the trunk as collected by the Qualysis system for the horizontal transfer task in the maximum reach and the two instructional conditions. This graph represents all trials for all participants in this task. As can be visualized there was limited motion during the task. While there were individual differences between the participants, there was minimal motion seen within the individual trials.

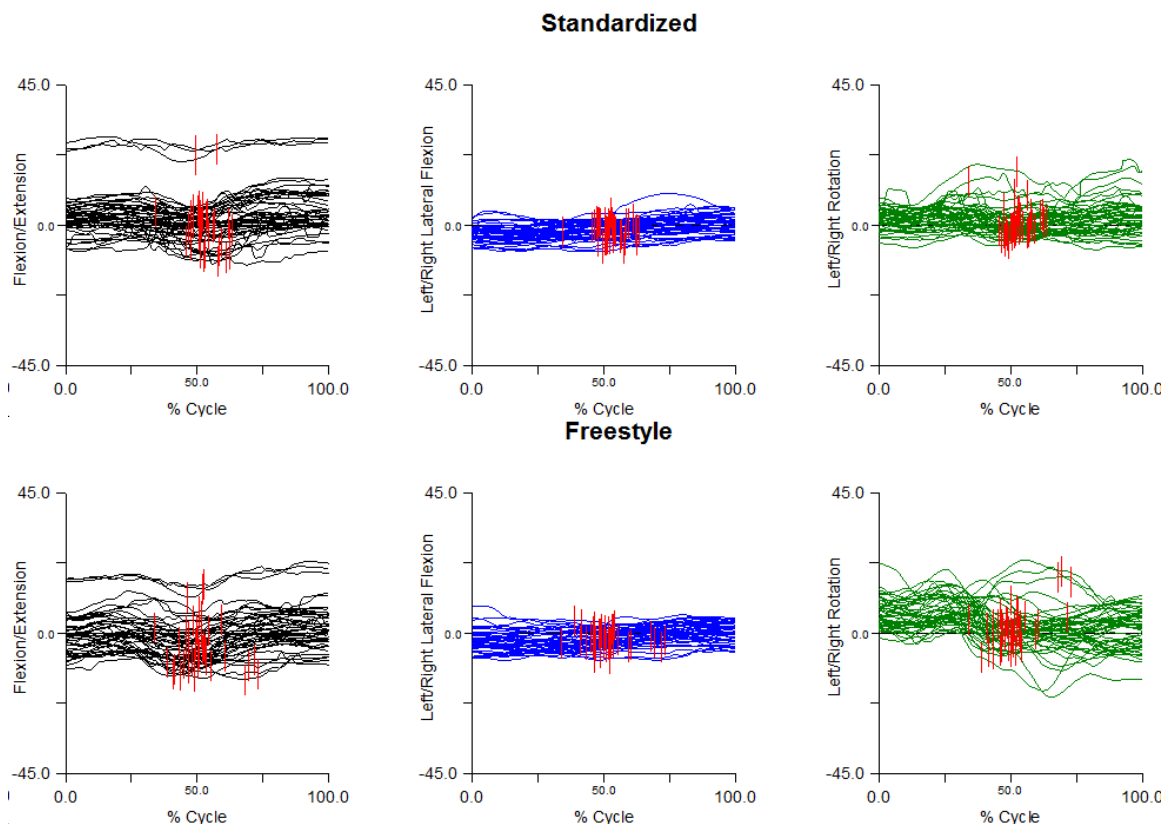


Figure 57. Angle-time graphs showing the angular position of the trunk with reference to the GCS for both the standardized and freestyle conditions as recorded by the Qualysis system. Angles are measured in degrees. Forward flexion and movements in the left are negative; Trunk extension and movements to the right are positive. The red lines represent the moment the lifting load was transfer from right to left hands.

Table 10. Average (Standard Deviation) max angular displacements of the trunk in relation to the GCS during the extended reach lift and horizontal transfer task. Standard deviation is included in brackets. Units are in degrees.

	Standardized			Freestyle		
	Flex/Ext	Lat. Flex.	Axial Rot.	Flex/Ext	Lat. Flex.	Axial Rot.
FOB	7.2 (3.3)	4.6 (2.5)	9.0 (3.9)	9.4 (3.9)	5.3 (2.1)	14.4 (6.9)
Qualysis	4.9 (2.7)	4.4 (2.5)	6.4 (3.3)	7.2 (3.9)	4.7 (1.8)	13.0 (6.7)
Difference	2.3 (1.8)	0.3 (1.6)	2.3 (2.6)	2.3 (0.9)	0.7 (0.9)	1.7 (1.1)

Flexion – Extension

A univariate ANOVA was performed to assess the effect of condition and sensor on the output. The analysis considered the main effects as well as the interactions. Shown in Figure 50 are the means for this data. There was a significant difference due to sensors ($F=47.56$, $df=1,49$, $p<0.001$). There was also a significant difference due to condition ($F=38.56$, $df=1,49$, $p<0.001$). Overall, the means (and SE) varied from 4.9 (± 0.4) to 9.5(± 0.4) with the freestyle condition having the greater difference.

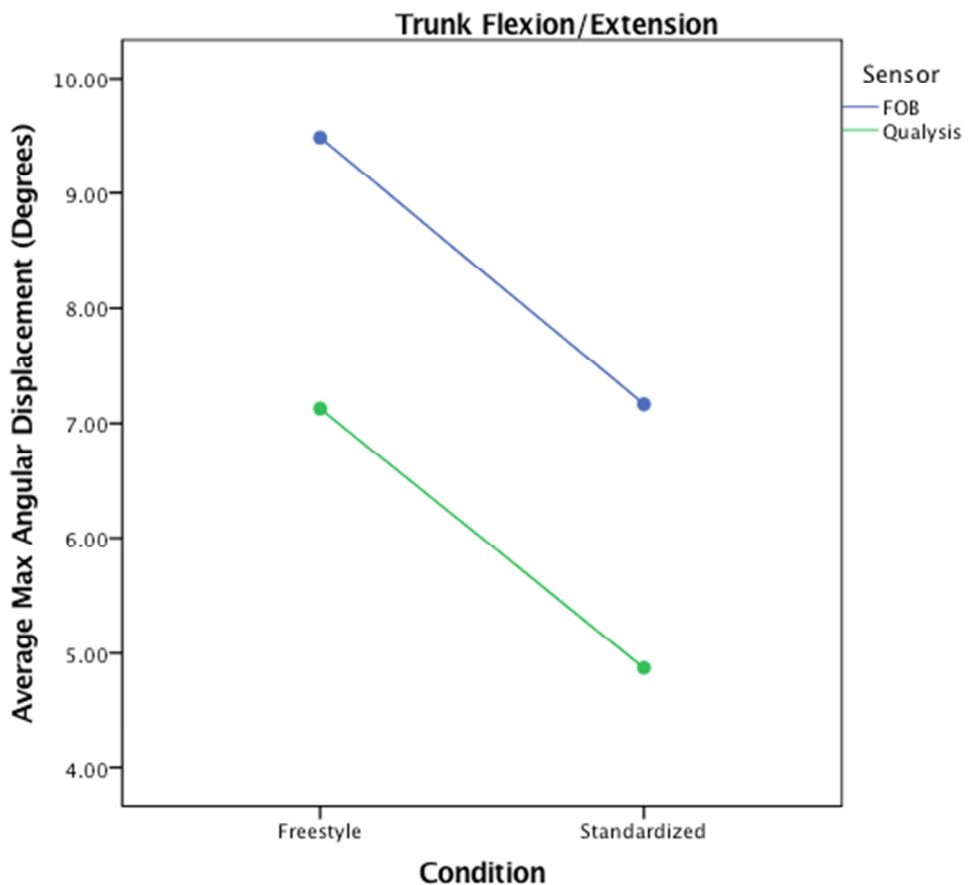


Figure 58: Graphical representation of the output from the univariate ANOVA

A Bland-Altman analysis was also performed to assess the agreement between the measures taken from the FOB and Qualysis systems. The max angular displacement data was used once again for this comparison. The mean difference of 2.3 (1.4) was significant ($t= 6.1$, $df = 30$, $p<0.001$). The 95%ile confidence interval was ± 2.8 degrees.

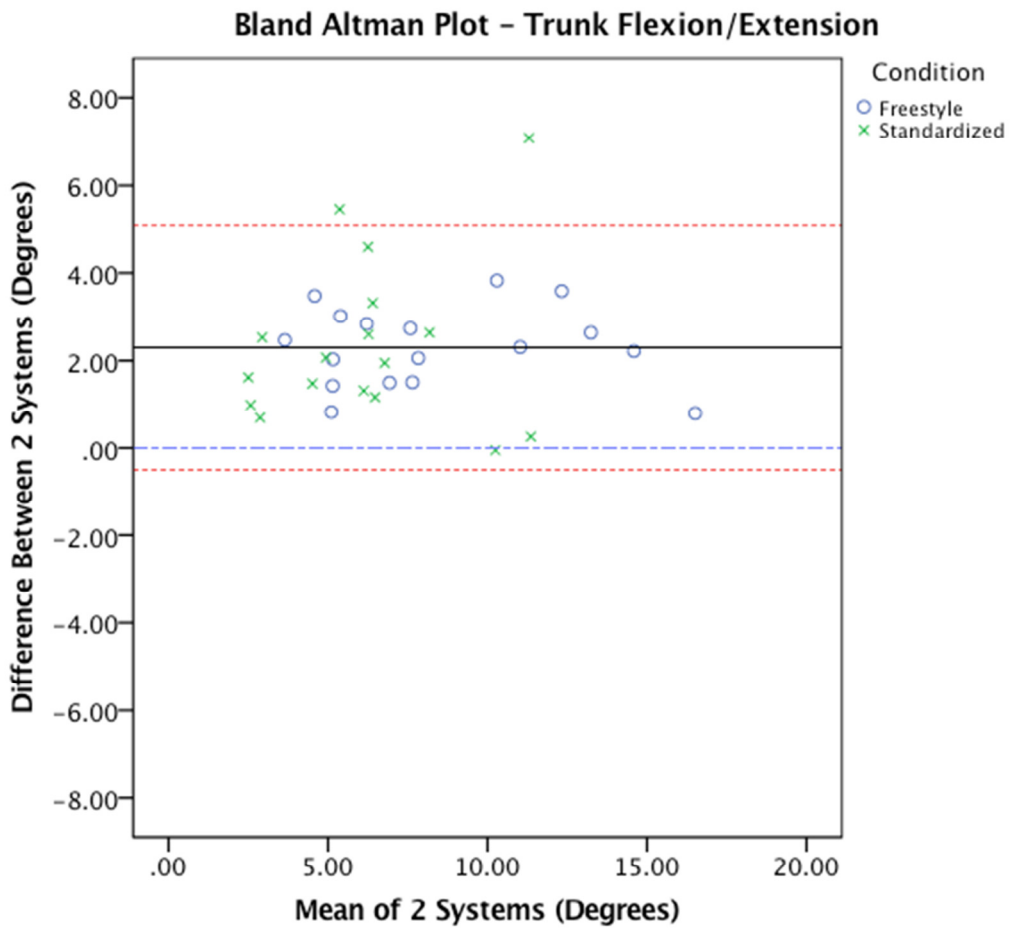


Figure 59: Bland-Altman Plot demonstrating the agreement between the FOB and Qualysis systems while recording trunk flexion/extension during the horizontal transfer task maximum reach task.

Lateral Flexion

A univariate ANOVA was performed to assess the effect of condition and sensor on the output. The analysis considered the main effects as well as the interactions. Shown below in Figure 52 are the means for this data. There was no significant difference due to sensors ($F=2.71$, $df=1,49$, $p= 0.106$). There also was no significant difference due to condition ($F=1.84$, $df=1,49$, $p= 0.18$). Overall, the means (and SE) varied from 4.3

(± 0.3) to 5.2(± 0.3) with the freestyle condition having the greater difference.

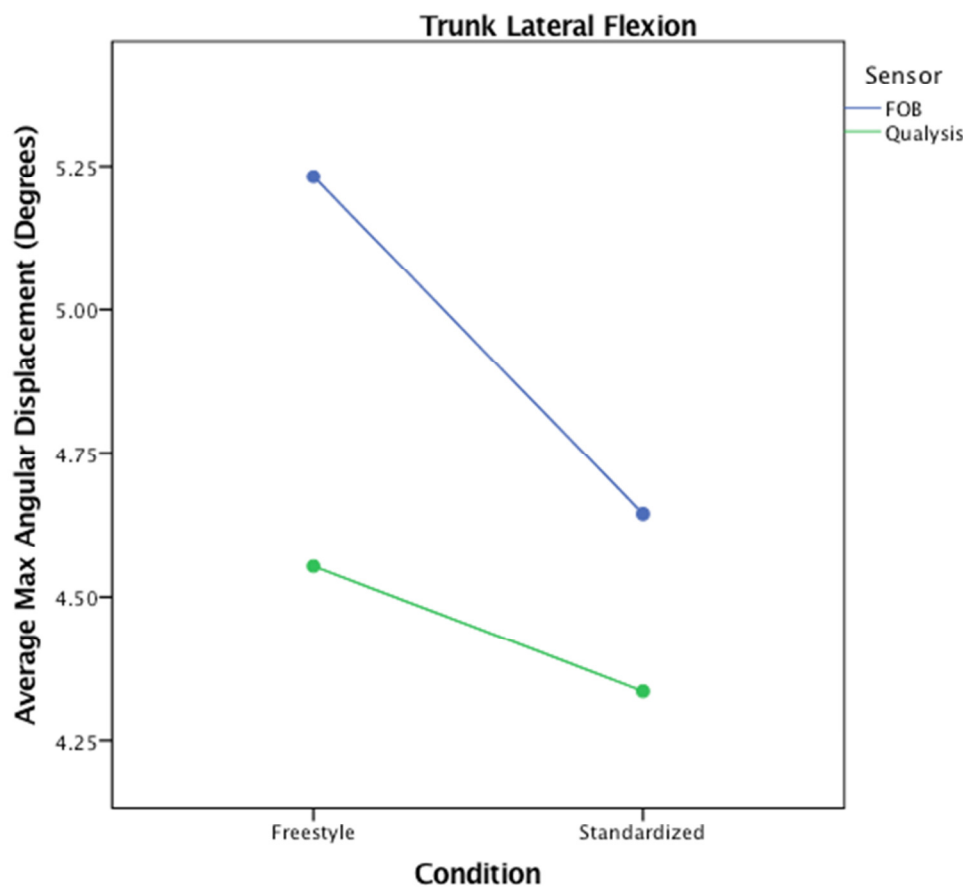


Figure 60: Graphical representation of the output from the univariate ANOVA results.

A Bland-Altman analysis was also performed to assess the agreement between the measures taken from the FOB and Qualysis systems. The max angular displacement data was used once again for this comparison. The mean difference of 0.5 (1.3) was insignificant ($t = -1.5$, $df = 32$, $p=0.125$). The 95%ile confidence interval was ± 2.6 degrees.

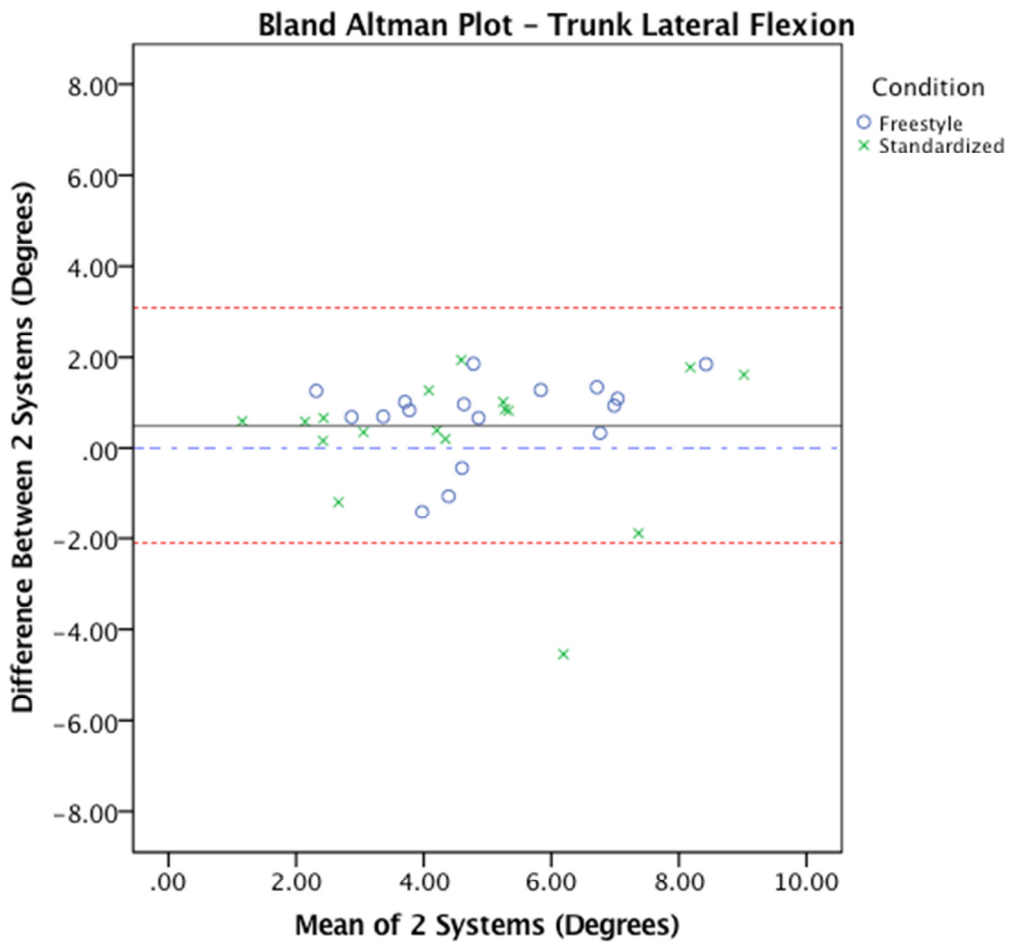


Figure 61: Bland-Altman Plot demonstrating the agreement between the FOB and Qualysis systems while recording trunk lateral flexion during the horizontal transfer task maximum reach task.

Axial Rotation

A univariate ANOVA was performed to assess the effect of condition and sensor on the output. The analysis considered the main effects as well as the interactions. Shown below in Figure 54 are the means for this data. There was a significant difference due to sensors ($F=9.98$, $df=1,49$, $p= 0.003$). There was also a significant difference due to condition ($F=56.81$, $df=1,49$, $p<0.001$). Overall, the means (and SE) varied from 6.5

(± 1.0) to 14.4(± 1.0) with the freestyle condition having the greater difference.

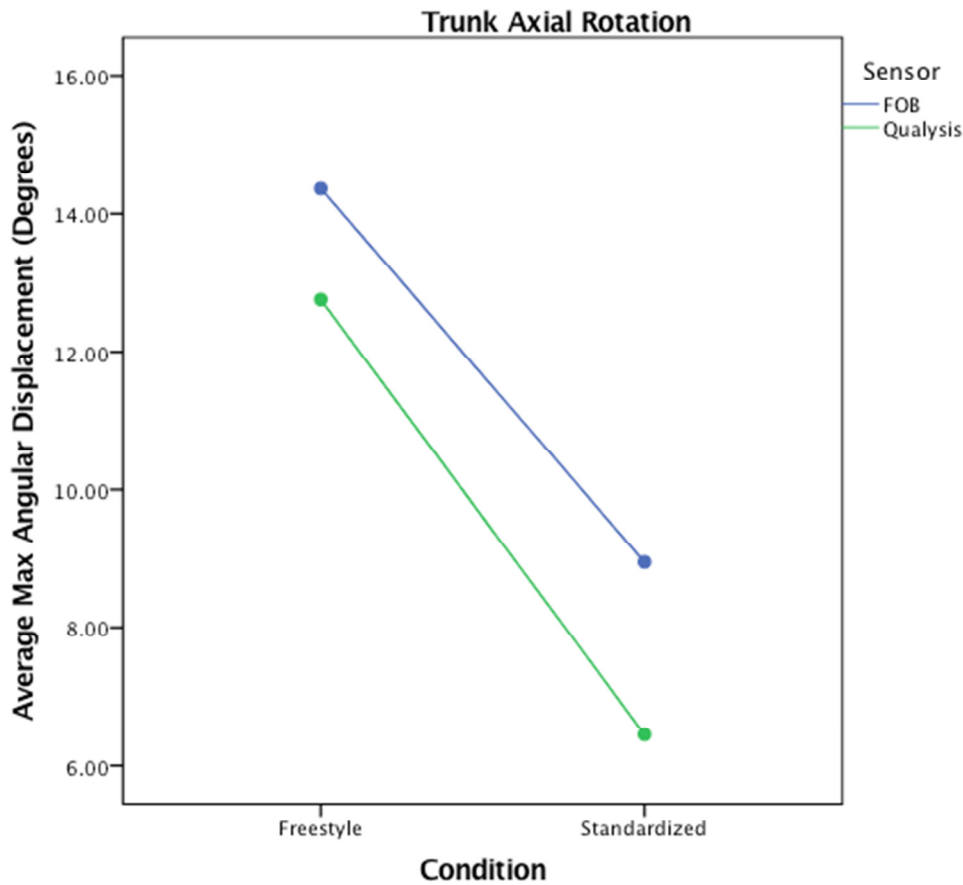


Figure 62: Graphical representation of the output from the univariate ANOVA results.

A Bland-Altman analysis was also performed to assess the agreement between the measures taken from the FOB and Qualysis systems. The max angular displacement data was used once again for this comparison. The mean difference of 2.1 (2.0) was significant ($t= 3.9$, $df = 33$, $p<0.001$). The 95%ile confidence interval was ± 4.0 degrees.

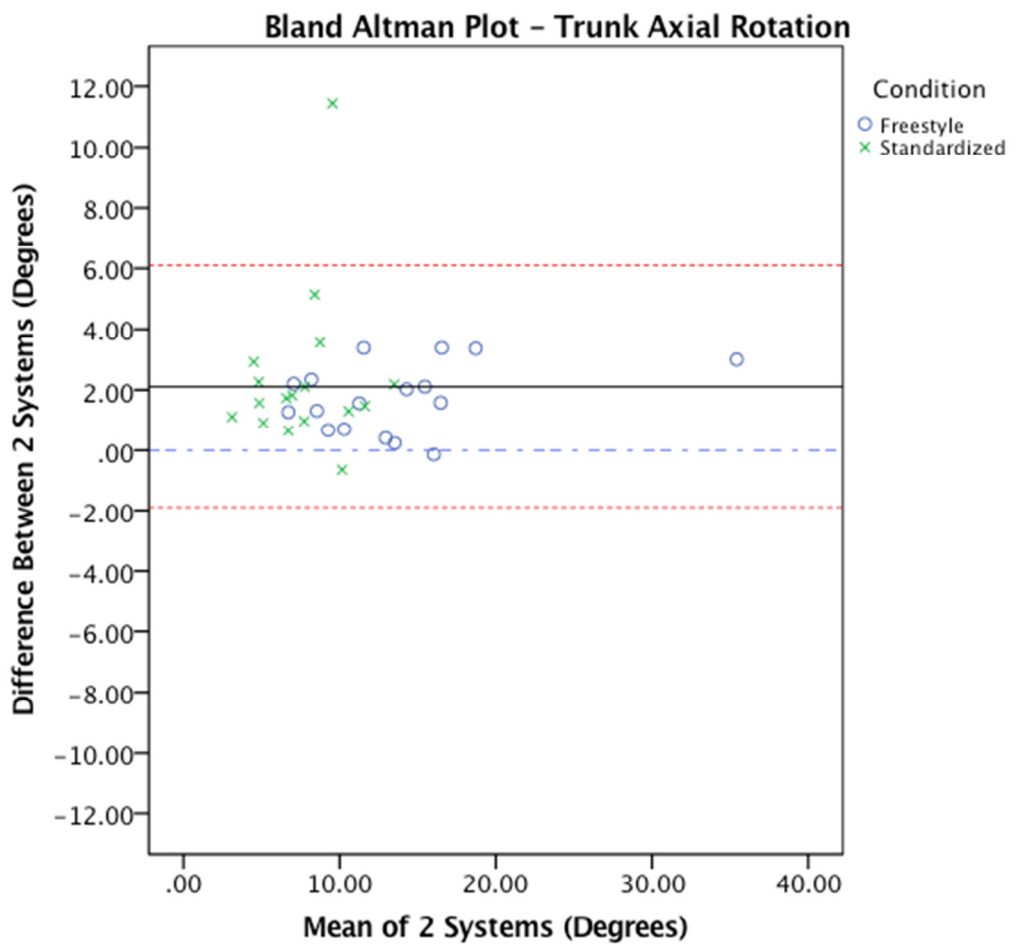


Figure 63: Bland-Altman Plot demonstrating the agreement between the FOB and Qualysis systems while recording trunk axial rotation during the horizontal transfer task maximum reach task. **Note:** The Y-Axis range was changed from the standard 8-8 to 12-12 in this sample subset.

Horizontal Transfer Task Maximum Reach - Pelvis

Shown in Figure 56 is a representative graph of the angular displacement patterns for the pelvis as collected by the Qualysis system for the horizontal transfer task in the maximum reach and the two instructional conditions. This graph represents all trials for all participants in this task. As can be visualized there was limited motion during the task. While there were individual differences between the participants, there was minimal motion seen within the individual trials.

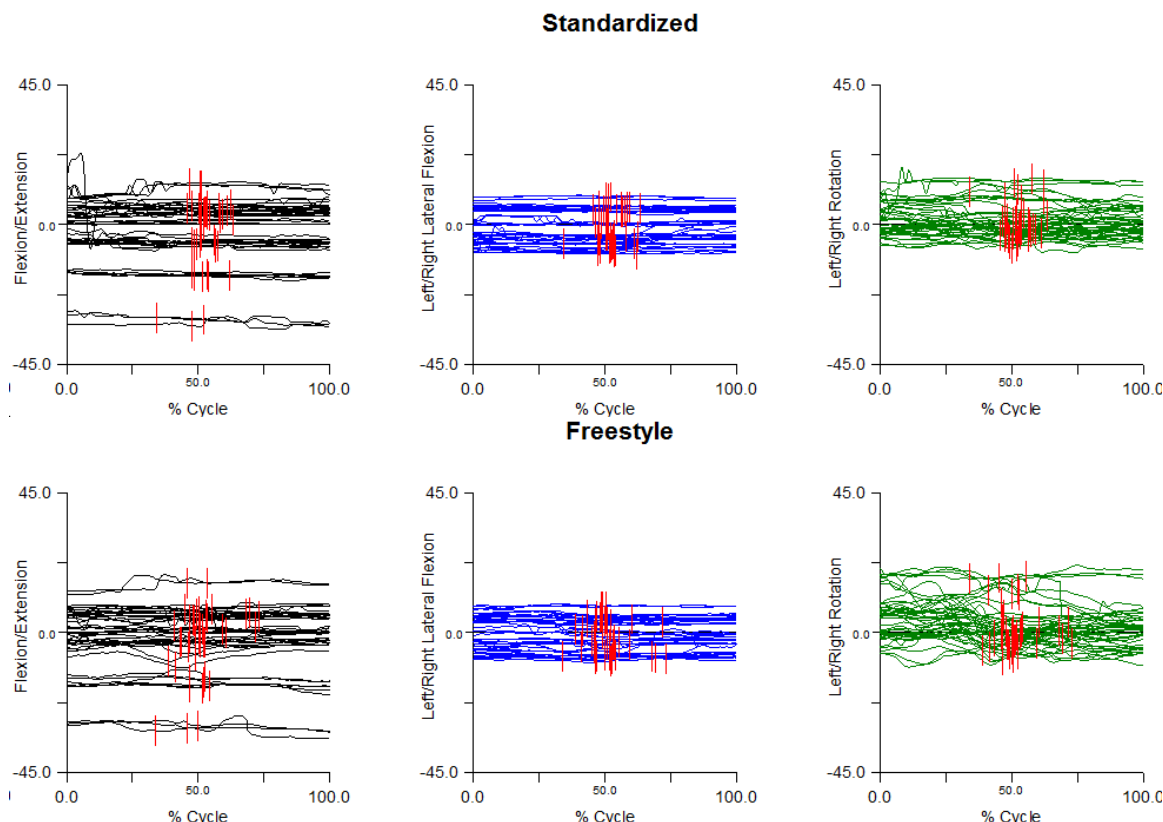


Figure 64. Angle-time graphs showing the angular position of the pelvis with reference to the GCS for both the standardized and freestyle conditions as recorded by the Qualysis system. Angles are measured in degrees. Forward flexion and movements in the left are negative; Trunk extension and movements to the right are positive. The red lines represent the moment the lifting load was transfer from right to left hands.

Table 11. Average (Standard Deviation) max angular displacements of the pelvis in relation to the GCS during the maximum reach lift and horizontal transfer task. Standard deviation is included in brackets. Units are in degrees.

	Standardized			Freestyle		
	Flex/Ext	Lat. Tilt	Axial Rot.	Flex/Ext	Lat. Tilt	Axial Rot.
FOB	2.3 (1.2)	1.1 (0.6)	5.0 (2.6)	3.4 (1.8)	1.9 (1.2)	8.9 (4.9)
Qualysis	1.0 (0.5)	0.6 (0.3)	3.2 (2.2)	2.0 (1.1)	1.2 (0.7)	7.5 (4.5)
Difference	1.2 (1.2)	0.6 (0.5)	1.7 (1.6)	1.4 (1.5)	0.9 (1.2)	1.6 (1.1)

Flexion – Extension

A univariate ANOVA was performed to assess the effect of condition and sensor on the output. The analysis considered the main effects as well as the interactions. Shown below in Figure 57 are the means for this data. There was a significant difference due to sensors ($F=42.69$, $df=1,49$, $p<0.001$). There was also a significant difference due to condition ($F=26.66$, $df=1,49$, $p<0.001$). Overall, the means (and SE) varied from 1.1 (± 0.25) to 3.5(± 0.25) with the freestyle condition having the greater difference.

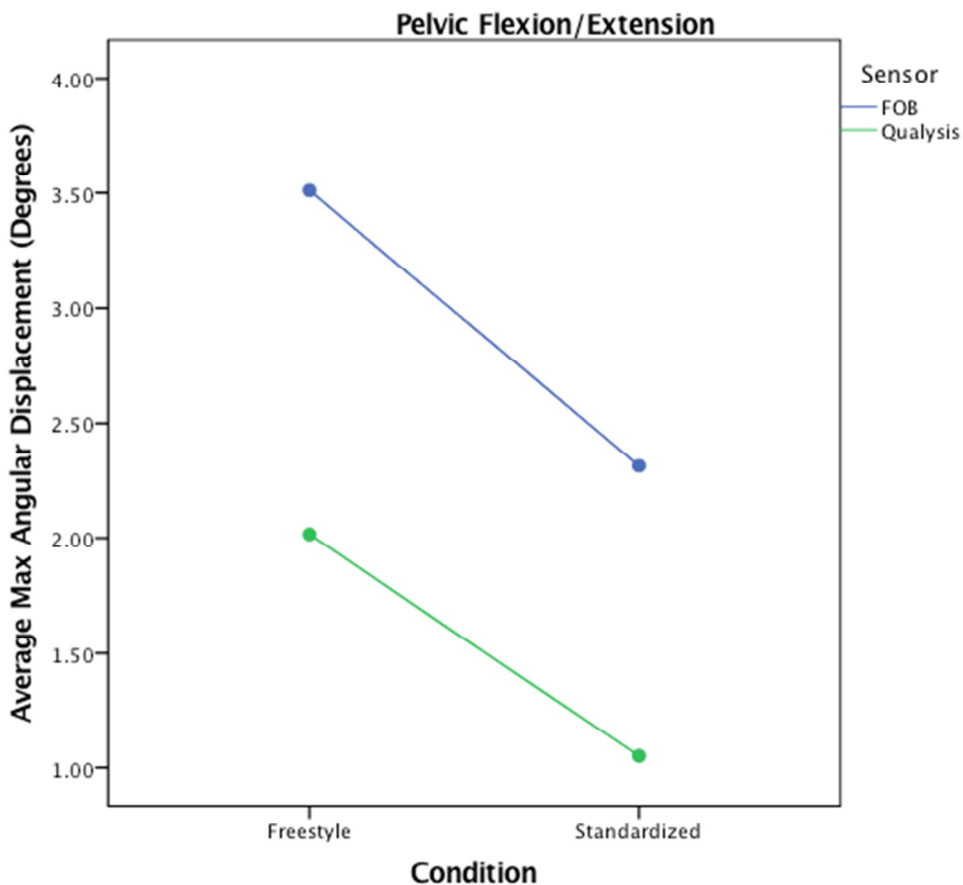


Figure 65: Graphical representation of the output from the univariate ANOVA results

A Bland-Altman analysis was also performed to assess the agreement between the measures taken from the FOB and Qualysis systems. The max angular displacement data was used once again for this comparison. The mean difference of 1.4 (1.4) was insignificant ($t = -0.2$, $df = 29$, $p=803$). The 95%ile confidence interval was ± 2.8 degrees.

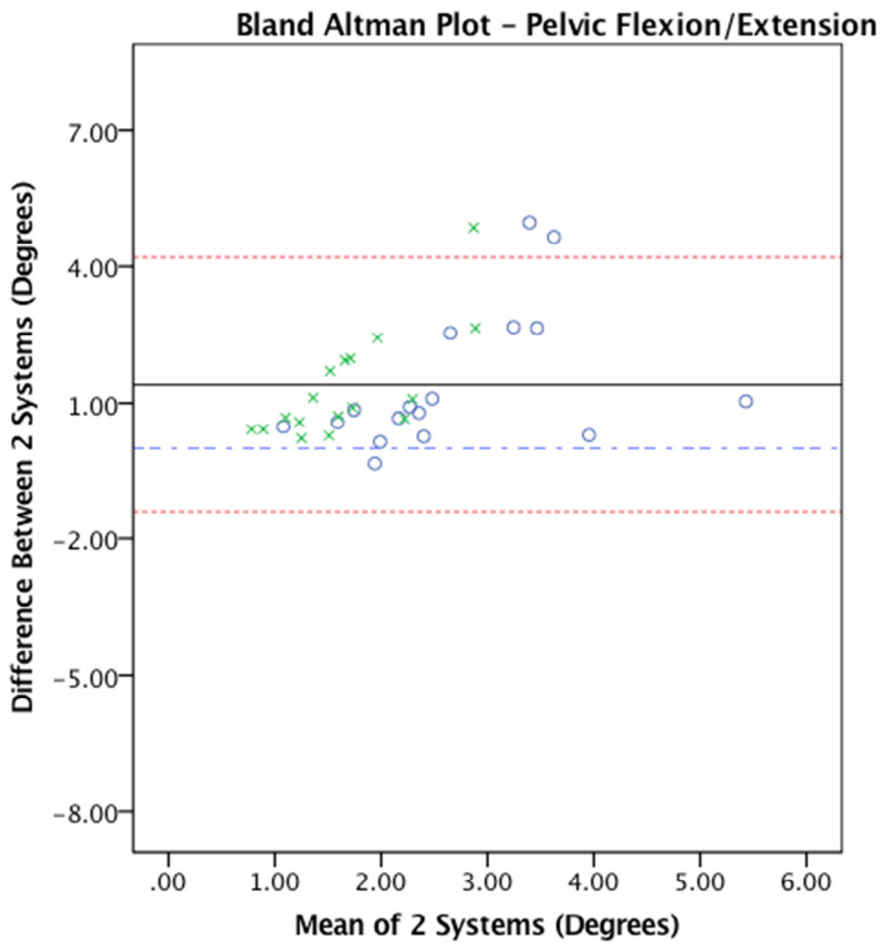


Figure 66: Bland-Altman Plot demonstrating the agreement between the FOB and Qualysis systems while recording pelvic flexion/extension during the horizontal transfer task maximum reach task.

Lateral Flexion

A univariate ANOVA was performed to assess the effect of condition and sensor on the output. The analysis considered the main effects as well as the interactions. Shown below in Figure 59 are the means for this data. There was a significant difference due to sensors ($F=39.79$, $df=1,49$, $p<0.001$). There was also a significant difference due to condition ($F=35.59$, $df=1,49$, $p<0.001$). Overall, the means (and SE) varied from 0.6

(± 0.15) to 2.0(± 0.15) with the freestyle condition having the greater difference.

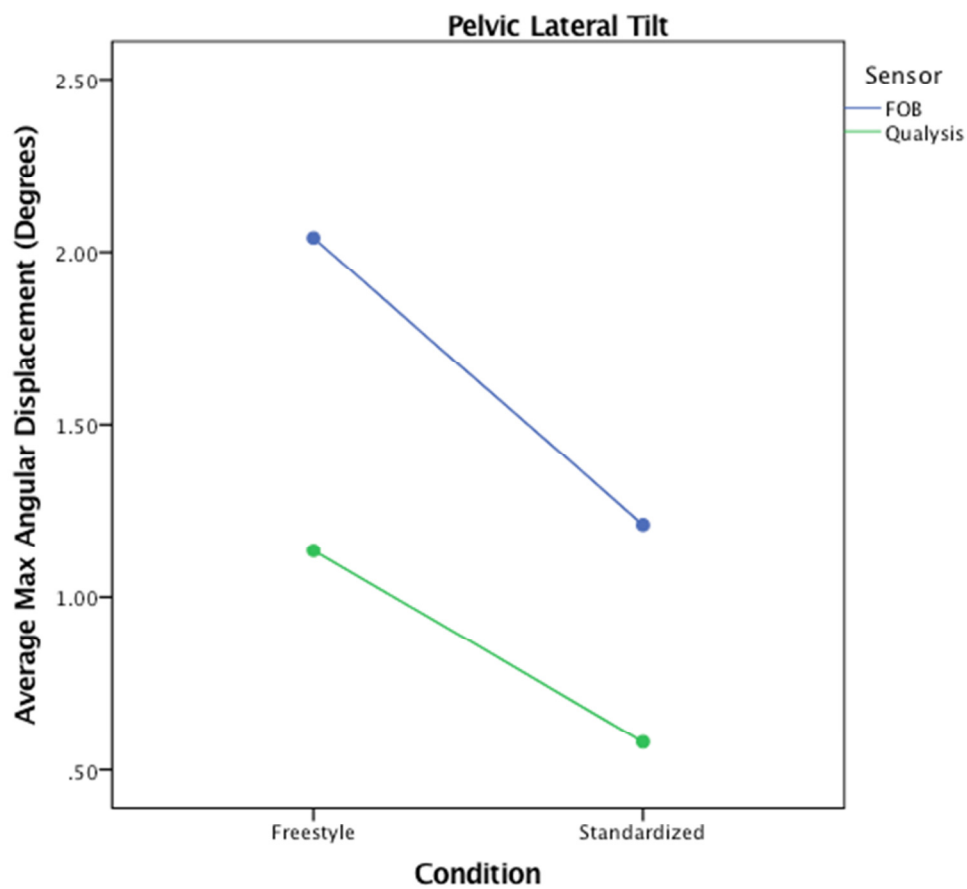


Figure 67: Graphical representation of the output from the univariate ANOVA results.

A Bland-Altman analysis was also performed to assess the agreement between the measures taken from the FOB and Qualysis systems. The max angular displacement data was used once again for this comparison. The mean difference of 0.8 (0.9) was significant ($t = -3.6$, $df = 33$, $p=0.001$). The 95%ile confidence interval was ± 1.8 degrees.

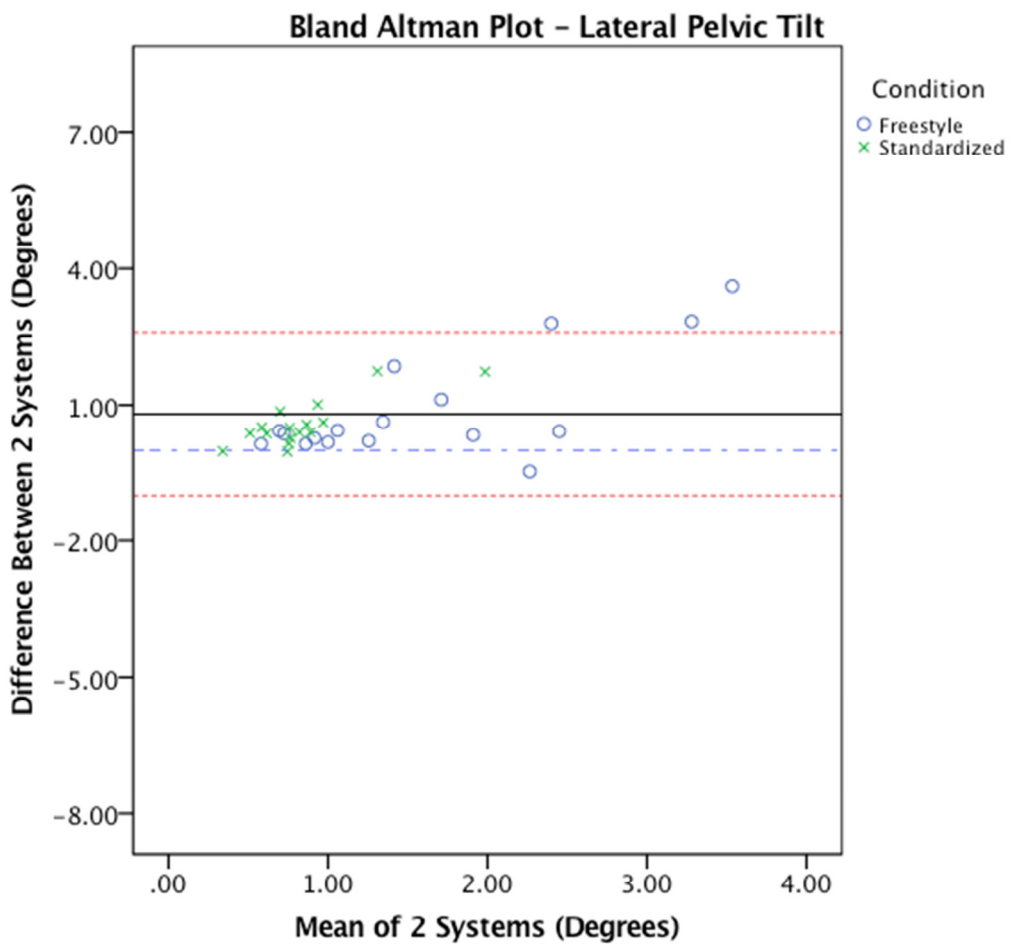


Figure 68: Bland-Altman Plot demonstrating the agreement between the FOB and Qualysis systems while recording pelvic lateral tilt during the horizontal transfer task maximum reach task.

Axial Rotation

A univariate ANOVA was performed to assess the effect of condition and sensor on the output. The analysis considered the main effects as well as the interactions. Shown below in Figure 61 are the means for this data. There was a significant difference due to sensors ($F=18.08$, $df=1,49$, $p<0.001$). There was also a significant difference due to condition ($F=80.57$, $df=1,49$, $p<0.001$). Overall, the means (and SE) varied from 3.2

(± 0.6) to 8.9(± 0.6) with the freestyle condition having the greater difference.

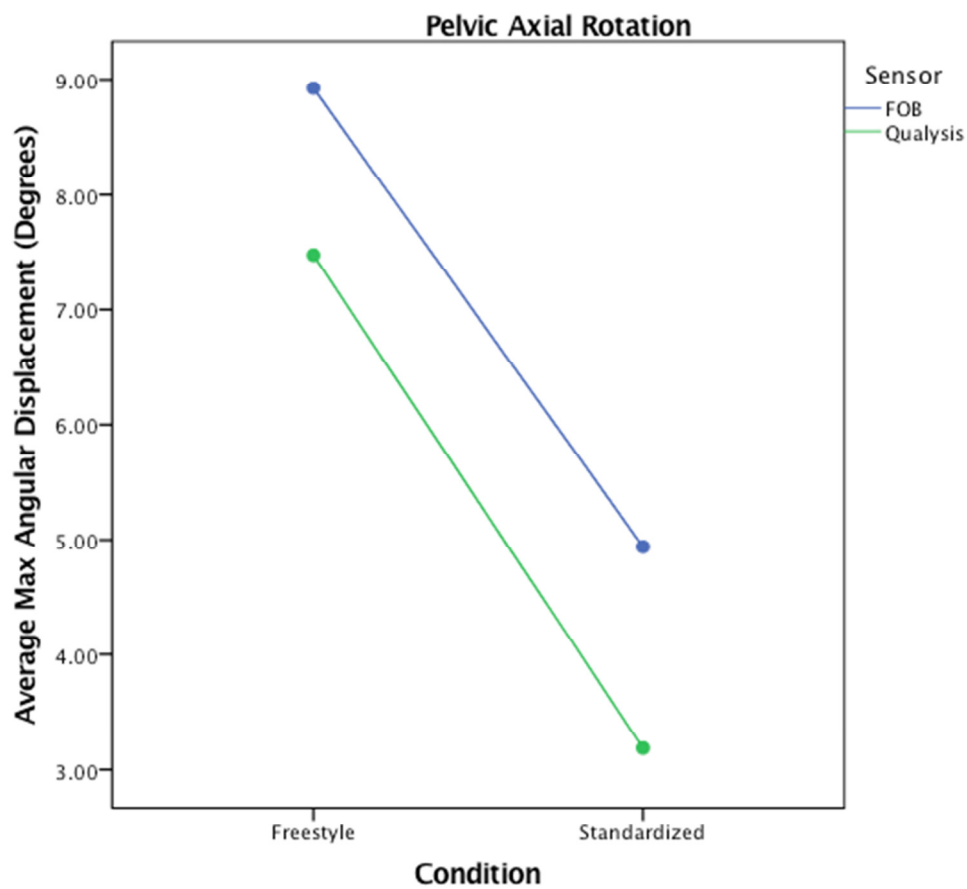


Figure 69: Graphical representation of the output from the univariate ANOVA results.

A Bland-Altman analysis was also performed to assess the agreement between the measures taken from the FOB and Qualysis systems. The max angular displacement data was used once again for this comparison. The mean difference of 1.6 (1.4) was significant ($t= 0.60$, $df = 28$, $p=0.552$). The 95%ile confidence interval was ± 2.8 degrees.

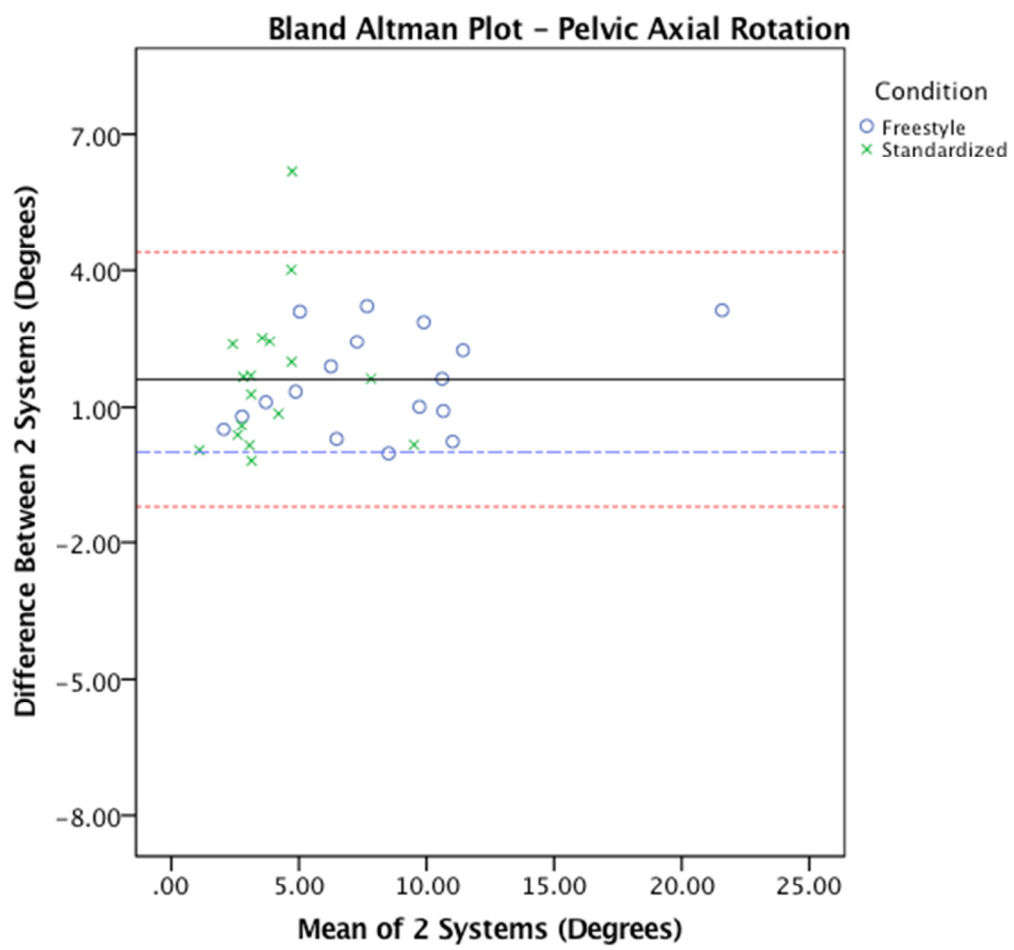


Figure 70: Bland-Altman Plot demonstrating the agreement between the FOB and Qualysis systems while recording pelvic lateral tilt during the horizontal transfer task maximum reach task.

Body Segment Angular Motion Patterns: LTM, HTTN, HTTM

Lifting Task Extended Reach

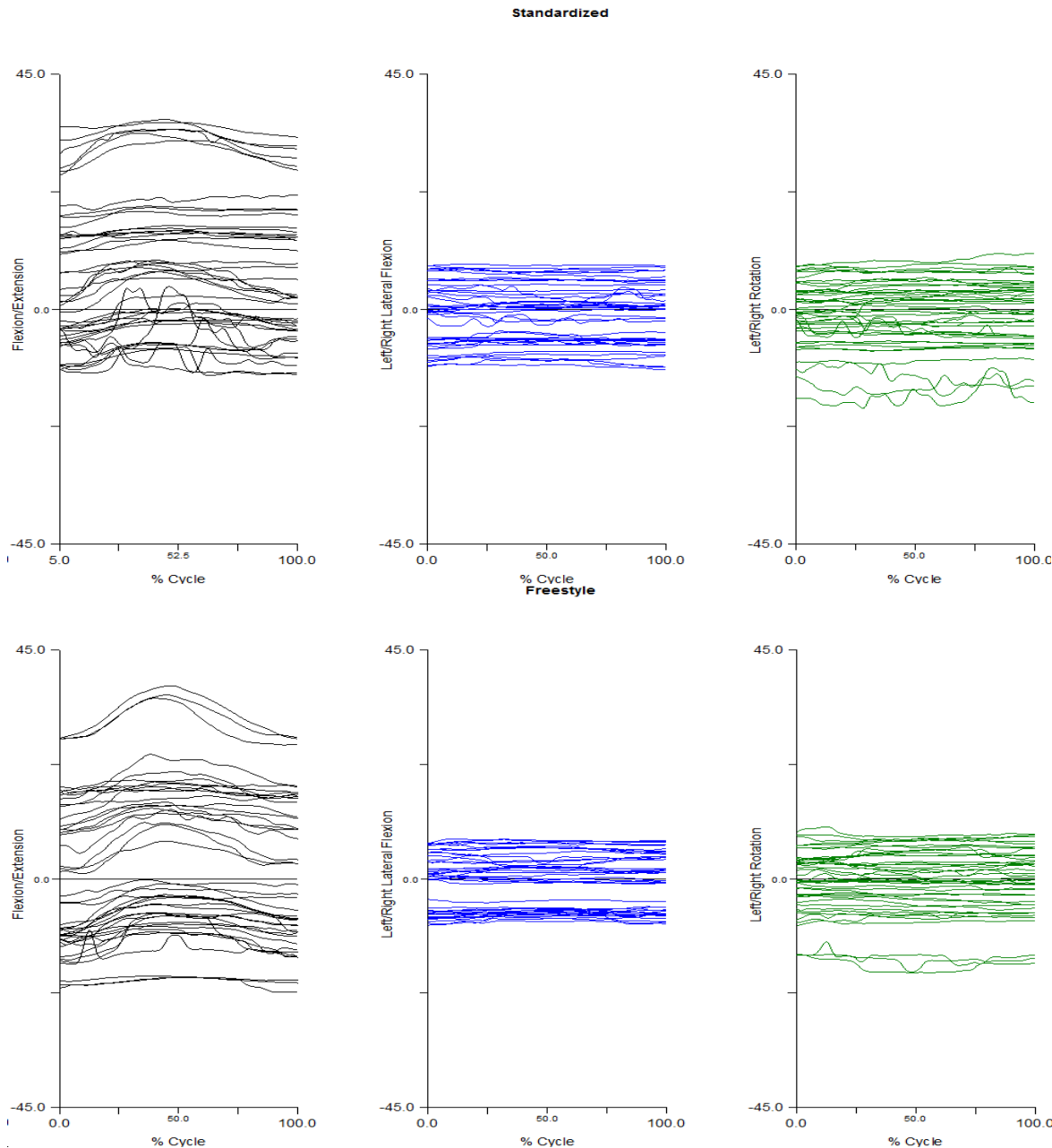


Figure 71. Angle-time graphs showing the angular position of the trunk with reference to the pelvis during the Lift & Replace Maximum Reach task.

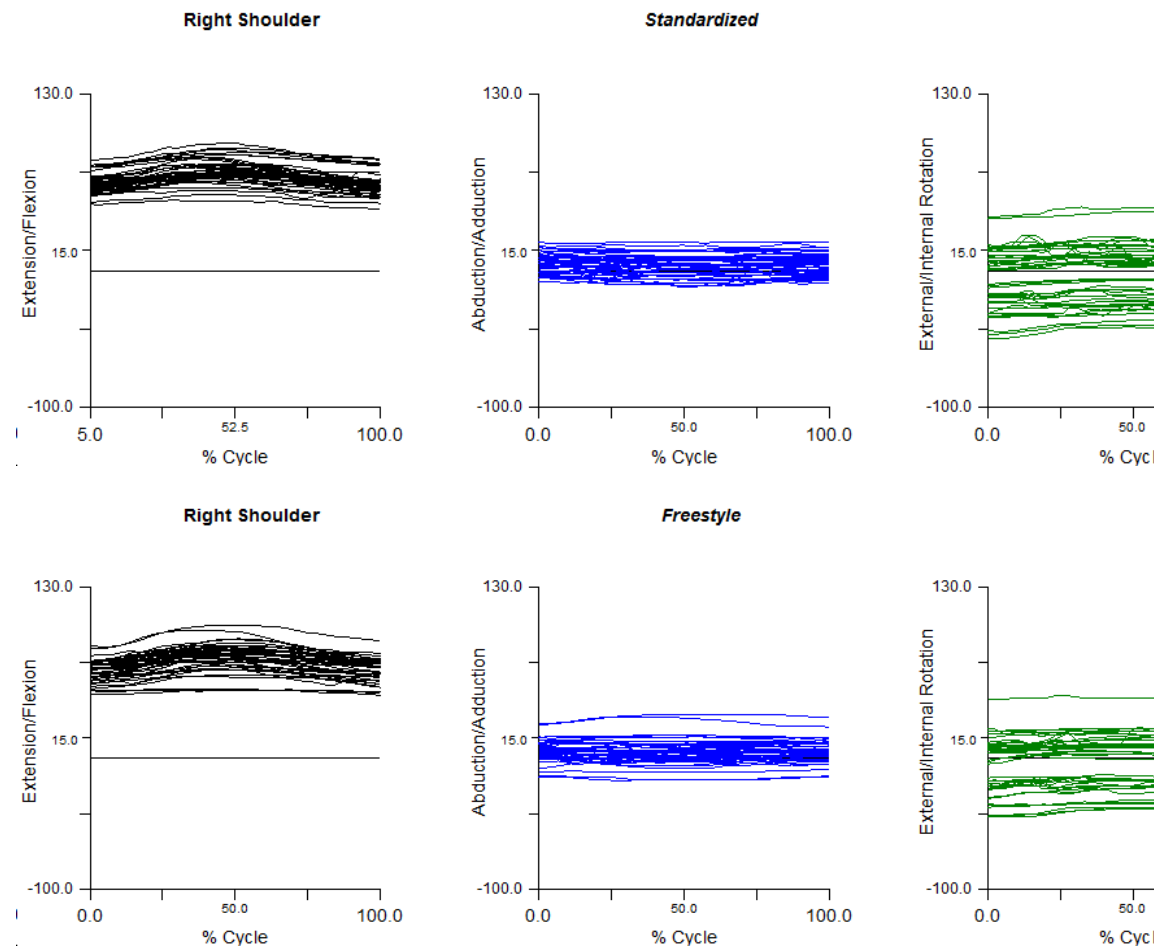


Figure 72. Angle-time graphs showing the angular position of the right upper arm with reference to the trunk during the Lift & Replace Maximum Reach task.

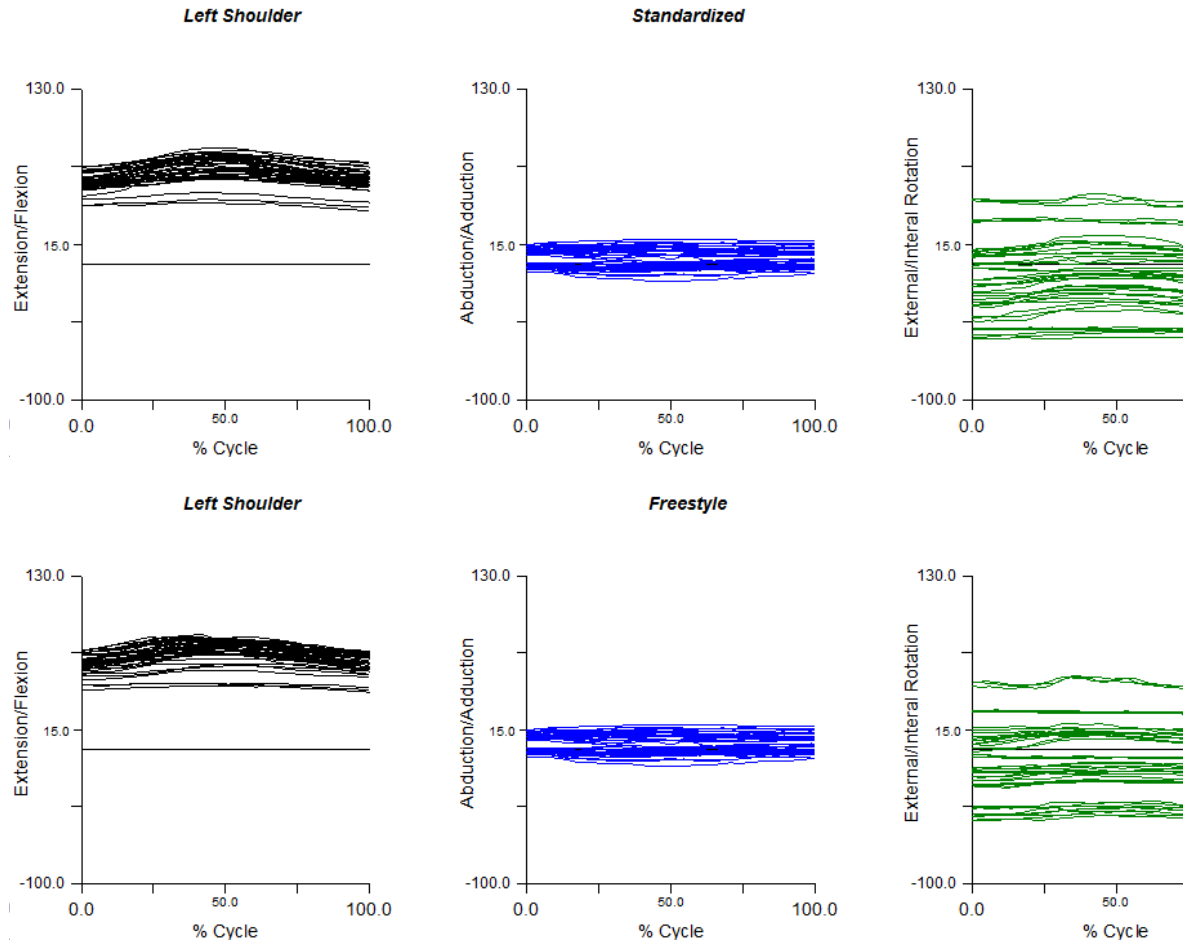


Figure 73. Angle-time graphs showing the angular position of the left upper arm with reference to the trunk during the Lift & Replace Maximum Reach task.

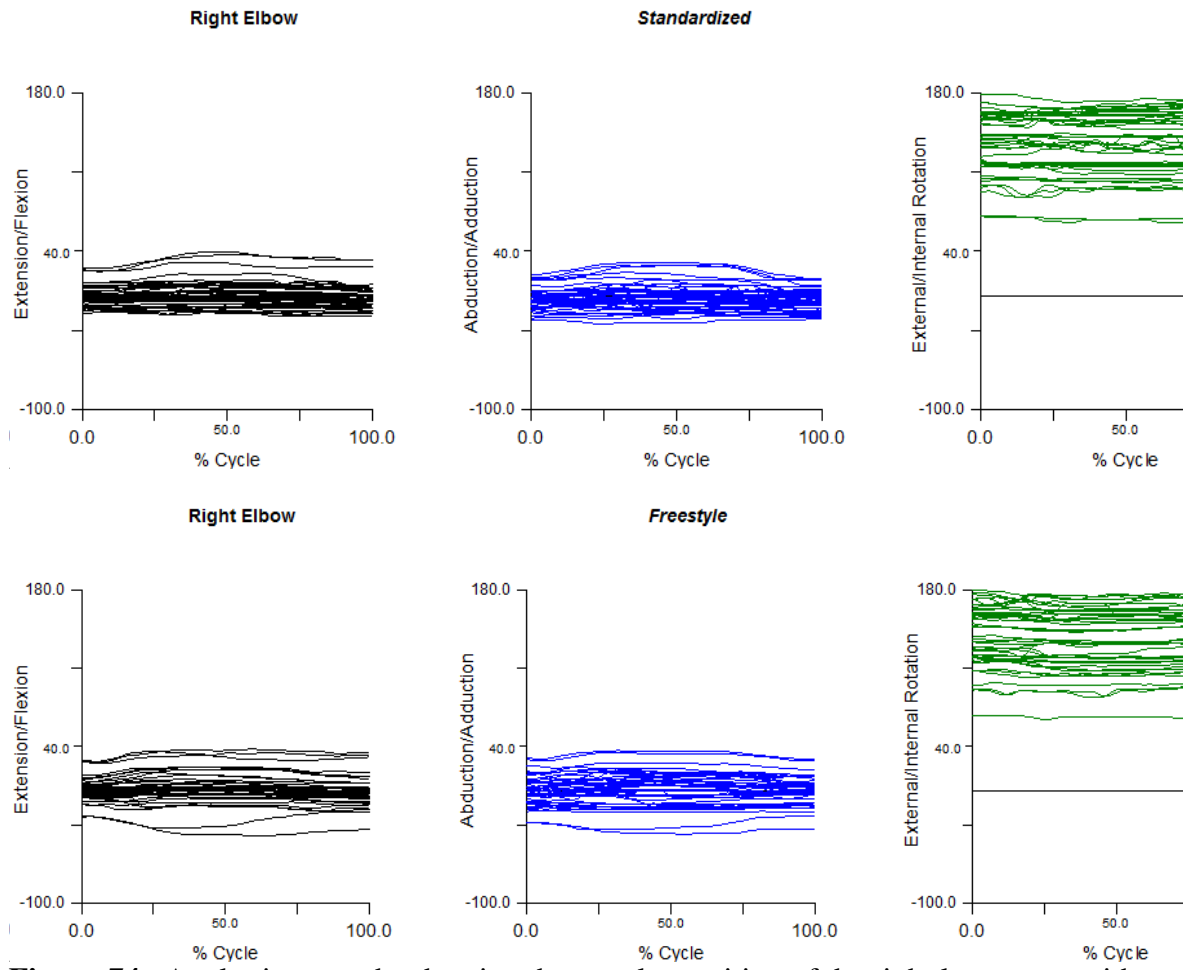


Figure 74. Angle-time graphs showing the angular position of the right lower arm with reference to the right upper arm during the Lift & Replace Maximum Reach task.

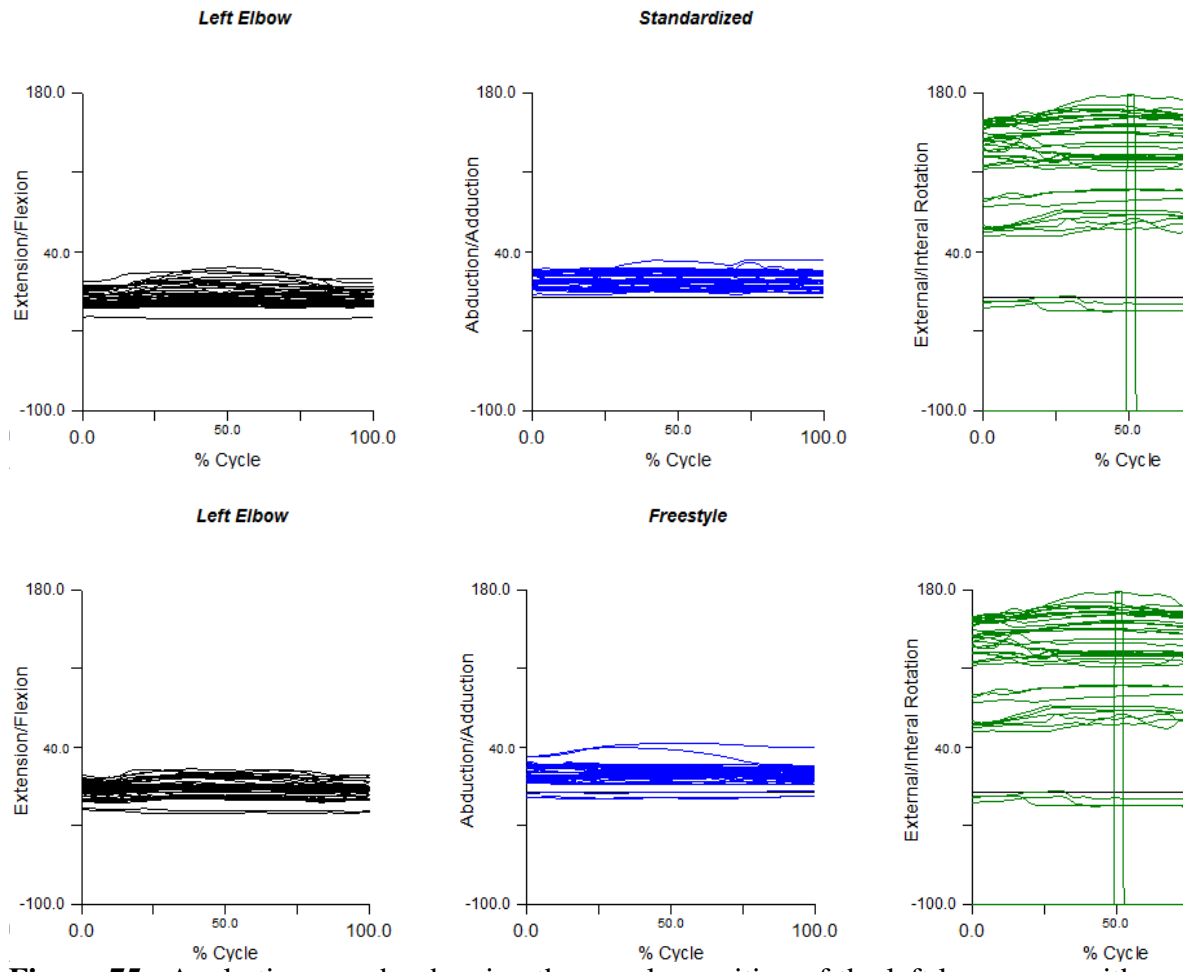


Figure 75. Angle-time graphs showing the angular position of the left lower arm with reference to the left upper arm during the Lift & Replace Maximum Reach task.

Horizontal Transfer Task Normal Reach

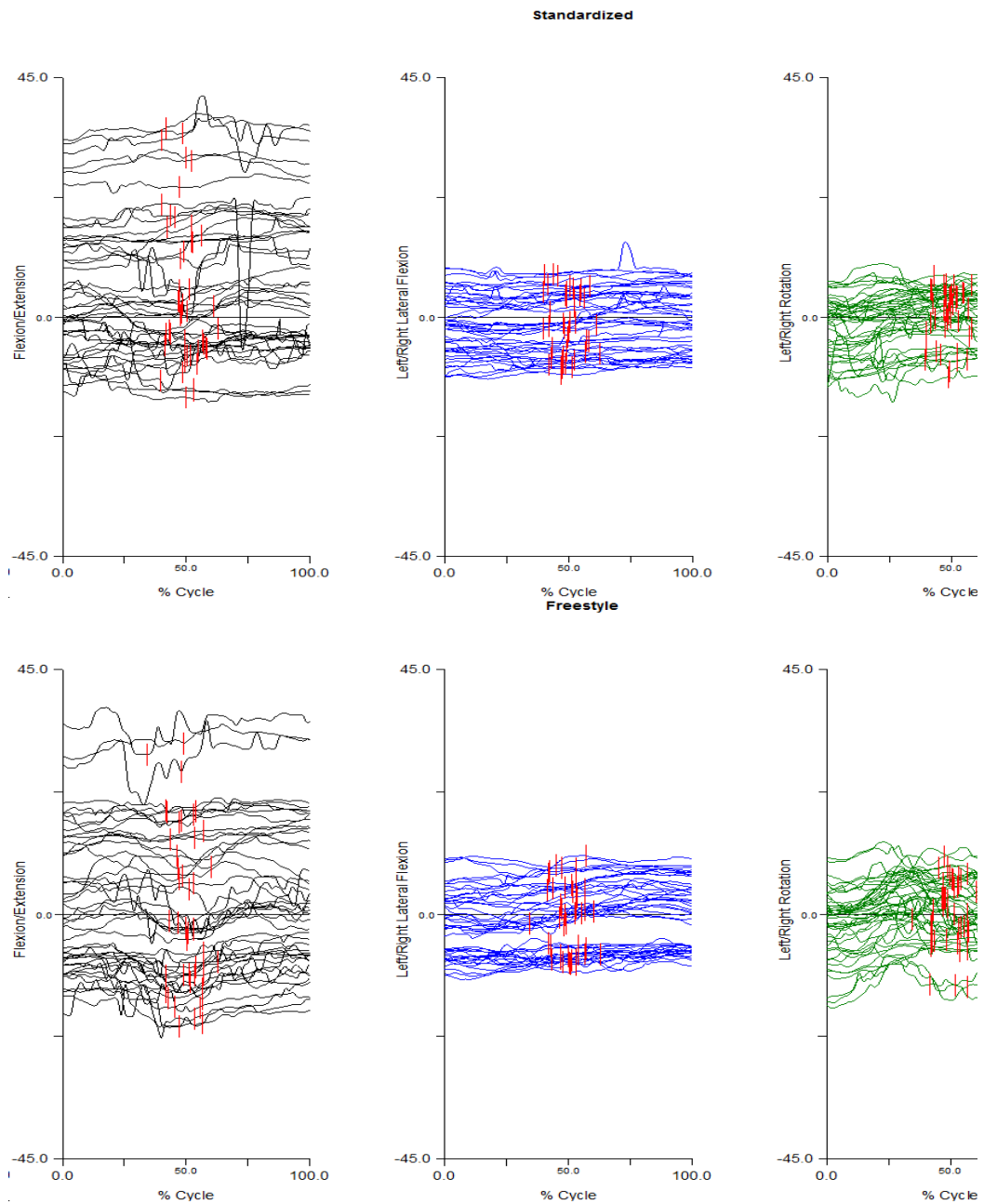


Figure 76. Angle-time graphs showing the angular position of the trunk with reference to the pelvis during the Horizontal Transfer Task Normal Reach condition.

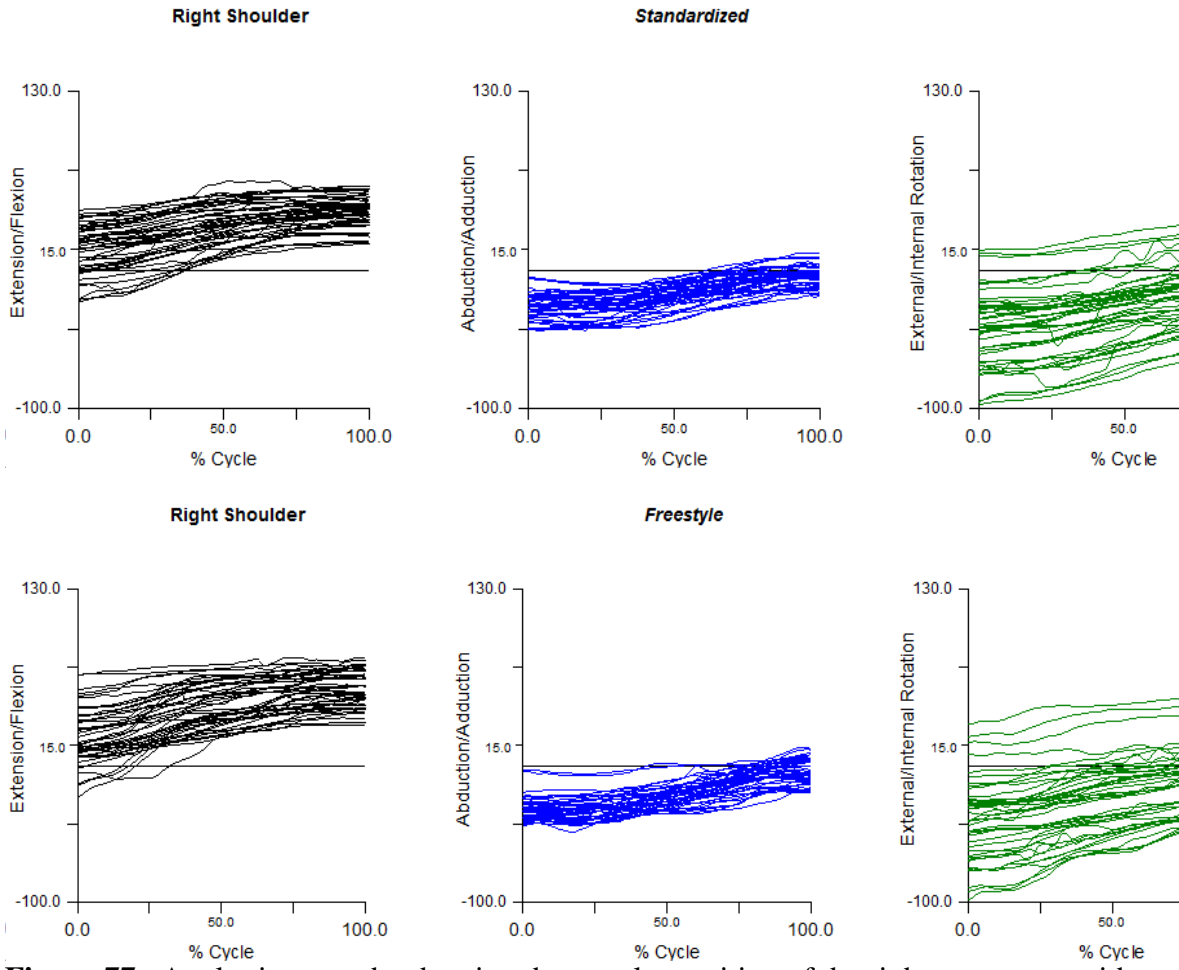


Figure 77. Angle-time graphs showing the angular position of the right upper arm with reference to the trunk during the Horizontal Transfer Task Normal Reach condition.

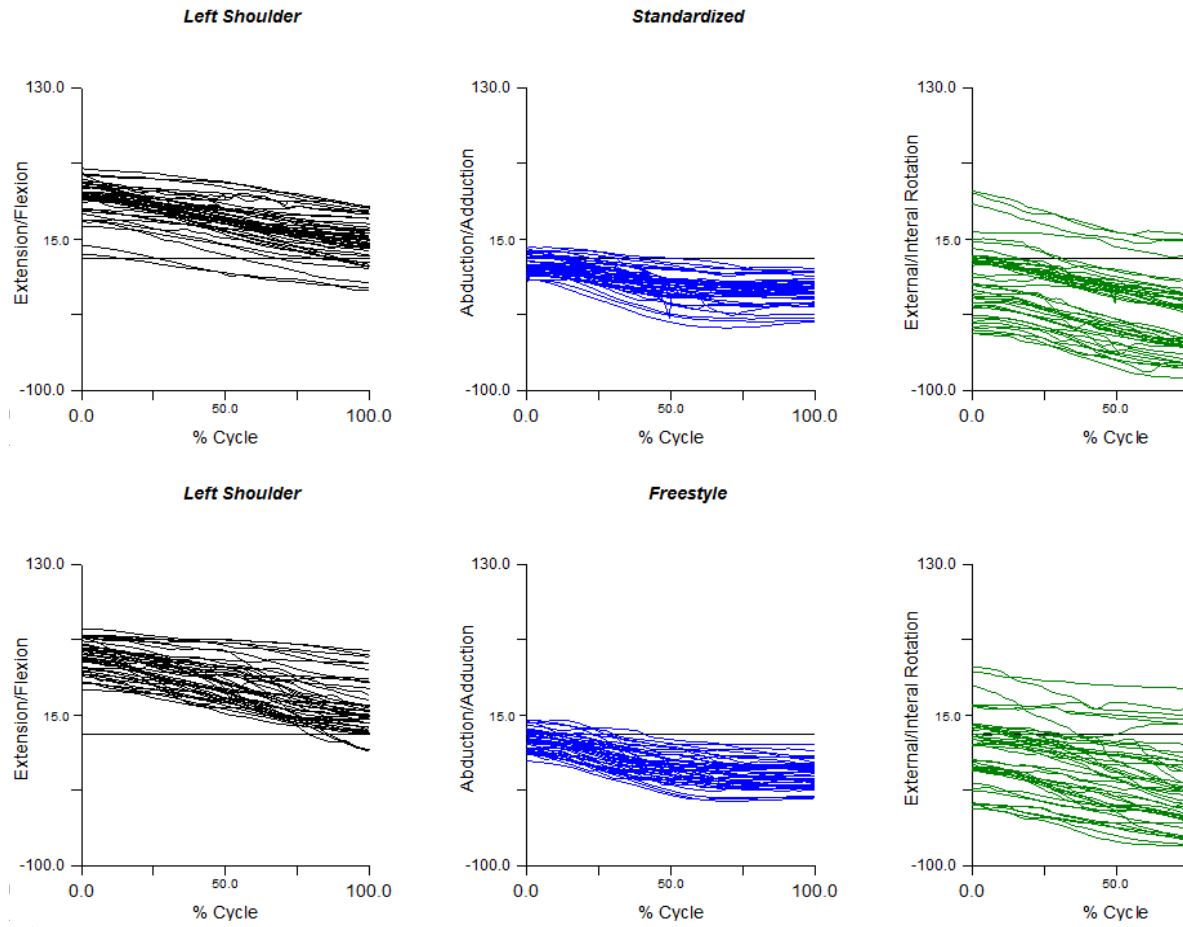


Figure 78. Angle-time graphs showing the angular position of the left upper arm with reference to the trunk during the Horizontal Transfer Task Normal Reach condition.

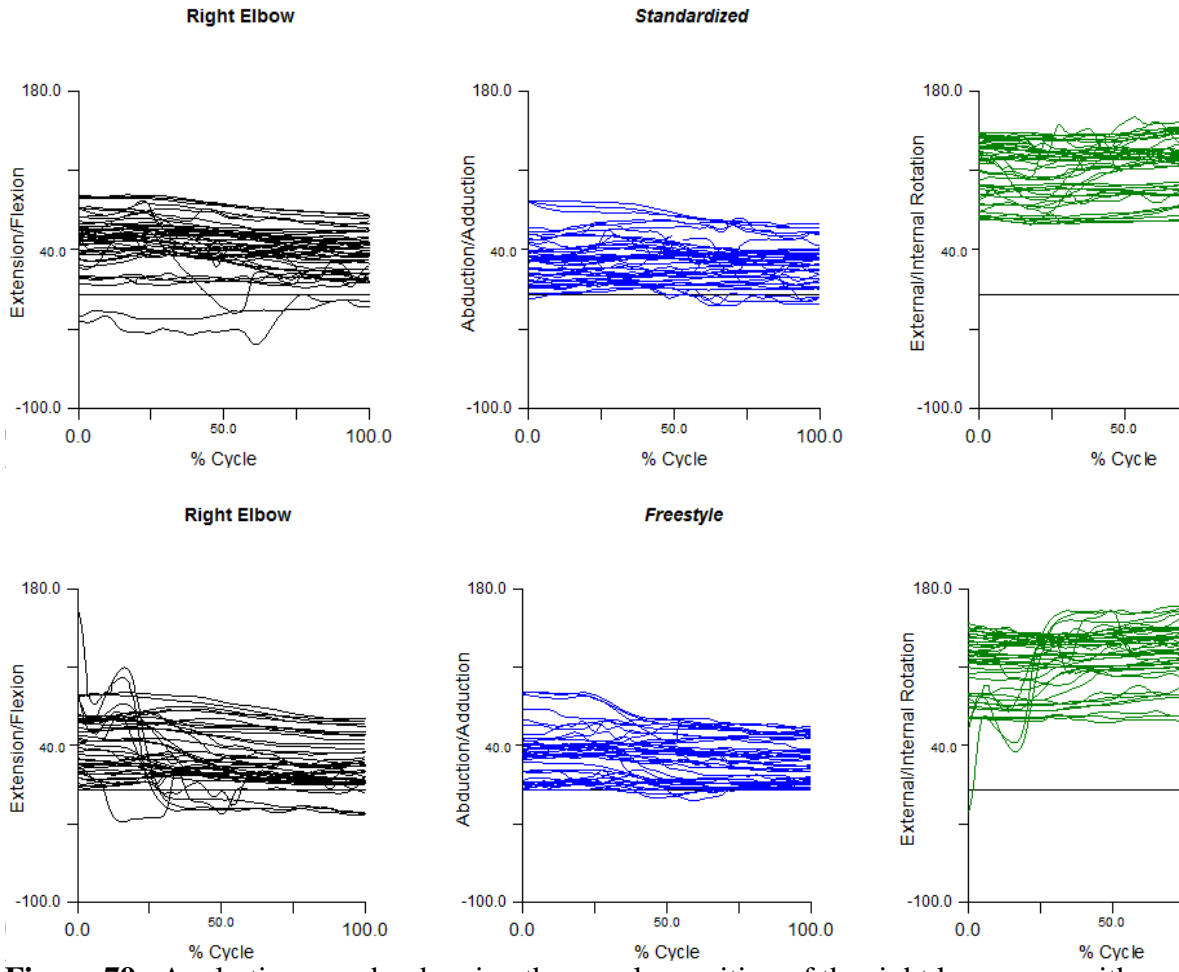


Figure 79. Angle-time graphs showing the angular position of the right lower arm with reference to the right upper arm during the Horizontal Transfer Task Normal Reach condition.

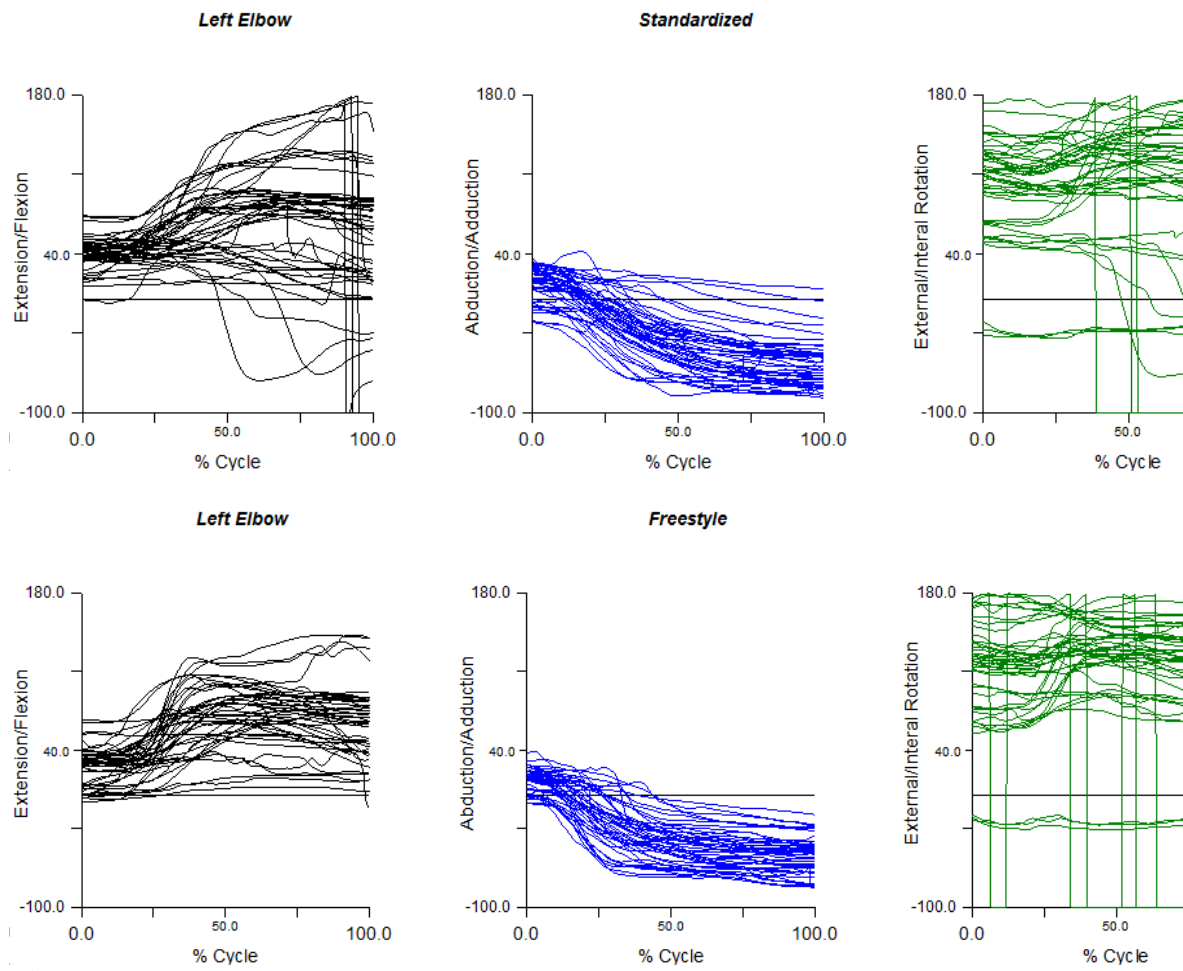


Figure 80. Angle-time graphs showing the angular position of the left lower arm with reference to the left upper arm during the Horizontal Transfer Task Normal Reach condition.

Horizontal Transfer Task Extended Reach

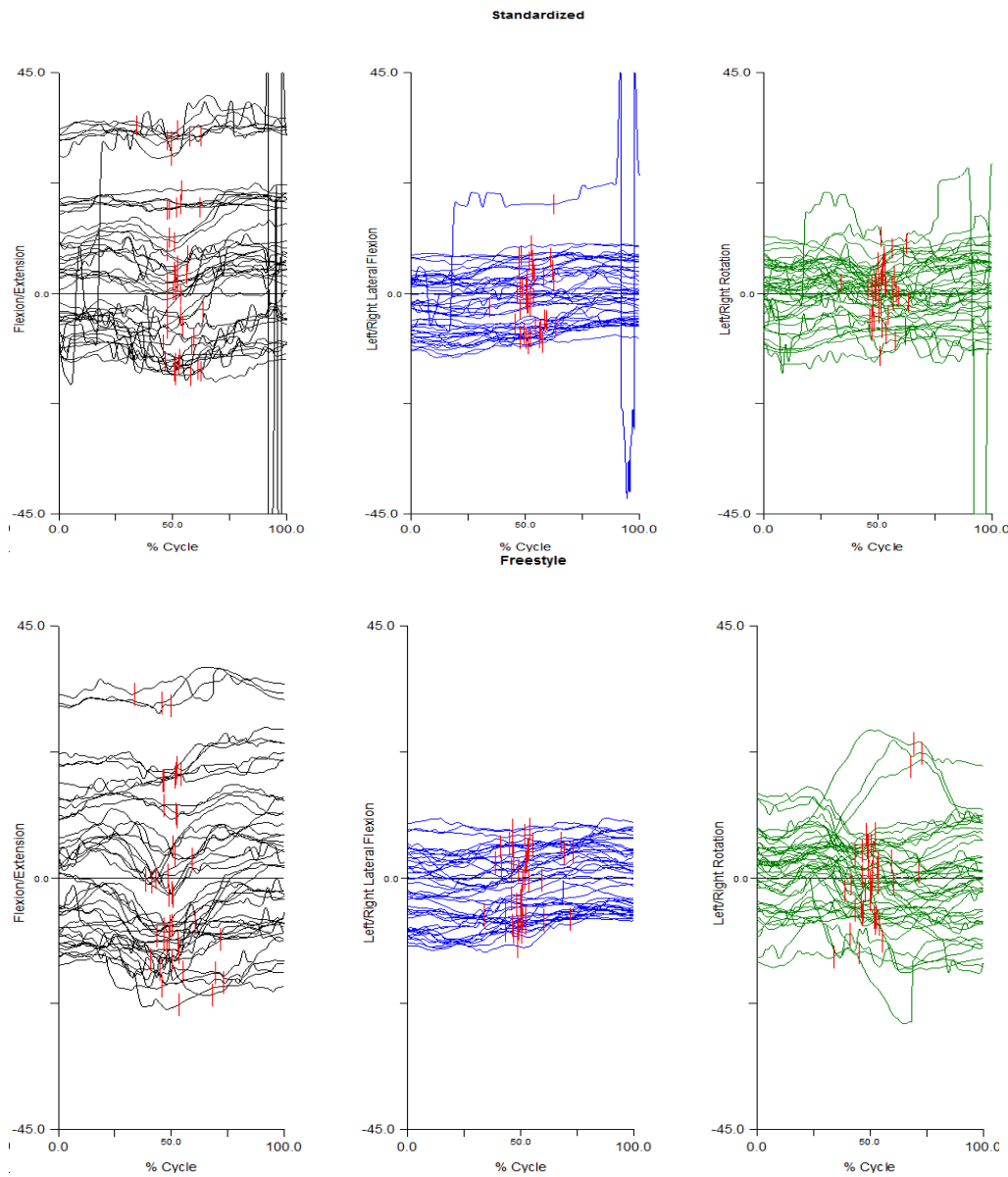


Figure 81. Angle-time graphs showing the angular position of the trunk with reference to the pelvis during the Horizontal Transfer Task Maximum Reach condition.

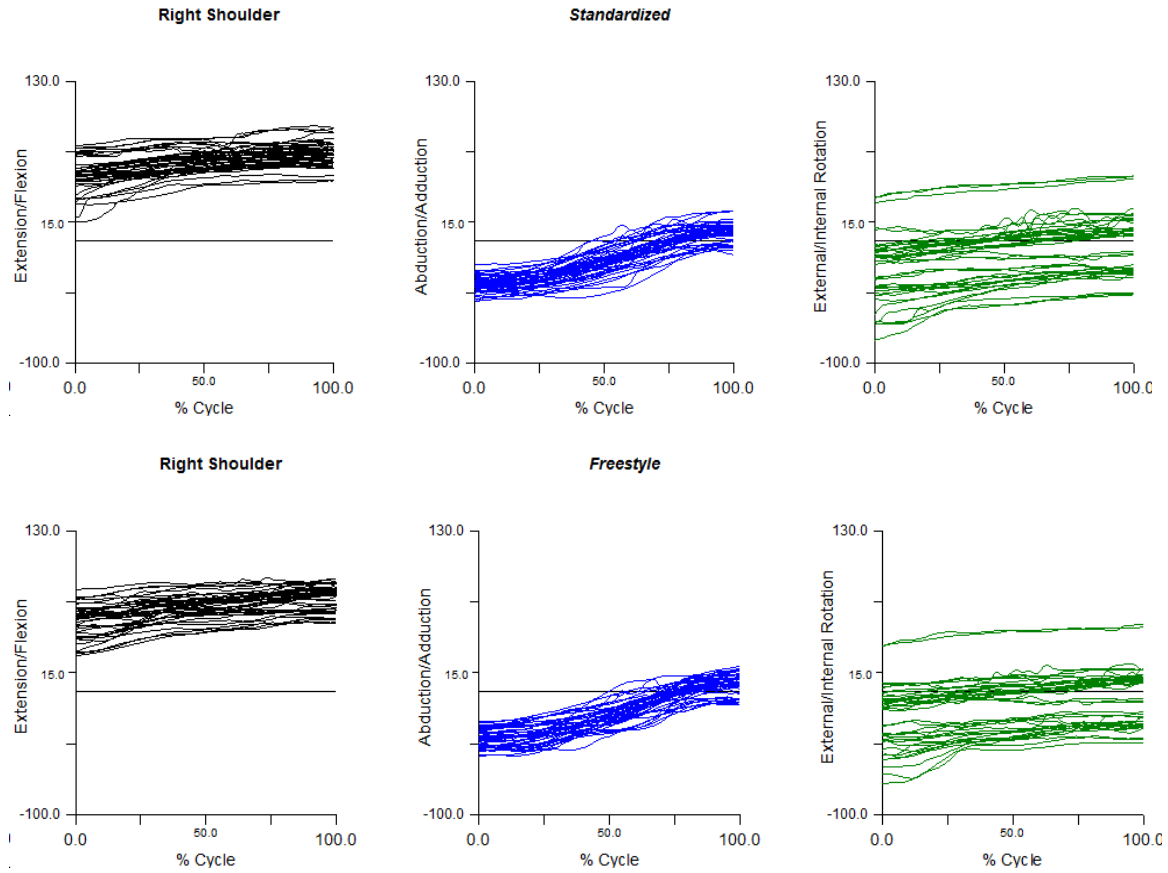


Figure 82. Angle-time graphs showing the angular position of the right upper arm with reference to the trunk during the Horizontal Transfer Task Maximum Reach condition.

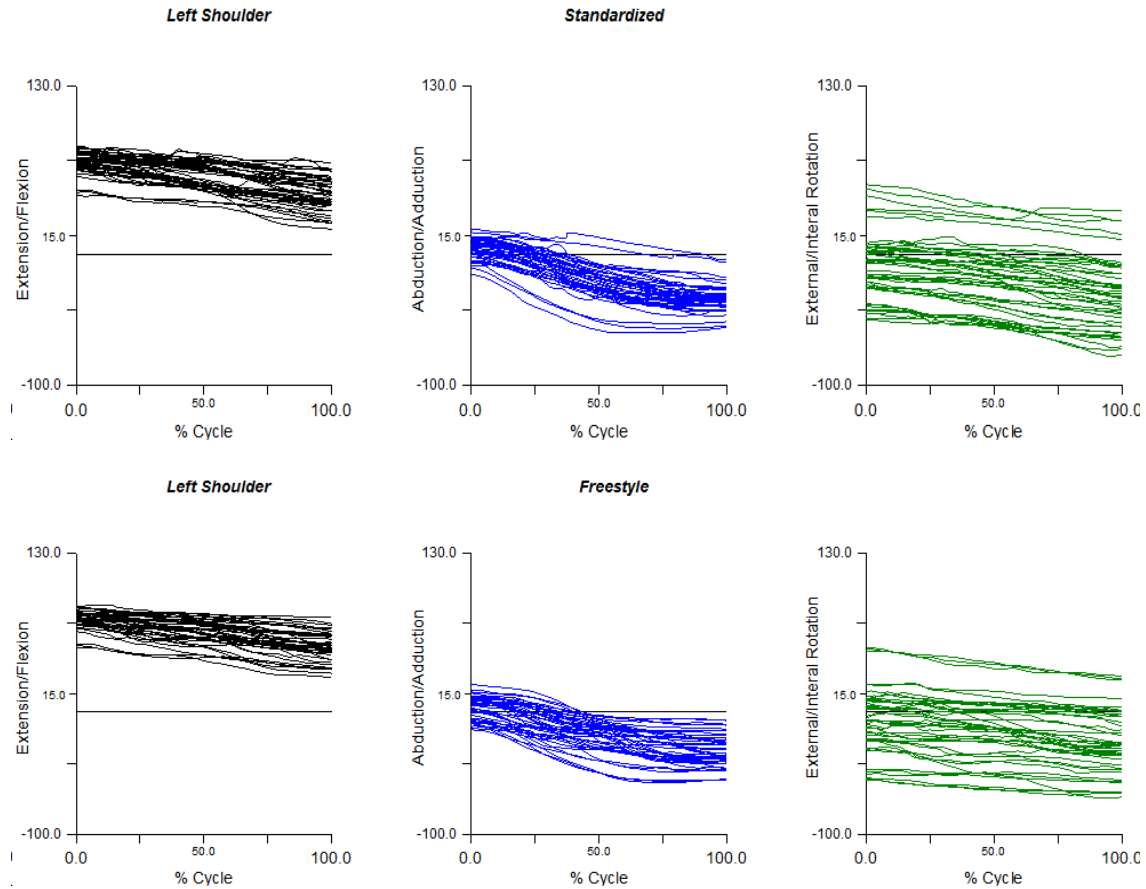


Figure 83. Angle-time graphs showing the angular position of the left upper arm with reference to the trunk during the Horizontal Transfer Task Maximum Reach condition.

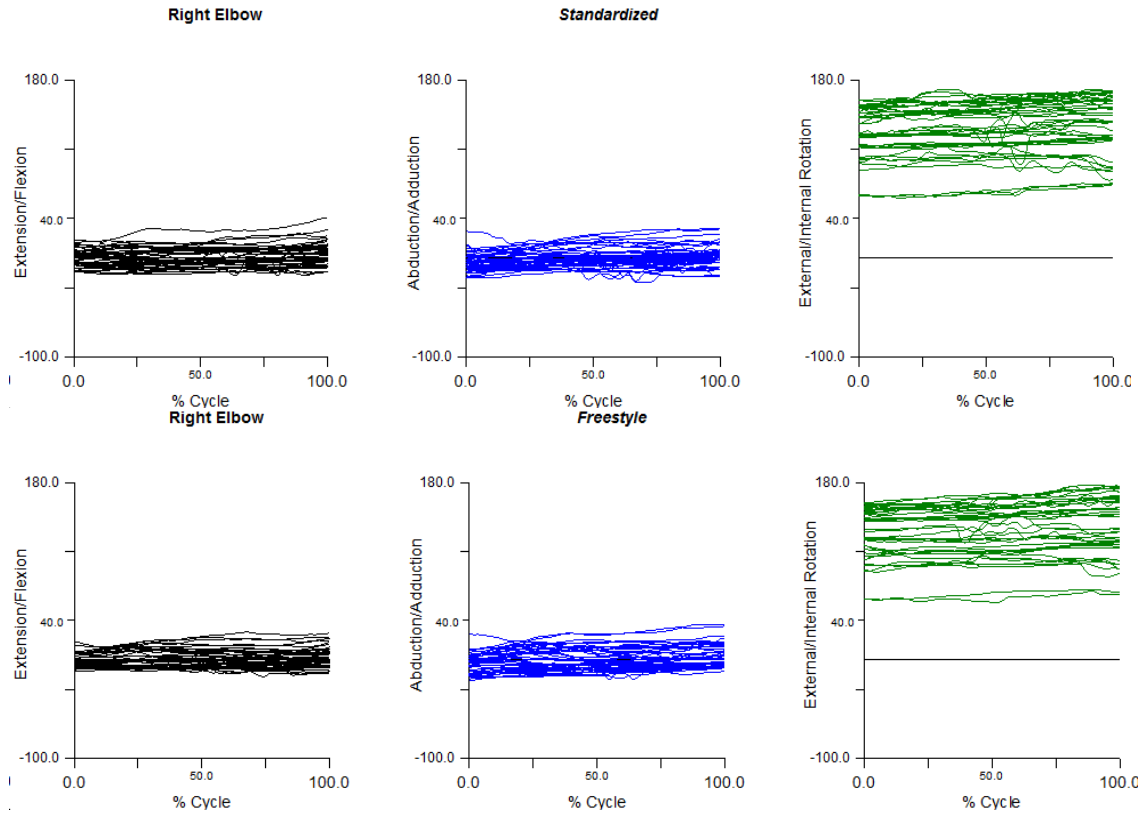


Figure 84. Angle-time graphs showing the angular position of the right lower arm with reference to the right upper arm during the Horizontal Transfer Task Maximum Reach condition.

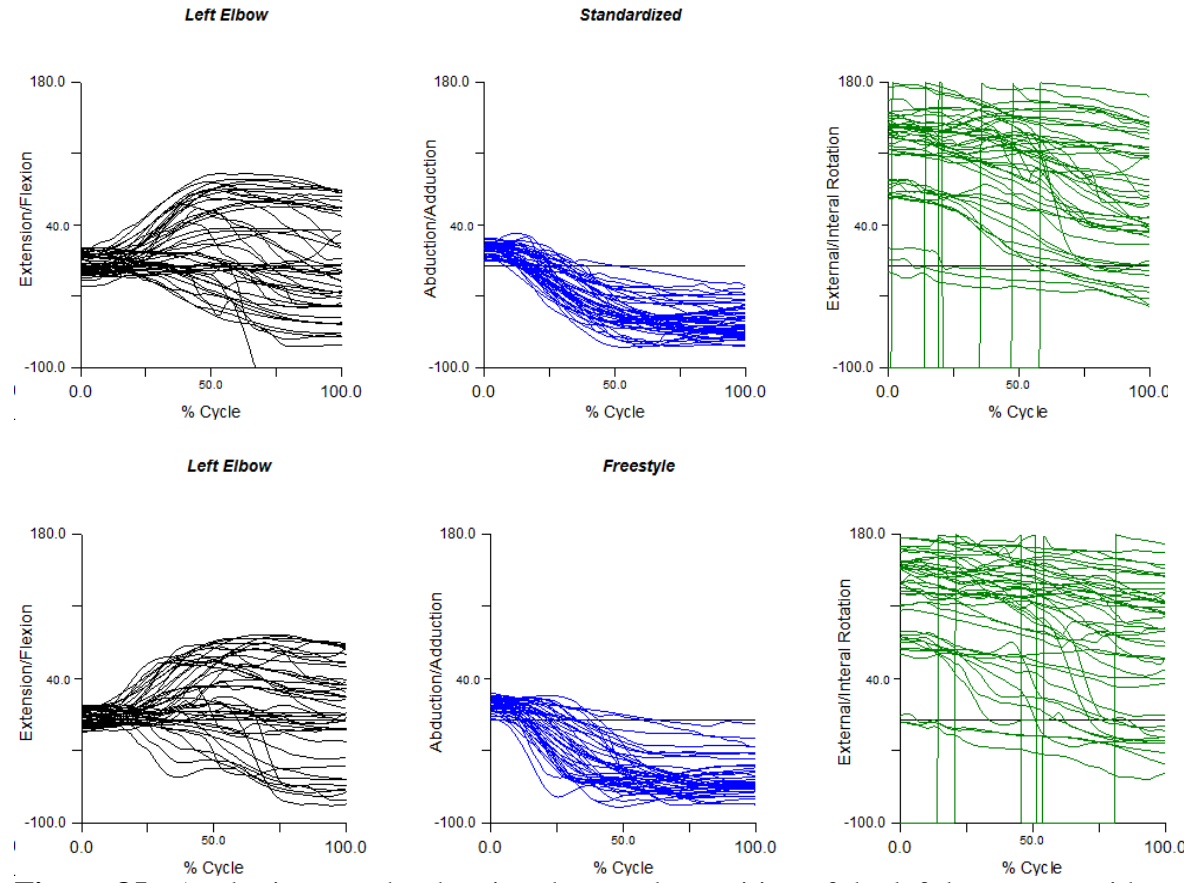


Figure 85. Angle-time graphs showing the angular position of the left lower arm with reference to the left upper arm during the Horizontal Transfer Task Maximum Reach condition.

Appendix B: Initial Screening Form

Specific health related questions for subjects of the study: *Three-dimensional kinematics of the upper limb during four functional transfer tasks*

The following narrative will be provided and read to each potential participant during the time period devoted to obtain informed consent. "This form is to help with the assessment of your upper extremity and back health. As you are being asked to move a 2.9 kg load through a series of standing lift and transfer tasks, we request a small amount of information regarding upper extremity joint health and past back problems. Please take time to read and understand the questions on this form."

If the potential participant answers yes to any of the questions listed above, they will be excluded from the study.

Have you ever had any of the following conditions?	Yes	No
Dislocated or separated either shoulder in the past year? If so, does it affect your arm reach?		
Do you suffer from arthritis, bursitis, tendonitis in either shoulder? Does this hinder your ability to perform daily activities?		
Any current pathologies of the arm or wrist that would limit ones ability to grasp or lift objects?		
An episode of back pain in the past 12 months that required you to miss work or seek medical attention?		
A current condition of the back or lower extremity that would inhibit your ability to stand for longer then one hour?		

If you have any further questions or want to seek clarification about anything found on this form, please contact Colin Wicks @ cl234046@dal.ca or 902-402-8275

Appendix C: Pilot Study

A preliminary study on one healthy male was performed in the fall of 2014 to assess the plausibility of collecting and processing kinematic data of the upper extremity. Only the normal and extended reach lift and replace tasks are presented. The transfer tasks were excluded from the pilot study to avoid over complicating a project that was meant to be completed in one semester. The pilot study sought to establish the proof in principle that the data could be collected and processed in a meaningful way. Programs were written manually to perform this analysis. Markers were placed in the positions listed in Table 1. Three trials for each condition were performed and recorded using the Optotrak Certus® camera system in the DOHM lab at Dalhousie University. A Matlab program was written which calculated the joint angles about the subject's elbows and shoulders; Microsoft Excel was then used to produce Figures 7 through 10 below. The program produced a series of angle-time histories over the period of the activity, which forms a motion pattern for both lifting conditions. These patterns are seen in the line graphs shown below in Figures 7 through 10. By convention, rotations about the segmental Y axis were internal/external rotation (pronation/supination in elbow), flexion/extension in the Z axis, while rotations about the X axis were adduction/abduction. The results for the wrist movements were excluded, as they were deemed insignificant after processing and visual review of the motion.

Shoulder Angle, Straight Arm Lift

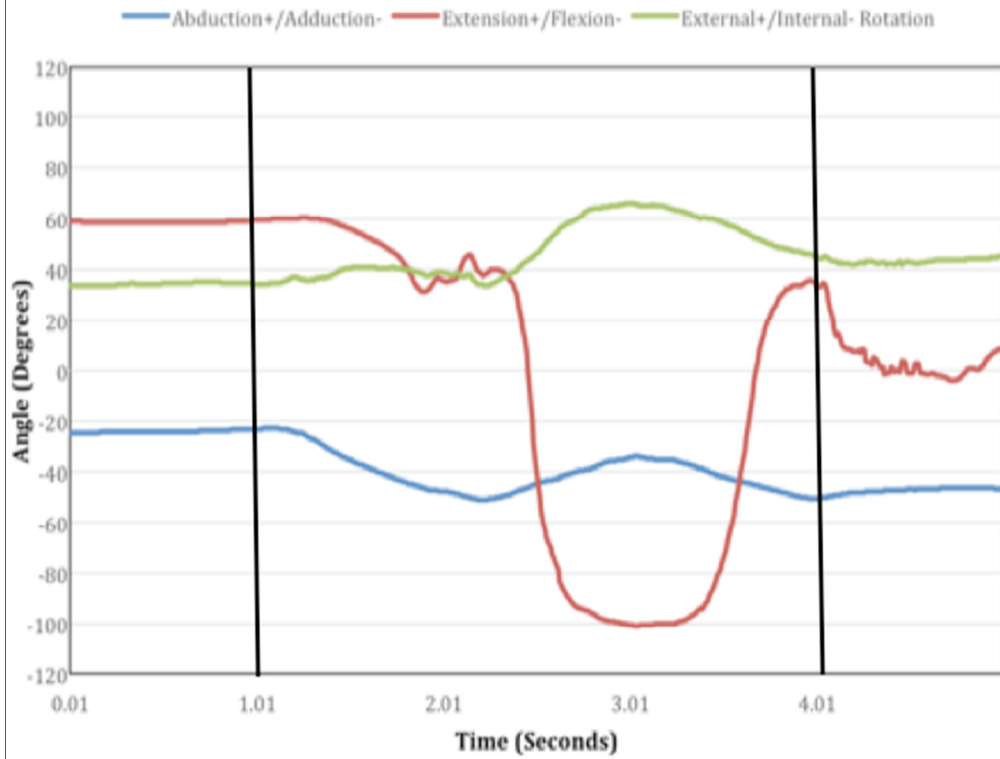


Figure 86: Shown above are the joint angles of the subject's shoulder joint during the straight-arm lift condition. The solid black lines signify the approximate start and end of the three seconds of lifting activity.

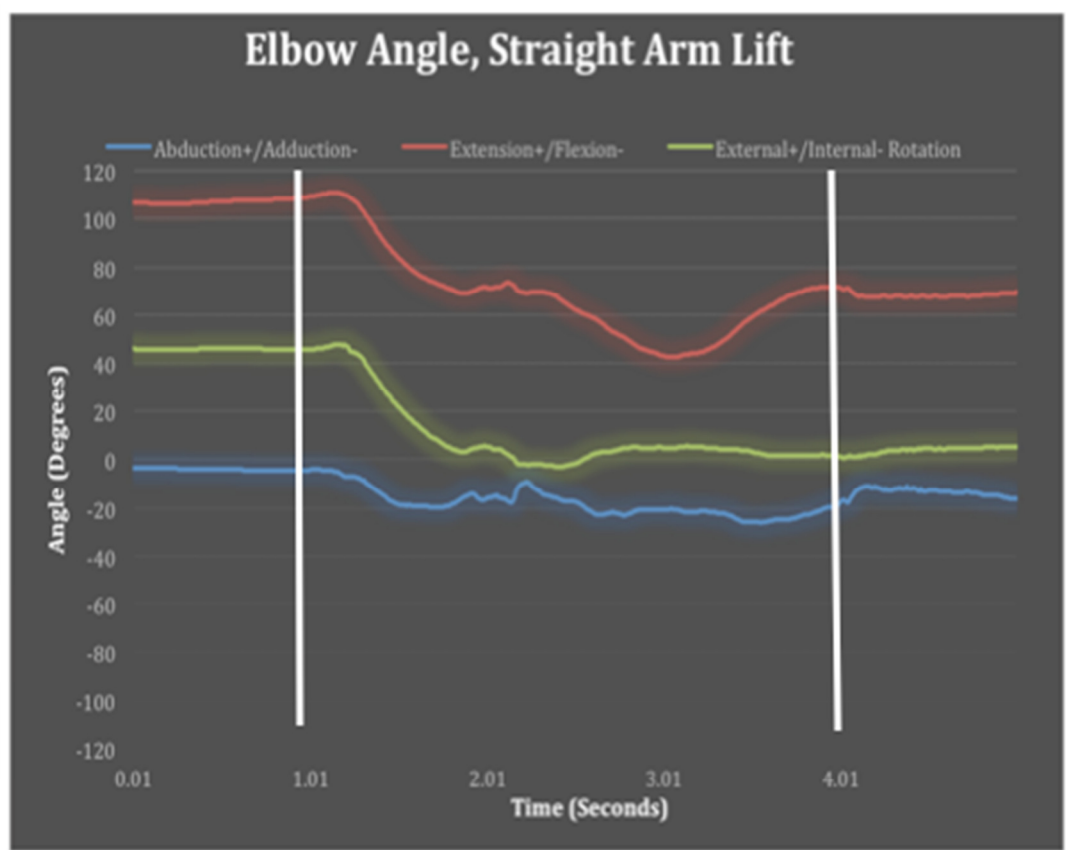


Figure 87: Shown above are the joint angles of the elbow joint during the straight arm lift condition. The solid white line signifies the approximate start and end of the three seconds of lifting activity.

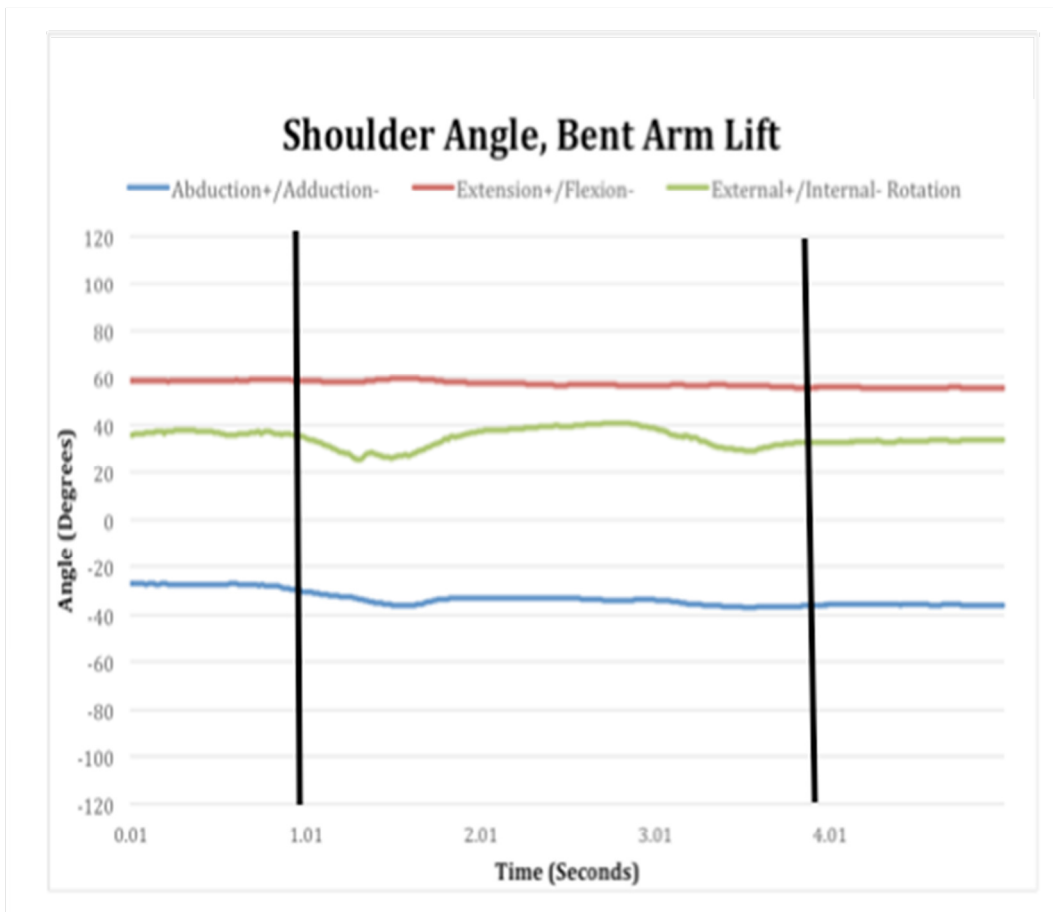


Figure 88: Shown below are the joint angles for the shoulder joint of the subject during the bent arm lift condition. The solid black lines signify the approximate start and end of the three seconds of lifting activity.



Figure 89: Shown below are the joint angles of the elbow joint of the subject during the bent arm lift condition. The solid white line signifies the approximate start and end of the three seconds of lifting activity.

The shoulder (humerus relative to thorax) patterns were as expected between the two conditions. The extended reach flexion angle was far greater (>100 degrees) than the bent arm trial, as expected. The shoulder joint did, however, reach almost 140 degrees of flexion during the extended reach trial, an excessive result considering the nature of the lift demonstrated. A single trial was collected however and a video of the lift was not recorded for future reference. Results for the elbow data were unexpected, especially for the bent arm lift (Figure 10). The rotations in the X and Y-axes, adduction/abduction and internal/external rotation respectively, were acceptable as the arm angles in both trials are in the same range (10 to -40 degrees), with the normal reach trial having slightly more adduction and internal rotation (pronation). The X and Y angles move symmetrically during the performed activity, further supporting a reasonable result. The unexpected result comes in the Z rotation, which would be elbow flexion and extension. One would expect the rotation angles for the normal reach trial to vary comparatively to those obtained from the shoulder during the extended reach trial. The elbow in the normal reach trial even flexed 30 degrees, when it was supposed to remain as straight as possible. The elbow only flexed 14 degrees according to the data collected in the selected trial for the normal reach condition, an unexpected result to say the least when one reflects on the humerus flexion of 140 degrees during the straight arm trial. More participants performing a larger number of trials would help in confirming if these unexpected results are an anomaly or not.

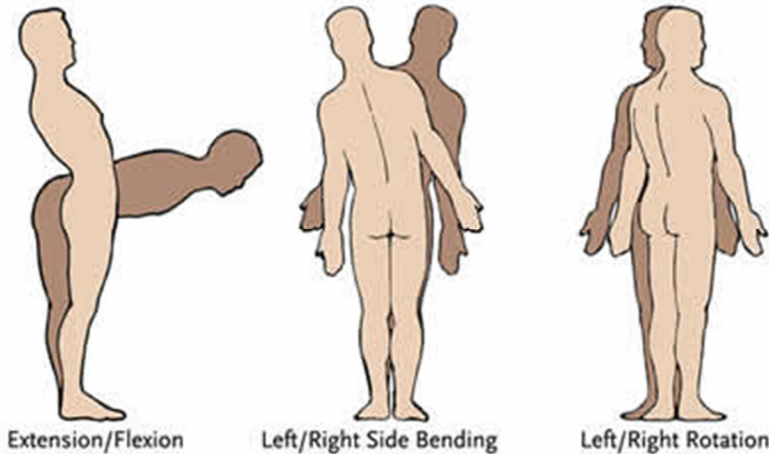
The study hoped to recreate motion pattern models similar to those in previous literature (van Andel et al., 2008). These models express the movement of segments in space as a sequence of rotations (angles) about pre-established anatomically relevant

coordinate systems. It can be concluded that the creation of a three-dimensional model of the upper extremity is feasible, and can be useful in expressing the motion of the human body. The results, even with the unexpected results, lead one to believe that the ISB guidelines can be emulated to provide joint angles that are relevant and easily deciphered by fellow researchers.

Appendix D: Qualysis - Visual 3D Verification Study

A verification study was performed prior to the commencement of participant testing. Its purpose was to assess the output of the Qualysis system when processed by the Visual 3D software, as well as to assure that the kinematic model created to process the kinematic data could be applied to different subjects other than the original. One subject was recruited to perform a series of static poses while wearing the exact marker set-up to be used in the main study. QTM sampled a second of data from the Qualysis motion tracking system for each pose, thus allowing Visual 3D to apply the model and calculate the relative angles of the trunk and both the right & left upper arms and forearms. A hand held goniometer was used to place the participants in the approximate position required for each set pose.

7.1 Trunk Analysis



The three positions chosen for the trunk analysis were:

		Frontal Flex.	L/R Rot.	Lateral Flex
45° Forward Flexion	Measured	-40	0	1
	Qualysis	-58	-2	1
20° Left Axial Rotation	Measured	0	-10	1
	Qualysis	-29	-5	1
30° Left Lateral Flexion	Measured	-15	12	-4
	Qualysis	-29	-2	-4

These positions were chosen because they covered angular displacements in each of the three degrees of freedom being examined in the study (X,Y,Z). The results clearly show that forward frontal flexion (X), left axial rotation (Z) and left lateral flexion (Y) are negative rotations about their respective axis'. In addition to the three trunk poses, the angles of the trunk were calculated in a static anatomic pose, in each of the trials performed specifically for the shoulder and forearm and during 4 poses selected from times during the four lifting conditions from the main study. It was expected that these angles would not surpass the more overt displacements in the trunk poses, which they did not. All the calculated trunk angles were assessed in Table 1below to determine the maximum angular displacement (MAD) for the trunk relative to the pelvis throughout all the trials. These ranges were deemed feasible and within the expected ranges for the set poses that were recorded.

Table 12. Calculated MAD of the trunk relative to the pelvis during the testing procedure.

	Flexion	L/R Rot.	Lateral Flex.
Maximum Angle Throughout Trials	1	4	0
Minimum (Qualysis)	-58	-5	-41
ROM (Degrees)	59	9	41

7.2 Upper Arm Analysis

The three positions chosen for the upper arm analysis were:

Position @ Shoulder	Right Arm			Left Arm		
	Flexion	Int/Ext Rot.	Ad/Abduction	Flexion	Int/Ext Rot.	Ad/Abduction
	Measured	92	24	-2	Measured	88
Abduction @ Shoulder						
Flexion @ Shoulder	Flexion	Int/Ext Rot.	Ad/Abduction	Flexion	Int/Ext Rot.	Ad/Abduction
	Measured	5		-98	Measured	5
	Qualysis	33	-51	-87	Qualysis	151
External Rotation						
Internal Rotation	Flexion	Int/Ext Rot.	Ad/Abduction	Flexion	Int/Ext Rot.	Ad/Abduction
	Measured	17	-30	-12	Measured	31
	Qualysis	35	-23	-18	Qualysis	36

These positions were chosen because they covered angular displacements in each of the three degrees of freedom being examined in the study (X, Y, Z). They also placed the upper arm in greater displacements than those expected during the study trials. The results clearly show that shoulder extension (X), internal rotation (Z) and abduction (Y) are negative rotations about their respective axes; Flexion, external rotation and adduction are all positive rotations. In addition to the three upper arm poses, the angles of both shoulders were calculated in a static anatomic pose, in each of the trials performed specifically for the trunk and forearm and during four poses

selected from times during the four lifting conditions from the main study. It was expected that these angles would not surpass the more overt displacements in the shoulder poses, which they did not.

All the calculated upper arm angles were assessed in Table 2 below to determine the MAD for the upper arm relative to the trunk throughout all the trials. Angles calculated in the Y and Z axis of the left arm were inversed so they would correspond with the right arm. The only anomaly within the data appears to be the flexion angle of the left arm during the abduction trial (highlighted in red above). It was decided that this was an error due to a possible gimbal lock, this data was omitted from further analysis. The calculated ranges shown below in figure # were deemed feasible for both arms and within the expected ranges for the set poses that were recorded.

Table 13. Calculated MAD for both shoulders relative to the trunk during the testing procedure

Upper Arm	Right Arm			Left Arm		
	Flexion/Ext.	Int./Ext.	Rot. Add./Abd.	Flexion/Ext.	Int./Ext.	Rot. Add./Abd.
Maximum Angle Throughout Trials	96	3	3	102	13	1
Maximum (Qualysis)	16	-84	-87	21	-60	-78
ROM (Degrees)	80	87	90	81	73	79

7.2 Forearm Analysis

The three positions chosen for the forearm were:

		Right Arm						Left Arm		
		Flexion	Int/Ext Rot.	Ad/Abduction	Flexion	Int/Ext Rot.	Ad/Abduction	Flexion	Int/Ext Rot.	Ad/Abduction
1 @ Elbow	Forearm	Measured	69	5	10	Forearm	Measured	69	8	
		Qualysis	39	49	52		Qualysis	Marker Error		
2 @ Elbow	Forearm	Measured	15	20	10	Forearm	Measured	10	20	
		Qualysis	-5	71	13		Qualysis	-7	2	
3 @ Elbow	Forearm	Measured	Flexion	Int/Ext Rot.	Ad/Abduction	Forearm	Measured	Flexion	Int/Ext Rot.	
		Qualysis	-5	79	9		Qualysis	-9	131	

These positions were chosen because they covered angular displacements in each of the three degrees of freedom being examined in the study (X, Y, Z). They also placed the forearm in greater displacements than those which were expected during the study trials. The results clearly show that elbow extension (X), internal rotation (Z) and abduction (Y) are negative rotations about their respective axis; Flexion, external rotation and adduction are all positive rotations. In addition to the three forearm poses, the angles of both shoulders were calculated in a static anatomic pose, in each of the trials performed specifically for the trunk and forearm and during 4 poses selected from times during the four lifting conditions from the main study. It was expected that these angles would not surpass the more overt displacements in the elbow poses, which they did not.

All the calculated forearm angles were assessed in Table 3 below to determine the range of motion (ROM) for the forearm relative to the trunk throughout all the trials. Angles calculated in the Y and Z axis of the left arm were inverted so they would correspond with the right arm. The manually measured angles for the 180° pronation trial were not recorded due to their difficulty in measuring and resulting lack of validity. Marker error prevented the software from calculating the angles for the left arm.

during the 90° flexion trial. The forearm data proved far harder to record and process, mainly due to the increased ROM and reduced size of the limb, resulting in the markers being far closer then in other areas of the body.

The main issue with the data is the angles about the Y axis (Adduction/Abduction) and the apparent lack of validity or common trend within the trials. Previous kinematic research looking at the upper extremity has omitted this degree of freedom from the elbow joint, mainly because it is not expected that this will change during motion. It appears that the software may be mistaking motion in the Z axis for motion in the Y. For this reason, the main research project will on focus on two degrees of freedom about the elbow and will exclude Y axis rotation from the statistical comparison.

The calculated ranges in the X and Z axes shown below in table 3 were deemed feasible for right arm and within the expected ranges for the set poses that were recorded. The results for the left arm were unexpected because X axis rotation wasn't near the amount of the right arm, this result can be explained however by the fact that the left arm was not recorded in the 90° flexion trial, therefore not capturing the left arm during its max moment of flexion.

Table 14. Calculated MAD for both elbows relative to the upper arms during the testing procedure

	<i>Right Arm</i>			<i>Left Arm</i>		
	Flexion/Ext.	Int./Ext.	Rot.	Add./Abd.	Flexion/Ext.	Int./Ext.
Angle Throughout Trials (Qualysis)	47	143		68	6*	151
ROM (Degrees)	-45	-47		-5	-28	-6
	92	96		73	34	157